U.S. Department
of Transportation
Federal Railroad
Administration

Office of Research,
Development and Technology
Washington, DC 20590

# Full-scale Grade Crossing Impact of a Single-frame Highway Truck into an LNG Tender: Pre- and Post-Test Analyses

DOT/FRA/ORD-24-14

Final Report | March 2024

# REPORT DOCUMENTATION PAGE

*Form Approved*
*OMB No. 0704-0188*



| **1. REPORT DATE** *(DD-MM-YYYY)* | **2. REPORT TYPE** | **3. DATES COVERED** *(From - To)* |
|---|---|---|
| 03-21-2024 | Technical Report | August 2018 – March 2022 |

**4. TITLE AND SUBTITLE**
Full-scale Grade Crossing Impact of a Single-frame Highway Truck into an LNG Tender: Pre- and Post-Test Analyses

**5a. CONTRACT NUMBER**
DTFR5317F00767

**5b. GRANT NUMBER**

**5c. PROGRAM ELEMENT NUMBER**

**6. AUTHOR(S)**
Michael Carolan* - ORCiD: 0000-0002-8758-5739
Dr. Shaun Eshraghi* - ORDiD: 0000-0002-8152-0838
Karina Jacobsen* - ORCiD: 0000-0002-3985-7349
Tatiana Mowry* - ORCiD: 0009-0007-0170-448X
Dr. Ulrich Spangenberg** - ORCiD: 0000-0003-2760-1394
Laura Sullivan* - ORCiD: 0000-0001-9146-8917

**5d. PROJECT NUMBER**
IAA RR28A520

**5e. TASK NUMBER**
VK347/VK348

**5f. WORK UNIT NUMBER**

**7. PERFORMING ORGANIZATION NAME(S) AND ADDRESS(ES)**
*Volpe National Transportation Systems Center
55 Broadway, Cambridge, MA 02142
**Transportation Technology Center, Inc.
55500 DOT Road, Pueblo, CO 81001

**8. PERFORMING ORGANIZATION REPORT NUMBER**

**9. SPONSORING/MONITORING AGENCY NAME(S) AND ADDRESS(ES)**
U.S. Department of Transportation
Federal Railroad Administration
Office of Railroad Policy and Development
Office of Research, Data, and Innovation
Washington, DC 20590

**10. SPONSOR/MONITOR'S ACRONYM(S)**
FRA

**11. SPONSOR/MONITOR'S REPORT NUMBER(S)**
DOT/FRA/ORD-24-14

**12. DISTRIBUTION/AVAILABILITY STATEMENT**
This document is available to the public through the FRA website.

**13. SUPPLEMENTARY NOTES**
COR: Melissa Shurland (FRA) and Francisco González, III (FRA)

**14. ABSTRACT**
FRA sponsored a research team from Transportation Technology Center, Inc. (TTCI) to execute a grade crossing side impact test of a heavy highway vehicle (dump truck) into a liquified natural gas (LNG) fuel tender at the Transportation Technology Center (TTC) in Pueblo, CO, on September 22, 2021. A team from Volpe National Transportation Systems Center (Volpe) conducted computational analyses to plan for the test. This report documents the development of the test procedures and setup and describes both the FE and the lumped-mass model used for pre-test planning. It outlines the measured results from the test to evaluate the crashworthiness of an LNG fuel tender and compares the test measurements and outputs from the numerical analyses. Finally, the report describes the subsequent post-test analyses performed to address the variations between the pre-test analyses and the actual test conditions.

**15. SUBJECT TERMS**
Fuel tender, alternative fuels, impact testing, finite element analysis, FEA

| **16. SECURITY CLASSIFICATION OF:** | | | **17. LIMITATION OF ABSTRACT** | **18. NUMBER OF PAGES** | **19a. NAME OF RESPONSIBLE PERSON** |
|---|---|---|---|---|---|
| **a. REPORT** | **b. ABSTRACT** | **c. THIS PAGE** | | 86 | **Francisco González, III** |
| | | | | | **19b. TELEPHONE NUMBER** *(Include area code)* **202-493-6076** |

**Standard Form 298** (Rev. 8/98)
Prescribed by ANSI Std. Z39.18

# METRIC/ENGLISH CONVERSION FACTORS

| ENGLISH TO METRIC | METRIC TO ENGLISH |
|---|---|
| **LENGTH (APPROXIMATE)** | **LENGTH (APPROXIMATE)** |
| 1 inch (in) = 2.5 centimeters (cm) | 1 millimeter (mm) = 0.04 inch (in) |
| 1 foot (ft) = 30 centimeters (cm) | 1 centimeter (cm) = 0.4 inch (in) |
| 1 yard (yd) = 0.9 meter (m) | 1 meter (m) = 3.3 feet (ft) |
| 1 mile (mi) = 1.6 kilometers (km) | 1 meter (m) = 1.1 yards (yd) |
| | 1 kilometer (km) = 0.6 mile (mi) |
| **AREA (APPROXIMATE)** | **AREA (APPROXIMATE)** |
| 1 square inch (sq in, $in^2$) = 6.5 square centimeters ($cm^2$) | 1 square centimeter ($cm^2$) = 0.16 square inch (sq in, $in^2$) |
| 1 square foot (sq ft, $ft^2$) = 0.09 square meter ($m^2$) | 1 square meter ($m^2$) = 1.2 square yards (sq yd, $yd^2$) |
| 1 square yard (sq yd, $yd^2$) = 0.8 square meter ($m^2$) | 1 square kilometer ($km^2$) = 0.4 square mile (sq mi, $mi^2$) |
| 1 square mile (sq mi, $mi^2$) = 2.6 square kilometers ($km^2$) | 10,000 square meters ($m^2$) = 1 hectare (ha) = 2.5 acres |
| 1 acre = 0.4 hectare (he) = 4,000 square meters ($m^2$) | |
| **MASS - WEIGHT (APPROXIMATE)** | **MASS - WEIGHT (APPROXIMATE)** |
| 1 ounce (oz) = 28 grams (gm) | 1 gram (gm) = 0.036 ounce (oz) |
| 1 pound (lb) = 0.45 kilogram (kg) | 1 kilogram (kg) = 2.2 pounds (lb) |
| 1 short ton = 2,000 pounds (lb) = 0.9 tonne (t) | 1 tonne (t) = 1,000 kilograms (kg) = 1.1 short tons |
| **VOLUME (APPROXIMATE)** | **VOLUME (APPROXIMATE)** |
| 1 teaspoon (tsp) = 5 milliliters (ml) | 1 milliliter (ml) = 0.03 fluid ounce (fl oz) |
| 1 tablespoon (tbsp) = 15 milliliters (ml) | 1 liter (l) = 2.1 pints (pt) |
| 1 fluid ounce (fl oz) = 30 milliliters (ml) | 1 liter (l) = 1.06 quarts (qt) |
| 1 cup (c) = 0.24 liter (l) | 1 liter (l) = 0.26 gallon (gal) |
| 1 pint (pt) = 0.47 liter (l) | |
| 1 quart (qt) = 0.96 liter (l) | |
| 1 gallon (gal) = 3.8 liters (l) | |
| 1 cubic foot (cu ft, $ft^3$) = 0.03 cubic meter ($m^3$) | 1 cubic meter ($m^3$) = 36 cubic feet (cu ft, $ft^3$) |
| 1 cubic yard (cu yd, $yd^3$) = 0.76 cubic meter ($m^3$) | 1 cubic meter ($m^3$) = 1.3 cubic yards (cu yd, $yd^3$) |
| **TEMPERATURE (EXACT)** | **TEMPERATURE (EXACT)** |
| [(x-32)(5/9)] °F = y °C | [(9/5) y + 32] °C = x °F |

## QUICK INCH - CENTIMETER LENGTH CONVERSION

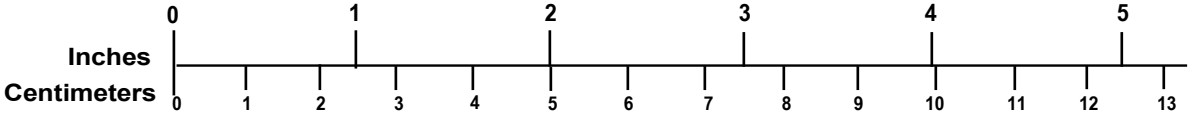


## QUICK FAHRENHEIT - CELSIUS TEMPERATURE CONVERSIO

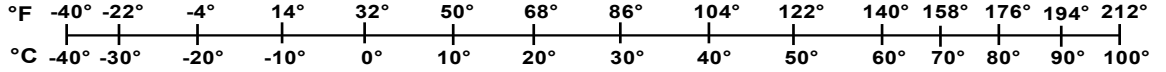


For more exact and or other conversion factors, see NIST Miscellaneous Publication 286, Units of Weights and Measures. Price $2.50 SD Catalog No. C13 10286

Updated 6/17/98

## Acknowledgements

The authors acknowledge the cooperation and assistance of Hector Villarreal and Devangkumar Patel of Taylor-Wharton Americas in providing engineering drawings, design information, and on-site support for the Liquified Natural Gas (LNG) tender used in this research. The authors also acknowledge the dedication of Taylor-Wharton Americas in ensuring the tender's vacuum was maintained in the days leading up to the test.

The authors acknowledge the cooperation and assistance of John Burgess and Steve Easterling of Airgas in providing information on the physical properties and filling procedures of liquid nitrogen (LN2) used in the test.

The authors are grateful to Texas A&M Transportation Institute (TTI) researchers for their assistance in developing a finite element (FE) model of a dump truck. Dr. Akram Abu-Odeh at TTI kindly shared and discussed the FE model TTI developed for a project for Texas Department of Transportation (TxDOT) which assisted the authors in developing their own dump truck FE model for the grade crossing impact simulation. The authors of this report also acknowledge the assistance of Dr. Gary Fry, P.E., formerly of the Transportation Technology Center, Inc. (TTCI), in making introductions to TTI and obtaining the dump truck model.

The authors acknowledge the cooperation of Dr. Steven Kirkpatrick of Applied Research Associates (ARA). ARA shared a finite element (FE) model of a locomotive they developed and provided insightful technical discussion of testing and modeling stainless steel at cryogenic temperatures. The authors also acknowledge the cooperation of the AAR Equipment Engineering Committee in obtaining the locomotive model.

The authors acknowledge the collaboration of the members of Association of American Railroads (AAR) M-1004 Technical Advisory Group, in particular Patrick Student and Dave Cackovic.

The authors acknowledge Dr. Przemyslaw Rakoczy (formerly of TTCI), in the preliminary test planning efforts at the Transportation Technology Center, and Travis Gorhum (formerly of TTCI), for test planning and preparation throughout the project.

The authors acknowledge cooperation, discussions, and technical information on freight truck (i.e., bogie) components and behaviors provided by Brian Marquis of Volpe and Ali Tajaddini of the Federal Railroad Administration (FRA).

The authors acknowledge the rail steel tensile test data shared by Dr. Pawel Woelke, P.E. (Thornton-Tomasetti) and Dr. Herman Nied (Lehigh University). The authors are also grateful for FRA's Dr. Robert Wilson's cooperation and coordination in facilitating this information sharing.

The authors acknowledge the cooperation and collaboration with FRA's Grade Crossing research program, Volpe's Marco DaSilva and Bill Baron, and FRA's Francesco Bedini Jacobini in documenting the post-impact scene using an unmanned aerial vehicle (UAV).

The authors acknowledge the technical assistance of the Volpe National Transportation System Center's John Wojtowicz, Dr. Benjamin A. Perlman, Aswani Krishnamurthy, and Wesley Peisch (former) in the planning, development, execution, and verification of the computational models

described in this report. The authors thank Volpe colleague Andrew Skrzypczak for helping with the post-test data processing included in this report.

Finally, inputs from FRA's Melissa Shurland and Francisco González, III, were valuable in developing the testing and modeling plans for this research. The authors also acknowledge technical discussions and assistance in developing testing plans provided by Mark Maday, Steve Clay, and Dr. Phani Raj of FRA's Office of Railroad Safety.

## Contents

## Illustrations

## Tables

## Executive Summary

The Federal Railroad Administration (FRA) sponsored a research team from Transportation Technology Center, Inc. (TTCI) to execute a grade crossing side impact test of a heavy highway vehicle (dump truck) into a liquified natural gas (LNG) fuel tender at the Transportation Technology Center (TTC) in Pueblo, CO, on September 22, 2021. A team from Volpe National Transportation Systems Center (Volpe) conducted computational analyses to plan for the test. The LNG fuel tender was specifically designed according to the Association of American Railroads (AAR) standard M-1004 specification for fuel tenders [1]. The tender was a double-walled tank (i.e., tank-within-a-tank) designed to carry a cryogenic liquid (i.e., LNG) as a locomotive fuel. The tender was purpose-built for testing with the structural features of a fuel tender, including all piping and valves found in normal service, but did not feature all the equipment required of a functional fuel tender (e.g., trucks, heat exchanger).

M-1004 includes criteria and procedures for the design of a protective housing of the fuel tender surrounding the external piping and valves. One method of demonstrating the housing's crashworthiness is through analysis of an impact scenario between a highway vehicle and the tender's protective housing. To conform with this standard, the test tender was coupled between two 6-axle freight locomotives and the protective housing was struck by an 80,000 pound dump truck modified to travel on railroad tracks.

The main objectives of the test were to demonstrate the crashworthiness of the LNG fuel tender's protective housing and the proper functioning of the cut-off valves during a side impact grade crossing collision. At the time of the test, no experimental data existed to evaluate the crashworthiness of the protective housing on an LNG fuel tender. Therefore, the experimental data would also be valuable to verify the realism of FE analyses conducted to demonstrate compliance with the requirements in M-1004.

The team used cryogenic liquid nitrogen (LN2) in place of LNG. Researchers targeted the impact speed to be no less than 40 mph, as required in M-1004. The impact speed, measured at approximately 42.6 mph (68.6 km/h), corresponded to an impact kinetic energy of approximately 4.9 million foot-pounds (6.6 MJ). All data were recorded successfully, and the tender resisted the impact without tearing either the inner or the outer tank, maintaining a vacuum between the tanks. The tender and locomotives derailed but remained upright. No leaks were observed in any of the piping following the impact, and the locomotive fuel supply valve functioned as intended during and after the test.

This report documents the development of the test procedures and setup and describes both the finite element (FE) and the lumped-mass model used for pre-test planning. It outlines the key measured results from the test to illustrate the collection of experimental data used to evaluate the crashworthiness of an LNG fuel tender and compares the test measurements and outputs from the numerical analyses. Finally, the report describes the lessons learned in testing and modeling the scenario described in M-1004.

# 1. Introduction

The Federal Railroad Administration (FRA) sponsored Volpe National Transportation Systems Center (Volpe) to support testing of a liquified natural gas (LNG) tender, provide test planning support, and develop a finite element model of the test scenario. The research was conducted between August 2018 and March 2022. FRA sponsored a September 2021 grade crossing impact test between an LNG fuel tender and a highway vehicle (represented by a dump truck) conducted at FRA's Transportation Technology Center (TTC) and performed by Transportation Technology Center, Inc. (TTCI), with computational analyses performed by Volpe. The LNG fuel tender is specifically designed to carry and deliver LNG as a fuel supply to connected locomotives. The LNG fuel tender used in this test had an outer tank[1] made of 3/4-inch-thick carbon steel and an inner tank made of 5/8-inch-thick stainless steel. This report documents the impact test and describes both the finite element (FE) and the multibody dynamics (MBD) model development and analyses. This report also includes comparisons of the test measurements and outputs from the analyses.

## 1.1 Background

The rail industry is interested in using alternative fuels such as LNG to power locomotives and is considering the use of modified and enhanced-design U.S. Department of Transportation (DOT)-113 tank cars as LNG fuel tenders.

The use of LNG as a locomotive fuel was tested in pilot projects at two railroads in the 1990s [2] using modified DOT-113 tank cars as fuel tenders. More recently, modified United Nations (UN) Portable T75 tanks, also called International Organization for Standardization (ISO) tanks, were used as fuel tenders for rail operation of trains transporting LNG.

In 2012, the Association of American Railroads (AAR) established the Natural Gas Fuel Tender (NGFT) Technical Advisory Group (TAG) to develop the specifications for the design and safe operation of alternative fuel tenders for dual fuel locomotives. These specifications are part of the M-1004 specifications for fuel tenders, which is intended to cover multiple tender configurations and multiple fuels [1].

Part of the development of the M-1004 specifications included developing accident scenarios of concern, specifically several potential accident scenarios involving the LNG tender. The analyses of the tender's structural performance under the postulated accident scenarios were performed by AAR using non-linear dynamic FE analysis. In addition, FRA entered into an agreement with the Volpe Center to evaluate the tender performance under the postulated accident scenarios using simplified multi-body dynamics analyses. These analyses evaluated the crashworthiness of the tender tank and its ability to contain the LNG without leakage.

No collision scenario test data on the survivability of various tender components such as valves, piping, and the pipe-to-shell weld joints necessary for the design of the tender as a fuel supply vessel existed before testing. No modeling was performed to demonstrate that the valves and piping would be able to withstand the accident scenario loads in M-1004 without leaking and while maintaining functionality. The grade crossing impact test conducted during this project was

[1] The phrase 'outer tank' is used throughout the report as opposed to the term 'jacket' used in M-1004 to highlight that the construction of the tender was a tank-within-a-tank design.

expected to provide data to help evaluate the survivability of the valve functions under such accident conditions. Additionally, it provided experimental data to evaluate the crashworthiness of an LNG tender designed to meet the M-1004 standard.

### *1.1.1 AAR Standard M-1004*

In 2013, the AAR's NGFT TAG began to develop specifications for tenders used for supplying fuel to dual fuel or alternative fueled locomotives. The preliminary steps for completing this process included identifying impact scenarios of concern, evaluating existing designs, and drafting idealized scenarios for evaluation. The group identified the following five collision scenarios of concern:

1. A head on collision between two locomotive-led freight trains
2. A side impact grade crossing collision between a highway vehicle and a natural gas tender
3. A rollover incident of the natural gas tender
4. A side impact into the shell of the natural gas tender
5. A head end impact into the natural gas tender

The NGFT TAG drafted these scenarios to be evaluated through FE analyses in which criteria must be met for a manufacturer to ensure a minimum level of crashworthiness performance for each idealized impact scenarios. Each scenario includes a description of the equipment involved in the idealized scenario, the impact conditions, and the required results. Additionally, the NGFT TAG developed an alternative set of static requirements that may be met in lieu of the dynamic requirements.

The purpose of these dynamic requirements is to minimize the potential for fuel release during accident conditions. The objective of the head and side impact scenarios is to ensure a minimum level of protection for the tank jacket and inner tank against punctures from blunt objects typical in derailment scenarios. The objective of the rollover scenario is to ensure a minimum level of protection for the top manway. The objective of the train-to-train and grade crossing scenarios are to ensure a minimum level of crashworthiness protection for the valves and control system.

## 1.2 Objectives

The objective of the full-scale LNG tender impact test was to demonstrate that an LNG tender design could contain its commodity under the grade crossing scenario prescribed in M-1004. The criteria for demonstrating compliance with this scenario includes the following: 1) the jacket does not puncture, 2) the inner tank is not breached, and 3) the only release of fuel is through normal operation of the pressure relief valve (PRV). Additionally, FRA sought to determine whether the protected valves within the housing continued to function as intended after the impact.

### *1.2.1 Full-scale Testing Objective*

The objective of full-scale testing was to evaluate the crashworthiness of an LNG fuel tender's protective housing (i.e., cabinet) surrounding external piping and valves and the proper

functioning of the cut-off valves under a grade crossing side impact. Using a full-scale test also addressed uncertainties in the modeling requirements and procedures detailed in M-1004 as it pertained to the execution of the test and the representation of the accident scenario in the various models.

### *1.2.2 Modeling Objective*

The objective of the pre-test modeling was to predict the potential outcomes of the test and to help guide the development of the test setup. Where a test parameter was not given in M-1004 or the performance of such a parameter was difficult or impractical to control, modeling was used to estimate the potential range of outcomes associated with such a parameter. The overall modeling approach was to represent the behavior of interest as simply as possible to produce a reasonable result. As the test setup evolved and modeling results were reviewed, the sophistication of the model was increased as necessary.

## 1.3 Overall Approach

The overall approach involved a collaborative research effort that culminated in conducting the test in September 2021. The main efforts included test planning meetings between FRA, TTCI, and Volpe, test preparation at TTC, pre-test modeling by Volpe, test implementation at TTC, and post-test data processing by Volpe and TTCI. The test conditions were developed based on the modeling scenario described in Section 11.9.1 of the M-1004 specifications for a highway-grade crossing collision. These test conditions covered the setup and main requirements of the physical test. Key test parameters not addressed by the specifications were evaluated before the test setup was finalized. Researchers from Volpe developed models to study the extraneous conditions that may arise during testing to inform the test planning phase. For example, the models were helpful in understanding the performance of the fuel tender upon impact as well as the potential of post-impact behaviors of the LNG fuel tender, locomotives, the couplers, and the track. Once the planning phase was completed, the test plan was developed and finalized.

The test preparation and implementation stage followed the planning phase, during which the team decided that a dump truck would serve as the single-frame highway vehicle colliding with the LNG fuel tender. The test articles (i.e., the LNG fuel tender, dump truck, and locomotives) were obtained and ancillary structures such as the track were prepared for the grade crossing side impact test. After preparation, the test articles were instrumented and positioned for testing.

The preparation phase was followed by test execution, post-test data acquisition, and test documentation. The test data acquired during this phase were used to assess the quality of pre-test models.

The modeling team developed two different models. A lumped-parameter MBD model was developed to represent the essential features of the impact using highly simplified geometry and inertial properties for the various bodies (e.g., locomotives, tender, dump truck, track structure). This model ran in a few minutes on a desktop computer and was used to quickly evaluate the relative significance of parameters as the test setup was developed.

The team also developed and executed a highly detailed FE model that included the locomotives, tender, dump truck, and track structure. This model featured detailed geometry for each body, nonlinear material properties, representations of the LN2 and gaseous nitrogen (GN2) filling the tender, and numerous linear and non-linear interactions (e.g., contact, constraints, and

connectors) between various parts of the model. The FE model ran for several days on a dedicated high-performance server; only a limited number of simulations could be run prior to the test.

## 1.4 Scope

The scope of the research included the following:

- Cryogenic tank car design requirements applicable to LNG fuel tenders and the unique features of such cars
- Analyses and test results for a highway-grade crossing impact between a dump truck and an LNG fuel tender
- Setup, execution, and results of the test
- The development and execution of models used in this project
- Modeling the LNG fuel tender steels, modeling the cryogenic liquid within the tank, and modeling the gas phase outage within the LNG fuel tender
- Overall results of the test and discussions of the pre-test modeling activities and post-test modeling adjustments
- Comparison of the test measurements and the model results

## 1.5 Organization of the Report

- Section 1 of this report includes the introduction and a description of the objectives, scope, and organization of the report.
- Section 2 describes the test environment and the development of the highway-grade crossing impact test setup.
- Section 3 describes the instrumentation used during the test and its placement. This description includes a discussion of the cameras used to capture the impact event.
- Section 4 presents the results of the test. These results include a summary of the measured test data.
- Section 5 describes the development and execution of the FE and lumped-mass models.
- Section 6 contains a comparison of the test results and measurements with corresponding results from the models.
- Section 9 summarizes the research conclusions.
- Section 10 contains a list of the references made in this report.

Several appendices are included in a separate document:

- Appendix A describes the camera and target positions used in the test.
- Appendix B presents all the measured data.
- Appendix C describes the design of the dump truck's suspension components.

- Appendix D describes the modeling of the tender's carbody.
- Appendix E describes the modeling of the three-piece freight trucks.
- Appendix F describes the modeling of the rail and track structures.
- Appendix G describes the outage volume and pressure calculations used to model the liquid and vapor within the tank.
- Appendix H presents the pre-test FE model results.
- Appendix I presents the pre-test multi-body dynamics model results.
- Appendix J describes the details of data processing the tie displacement measurements.
- Appendix K describes the detailed dump truck model development.

# 2. Test Development

Planning for and developing the fuel tender grade crossing impact test required the construction of a fuel tender, design and construction of track structures, and development of a test implementation plan. While the existing M-1004 standard described the impact scenario and conditions for the impact, numerous interpretations, simplifications, and alterations were made to safely implement a full-scale, physical impact test. This chapter documents the development of the test article (i.e., LNG fuel tender), how the test conditions met the conditions laid out in M-1004, and when necessary, how the test conditions varied from conditions specified in M-1004.

## 2.1 LNG Fuel Tender

M-1004 contains design specifications for several potential tender styles. Tenders constructed according to M-1004 may carry fuel in either liquefied or compressed gas states and may be constructed like a tank car (i.e., the fuel tank is integrated within the carbody structure), like an intermodal car (i.e., the fuel tank can be removed from the carbody), or with a carbody enclosing the fuel tanks. The test described in this report used a tank car-style tender, so the discussion in this section will focus on that tender's design features.

### *2.1.1 Design Features*

The tender used in this test was designed and constructed to transport cryogenic LNG. It featured a 5/8-inch-thick inner tank made from ASTM A240 Type 304 stainless steel, an annular space containing multi-layer insulation (MLI) and held under vacuum, and a 3/4-inch thick outer jacket made from AAR TC128-B carbon steel. A DOT-113C120W9 tank car designed to transport LNG in commerce features similar construction using similar materials but is only required to have a 3/16-inch thick inner tank and 9/16-inch thick outer tank[2].

While a fuel tender may resemble a tank car, a tender differs from a tank car in several significant ways. A tank car will typically not be placed adjacent to an occupied locomotive, while a tender must be coupled directly to the locomotive(s) it is fueling. A tender features a continuous through sill between the couplers at both ends that is designed to carry the in-train longitudinal forces that develop during operations. A tender must also feature piping, valves, and other specialized equipment to allow fuel to flow between the tender and the locomotive. M-1004 requires that this plumbing, which is pressurized and contains fuel during operations, is contained within a protective housing to reduce the likelihood of fuel loss during an impact. Finally, the amount of fuel contained within the tender will vary during the trip as fuel is consumed by the locomotive(s). The mass of fuel within the tender will decrease, while the volume of the outage (i.e., the space occupied by vapor above the liquid level) will increase as fuel is consumed.

[2] At the time the tender grade crossing test was conducted, LNG was authorized to be transported via DOT-113C120W9 tank cars. A notice of proposed rulemaking (NPRM) was subsequently issued to suspend the transportation of LNG via tank cars (86 FR 61731). A Final Rule suspending the transportation of LNG via tank cars was published on September 1, 2023 (88 FR 60356).

### 2.1.2 Static Load Requirements

Chapter 11 of M-1004 contains "Crashworthiness Requirements" for a fuel tender, including the grade crossing impact scenario evaluated in this test. A tender designed to meet M-1004 has the option of complying with the dynamic grade crossing impact scenario, or, alternatively, complying with prescribed static load cases. The grade crossing impact scenario is an evaluation of the protective housing around the piping and valves. M-1004 contains alternative static loads that would also act on the protective housing. Development of the static load requirements and the grade crossing impact scenario were previously documented in a report to the AAR [3].

The tender used in the grade crossing impact test was designed using M-1004's static load requirements. While not the primary objective of the test, the results of the test provided additional insight into whether the static design loads were sufficient to resist dynamic impact forces from the accident scenario.

## 2.2 Test Conditions Specified in M-1004

The M-1004 standard provides a set of requirements to simulate a grade crossing impact and demonstrate the structural integrity of an LNG fuel tender and the survivability of its valves. To ensure the collision scenario is evaluated consistently by different entities at different times, M-1004 contains specific requirements on the lading and outage conditions, the equipment (e.g., vehicles) involved in the collision, and the parameters of the impact. Each of those areas is described in the subsequent sections.

### 2.2.1 Lading and Outage

Chapter 11.7.1.1 of AAR M-1004 contained the lading and outage initial conditions for the dynamic impact scenario. Prior to the test, the value given in M-1004 for initial vapor pressure was changed. Additionally, the team planned to use LN2 rather than LNG within the tender for the actual full-scale test, necessitating additional changes. The three sets of parameters are summarized in Table 1.

**Table 1. Lading and Outage Properties in M-1004 and Test**

| Parameter | Value in M-1004 (2020) | Proposed New Value in M-1004 (2021) | Actual Test Condition |
|---|---|---|---|
| Commodity in Tank | LNG | LNG | LN2 |
| Minimum Outage (% by volume) | 15% | 15% | 36 in H2O (55%) |
| Initial Vapor Pressure (psig) | 150 (1.034 MPa) | 25 (0.172 MPa) | 25 (0.172 MPa) |
| Initial Vacuum Pressure (psia) | 0 (perfect vacuum) | 0 (perfect vacuum) | <100 micron |
| Inner Tank Temperature (°F) | -260 (111 K) | -260 (111 K) | ≤ -304.5 (86 K) |

The test conditions were chosen to match the proposed new values in M-1004 as closely as possible. However, while LNG and LN2 are both cryogenic liquids, there are several important physical differences between them that affected the test setup. M-1004 prescribed an initial pressure (25 psig) and temperature (-260 °F) for the liquid within the tank. However, LN2 cannot exist as a liquid at that pressure and temperature. The test team decided it was more important to

match the initial pressure given in M-1004, since pressure could influence the apparent stiffness of the inner tank. This decision resulted in an inner tank that would be colder than prescribed in the standard.

Additional details on the volume calculations are provided in Appendix G. Atmospheric pressure was assumed to be 12.3 psia [4] based on Pueblo, CO's altitude of approximately 4,700 feet [5]. Under saturation conditions (25 psig, -304.5 °F), LN2 has a density of 764.1 kg/m$^3$ [6]. At the conditions given in M-1004, LNG has a density of 423.6 kg/m$^3$. This left the test team with two options for filling the tank with LN2 at 25 psig. M-1004 gives a minimum initial outage value, which corresponds to a particular mass of LNG based on the volume of the tank. Using LN2, the tank could either be filled to match the equivalent *volume* of LNG that would be carried under M-1004's conditions, or to match the equivalent *mass* of LNG that would be carried under M-1004's conditions. In an impact test to a DOT-113 cryogenic tank car conducted by FRA several months prior to the tender grade crossing test, LN2 was used to fill the tank car to a similar volume as that used in service [7]. However, volume-matching was chosen in that test because the large deformation of the DOT-113 tank under the impact would be substantially affected by the initial outage. Preliminary FE modeling in this research showed that the inner tank would experience very little deformation during the grade crossing impact. Additionally, matching the volume of LNG with LN2 results in a substantially additional mass of lading. Since the grade crossing impact scenario was expected to result in significant roll of the tender, having a larger mass of liquid in the tank than normal operations could exacerbate the roll issue. Thus, the test team chose to fill the tender with a mass of LN2 that corresponded to the mass of LNG that would be carried under the conditions prescribed in M-1004. This resulted in a filling level of approximately 45 percent of the tender's volume, leaving a 55 percent outage volume. The liquid height gauge was used to monitor the filling of the tender, with a target value of 36 inches of water corresponding to the target filling volume (refer to Figure 10 in Section 2.3.2).

Additionally, M-1004 stated that a perfect vacuum was to be assumed for the annular space between inner tank and jacket. While this is possible in a numerical simulation, in a physical test a perfect vacuum is not attainable. A vacuum of < 100 micron was targeted for the test. This simplification was not expected to have a significant effect on the impact response of the tank during the test.

### 2.2.2 Equipment

M-1004 describes the rail and highway vehicles used in the impact scenario. The tender undergoing evaluation is to be coupled to two 6-axle freight locomotives. This arrangement is meant to represent typical freight operations using a fuel tender simultaneously providing fuel to two locomotives. The tender is to be struck by a highway vehicle with a mass and impact velocity as described in the subsequent section. The details of the tender itself (e.g., dimensions, weight, piping arrangement, etc.) will vary from design-to-design and are to be determined by its manufacturer. M-1004 further states that FE models of the locomotives and highway vehicle can be provided by the AAR to an entity evaluating a tender according to the standard.

### 2.2.3 Impact Parameters

Table 2 summarizes the impact parameters used in the grade crossing side impact test of the LNG fuel tender. The parameters were chosen based on Chapter 11.9.1 of M-1004.

**Table 2. Summary of Impact Parameters**

| Parameter | Value |
|---|---|
| Highway Vehicle Type | Dump Truck |
| Highway Vehicle Weight | 80,000 lbf |
| Highway Vehicle Speed | 40 mph |
| Impact Location | Center of Protective Housing |

Chapter 11.9.1.1 of M-1004 states, "The tender shall be stationary on the grade crossing coupled between two locomotives. The tender shall be impacted by a single-frame vehicle weighing 80,000 lbf, at an area between body bolsters at the center of a section of a side protective housing structure nearest the center of the tender" [1]. A dump truck was chosen as the impact vehicle, ballasted to 81,350 lbf, and the target impact location was centered on the protective housing.

Chapter 11.9.1.2 of M-1004 states, "The speed of the [highway] vehicle at moment of impact shall be 40 mph. The track in the grade crossing shall be assumed tangent and level. The highway leading into the grade crossing shall be level, at 90° to the track and at the height of the top rail" [1]. The test setup was designed to place the top surface of the running rail of the track upon which the dump truck was traveling, at the same height as the top of the rails on which the tender and locomotives were standing. The target speed for the dump truck was chosen to be no less than 40 mph at the time of impact. While an overspeed impact could cause damage that would not have resulted from a 40-mph impact, an underspeed impact would not provide confidence that the tender met the requirements of M-1004. If the impact occurred at more than 40 mph and the tender met the criteria of M-1004, then the tender design would have been shown to be even more resilient than required by the standard.

## 2.3 Test Conditions Not Specified in M-1004

The M-1004 specifications provide a set of requirements to simulate a grade crossing impact and evaluate the structural integrity of an LNG fuel tender and the survivability of its valves. These specifications provide a broad overview of the impact scenarios with some details related to the placement of the tender between two locomotives, the speed and weight of the single-frame highway vehicle, and the layout of the crossing. The modeling setup as specified in M-1004 is shown in Figure 1. The modeling conditions required the single-frame vehicle to weigh 80,000 lbf and impact the tender at 40 mph.

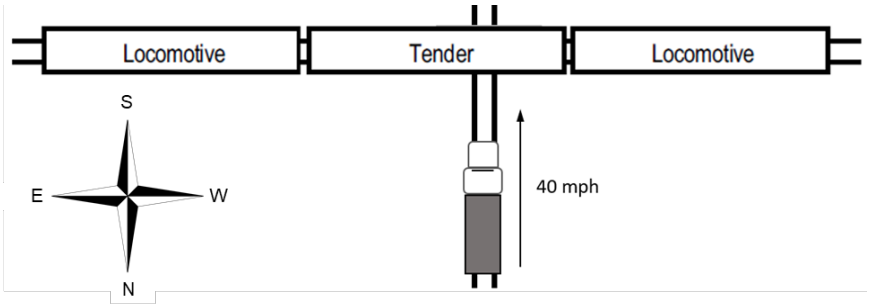


**Figure 1. Highway-Grade Crossing Impact Specified in M-1004 for Modeling and Adapted for the Test [1]**

However, the M-1004 specifications were focused on modeling, and the test setup and impact test described in this report were developed to emulate the modeling conditions. There were key test parameters that needed evaluation that were not fully addressed by the specifications before the test setup was finalized. The following section describes the key components and parameters required for a physical test.

### 2.3.1 Dump Truck as the Single-Frame Vehicle

M-1004 specifications require a single-frame vehicle to impact the fuel tender. A 1994 FLD 120 dump truck was selected as the single-frame vehicle for testing (Figure 2). The test conditions would result in a severe impact, necessitating a vehicle trajectory that would have to be controlled externally. In a modeling environment, the trajectory of the vehicle can easily be controlled, but during the test, control of the vehicle's trajectory is much more difficult and complex. Additionally, the M-1004 specifications provided a target test speed of 40 mph for the impact so the velocity of the dump truck needed to be controlled precisely for the test.

The test team considered several potential techniques for achieving this control. Researchers explored the installation of remote-controlled actuators to steer and accelerate the dump truck via radio signal which allowed a human controller to make corrections to either the velocity or the trajectory prior to impact. This also offered the most realistic situation because the dump truck required minimum structural modification to accommodate the remote-controlled setup. However, the team abandoned this approach due to the following three challenges.

1. If researchers drove the dump truck remotely, the engine would need to be running during the test, which required the truck engine to be loaded with a full complement of fluids, including diesel fuel. This situation could have led to a potential environmental and/or safety hazard following impact.
2. Because the dump truck load would equal 80,000 lbf (per M-1004), the test team anticipated a longer stretch of straight paved roadway was needed to reach an impact speed of 40 mph than was available.
3. As is typical of most heavy trucks, the dump truck used in this test featured a manual transmission, greatly increasing the complexity of a remote-driving setup. Therefore, given the uncertainties of developing a remote-driving setup and the fact that there would only be one opportunity to run the test, the team sought a more reliable method of controlling the velocity and trajectory of the dump truck.

A second concept involved keeping the dump truck on its own wheels but using a separate vehicle to increase its speed to 40 mph. This concept would allow the team to drain the fluids from the dump truck prior to the test, thereby removing the environmental and safety hazards. Directing the trajectory of the truck, however, would still require either a remote-controlled steering wheel, a guideway, or another similar setup to ensure the dump truck struck the tender at the desired location. Like the remote-driven dump truck, a dump truck propelled externally would still require a flat, straight section of pavement for the dump truck to travel on to the point of impact. While the dump truck could have been "shoved" up to speed by a second vehicle while being allowed to roll on its own tires up to the tender, the substantial rolling resistance of rubber tires on pavement was expected to result in a substantial decrease in speed between the point of separation with the powered vehicle and the point of impact. Again, given the need to hit

the tender at a precise location and at 40 mph, shoving the dump truck up to speed on its own tires was thought to present a high risk of an unacceptable impact condition.

The team also considered the option of using a cable to pull the dump truck up to speed, as opposed to pushing it up to speed and allowing it to coast. The use of a cable to pull the dump truck would allow researchers to control the velocity up to the point of impact. However, it would also require a way to remotely steer the truck or provide a guideway to control the truck's trajectory, a long stretch of paved road leading up to the point of impact, and a suitable towing vehicle or piece of equipment capable of accelerating the 80,000 lbf dump truck up to a minimum of 40 mph in a distance shorter than the length of the paved road.

The team instead chose to use a dump truck converted for use as a high-rail vehicle (see Figure 2). With the dump truck modified to roll on two railroad wheelsets on existing track, the dump truck's trajectory could be effectively controlled by the railroad tracks on which it traveled. The anticipated low rolling resistance between the steel wheels and the steel rail would allow the dump truck to be "shoved" up to speed by a locomotive before it coasted into the point of impact with the tender. The dump truck would run on an existing track at TTC, while the locomotives and fuel tender would be positioned stationary at a 90-degree angle to the dump truck (as shown in Figure 3).

**Figure 2. Side and Front View of the 1994 FLD 120 Dump Truck**

**Figure 3. Oblique View of Dump Truck Aligned at the Impact Point with the Tender**

An assessment of the rail performance and stability of the dump truck fitted only with the wheelsets as it traversed the track was performed in NUCARS®.[3] The NUCARS assessment determined that additional suspension between the dump truck body and the wheelsets would be required to ensure the adequate performance and stability of the dump truck. Truck leaf springs were selected as the suspension type and the railway wheelsets were redesigned to connect to the dump truck body through the leaf spring assembly. A three-dimensional representation of the suspension assembly is shown in Figure 4, and the final assembly, as fitted to the dump truck, is shown in Figure 5. Figure 6 shows the dump truck as fitted with the railway wheelsets and suspension. This figure shows that the bottoms of the tires on the dump truck were located just above the top of the rail. The details of the NUCARS assessment and the suspension design can be found in Appendix A.

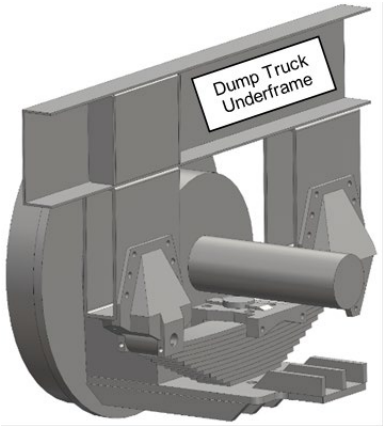


**Figure 4. Sectioned View of Suspension Attachment Between the Railway Wheelset and Dump Truck Underframe**

**Figure 5. Structural Attachment Between Railway Wheelset and Dump Truck Body**

[3] NUCARS® is a registered trademark of Transportation Technology Center, Inc.

**Figure 6. Dump Truck Fitted with the Leaf Spring Suspension and Railway Wheelset**

After the suspension was fitted the team loaded the dump truck with steel weights to increase its gross weight to 80,000 lbf, as specified in M-1004. The weights were secured to the bed of the dump truck to limit their movement during impact. The arrangement of the weights and restraining system is shown in Figure 7. The final gross weight of the dump truck was 81,350 lbf.

**Figure 7. Arrangement of the Dump Truck Bed Loaded with Weights and Restraining System**

The impact scenario was designed to transfer all the kinetic energy of the dump truck along its rolling direction to the LNG tender. However, the strength of the structural connection between the dump bed and the underframe was unknown. During the pre-test modeling of the impact event, it appeared possible that the dump bed could separate from the underframe and rotate around the cab of the dump truck before impacting with the LNG fuel tender. To increase the structural rigidity between the dump bed and its underframe, the dump bed was welded with 12-inch-long welds to the underframe. These welds were made to the front and the rear of the bed as shown in Figure 8. Damage to these welds and the dump bed during the test are discussed in Section 4.1.

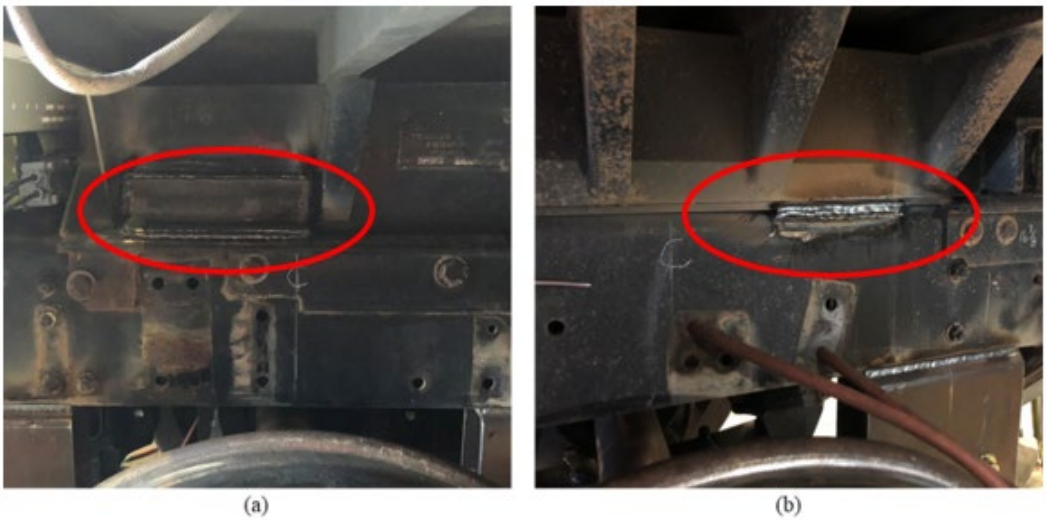


**Figure 8. Welds (circled in red) between the Dump Bed and Underframe at (a) the Front and (b) the Rear of the Dump Truck**

Speed upgrade tests were performed to determine that the dump truck, modified to roll like a hi-rail vehicle, could negotiate the test track safely at 40 mph. A brake system was designed and installed and the rear of the dump truck was fitted with a railway coupler to allow the truck to be hauled by a locomotive (Figure 9).

**Figure 9. Railway Coupler Fitted to Dump Truck**

After the speed upgrade tests were executed, the team found the dump truck was stable up to 50 mph and the performance of the vehicle was adequate for the test. These speed tests established that the dump truck was sufficient to act as the impact vehicle in the test setup. It could be pushed by a locomotive to reach the required 40 mph and then uncoupled from the locomotive and released at a set point on the test track. Further speed trials were performed to determine the release speed and the point of release.

### 2.3.2 LNG Fuel Tender

FRA procured an LNG fuel tender for the test that was designed and constructed according to the M-1004 specifications. The fuel tender was a tank-within-a-tank design with a 3/4-inch carbon steel outer tank and an inner tank made of 5/8-inch stainless steel. A vacuum was introduced in the annular space between the outer and inner tanks to insulate the inner tank which contained a cryogenic fluid from the outer tank that is usually exposed to ambient temperature. The fuel tender was designed to have a maximum water capacity of 29,926 gallons when filled to a 5 percent outage with LNG. The M-1004 requires the outage to be pressurized to 25 psig in the model with a minimum of 15 percent outage[4]. The empty weight of the fuel tender fitted with freight trucks was 197,325 lbf.

Since the test could not be executed with LNG due to safety and environmental concerns, the team used liquid nitrogen (LN2) as a surrogate cryogenic liquid. LN2 is inert and therefore does not present the same environmental hazards as LNG when released into the atmosphere, eliminating safety concerns. LN2 is denser than LNG, so researchers decided to fill the LNG fuel tender to the maximum weight capacity rather than the maximum volume capacity. This meant that only 13,123 gallons of LN2 was required for the impact test, which filled the tank to roughly 45 percent by volume[5]. This outage volume did not conform to the specifications; however, researchers were required to make some concessions since the test lading was LN2 as opposed to LNG. Filling the tank to 85 percent by weight with LN2 was deemed to be more representative of a tank filled to 85 percent by volume with LNG than a tank filled to 85 percent by volume with LN2. The test team determined that matching the inertia of an LNG-filled fuel tender was more important than matching the pressure-volume relationship inside the inner tank. As will be discussed in Section 5, the FE models predicted no change in inner tank volume during the test. This behavior also supported the decision to match the mass of LN2 to the mass of LNG that would be used in service, rather than filling the tank with LN2 to an outage of 15 percent.

There was no instrumentation to accurately determine the volume of LN2 in the tank. The pressure gauge that estimates the fill weight in inches of water was used to determine when the tank was filled with the adequate volume of LN2. To reach the required volume, the pressure gauge needed to reach 36 inches of water. The final pressure and fill volume are shown on the gauges in Figure 10.

[4] At the time test plans were originally developed, M-1004 required a 15 percent outage at 150 psig. The pressure was subsequently reduced to 25 psig prior to the test being conducted.

[5] The volume and outage percentages are based on an assumed LN2 filling pressure of 15 psig. The outage volume calculations in Appendix G [3] reflect the measured test pressure of 25 psig.

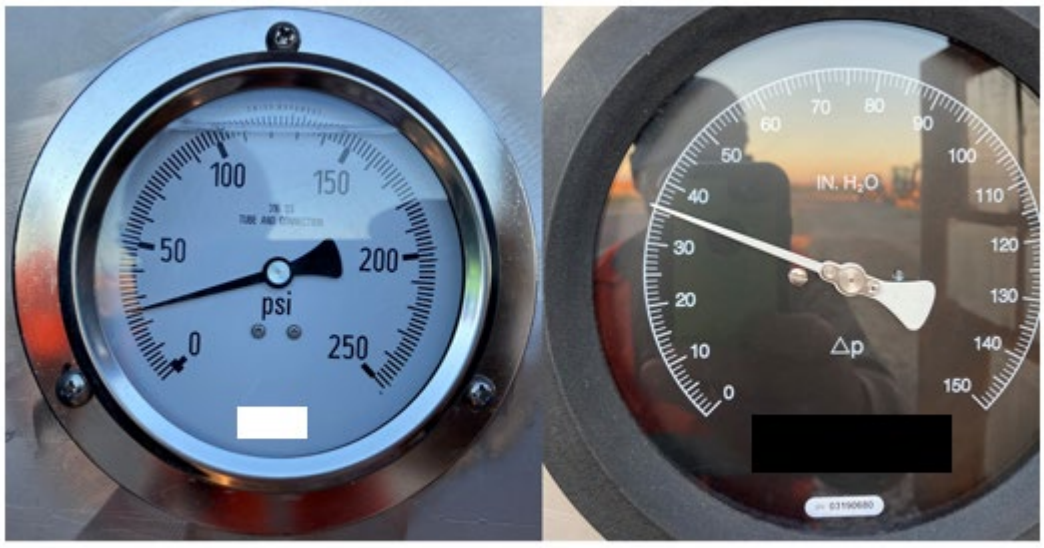


**Figure 10. (a) Pressure Gauge and (b) Inner Tank Fill Volume Related to Pressure in Inches of Water**

### 2.3.3 Locomotives

The research team used scrapped locomotives fitted with F-type couplers in testing; these served only as reaction masses in the test setup. Despite the possible influence on the restraint of the fuel tender during the test, M-1004 does not specify a required coupler type for the coupled locomotives, nor the locomotive weight. However, M-1004 does state that AAR will provide FE locomotive models to any applicant performing dynamic impact simulations following M-1004 standards. The locomotive models that were made available by AAR weighed 420,000 lbf. (The development of the models provided by AAR is documented in the Appendices.) When weighed on the scales at TTC, the locomotive on the east end of the setup (refer to Figure 1) weighed 363,000 lbf and the locomotive at the west end (refer to Figure 1) weighed 358,000 lbf, which is less than the locomotives in the AAR models. The team did not consider this a problem since the locomotives functioned as reaction masses on either side of the tender and the actual test locomotive weights were within 85 percent of the indicated weight. The locomotives were arranged in the typical configuration during operation with a fuel tender. Both F-ends were facing away from the tender.

### 2.3.4 Track

The test was designed to run the dump truck from north to south on the test track before impacting the fuel tender. A section of track running from east to west was constructed at a 90-degree angle to the existing test track. The locomotives and tender were staged on this section of track before impact. M-1004 does not specify either the track Class or the stiffness of the track in the vicinity of the level crossing; it only specifies that the track should be tangent and level. Additionally, it requires the highway leading into the level crossing be level and at the height of the top of the rail.

The test section of constructed track extended roughly 130 feet to each side of the center of the existing test track. The continuity of the track was broken and the section of track that was constructed was continuous from east to west. Class 3 American Railway Engineering and Maintenance-of-Way Association (AREMA) ballast was used for the ballast bed. Concrete ties supported the rails with a 24-inch center-to-center spacing. Secondhand 136RE rails and some 141RE rails were used in the track construction but brand new fasteners were used to clamp the rails to the ties. No measurements were taken to confirm the track Class, but the track was constructed and tamped to conform to FRA's Class 4 track specifications [8]. Figure 11 shows the section of track under construction.

**Figure 11. Track Section Under Construction (West View)**

Though all the test articles were constrained to running on rails, the test site was prepared for a level crossing impact. A level crossing surrogate, as shown in Figure 12, was constructed out of wooden ties to represent a typical level crossing that could be found in a rural setting.[6] The track construction was representative of typical track that could be encountered in service, along with a level crossing simply laid on top of the crossing and not adding any additional stiffness to the track.

[6] At the time test preparations were being made, AAR M-1004 did not provide any specific dimensions for the level crossing. Subsequently, AAR M-1004 was revised to include a width of the grade crossing based on a two-lane roadway with two shoulders, having a total width of approximately 48 feet.

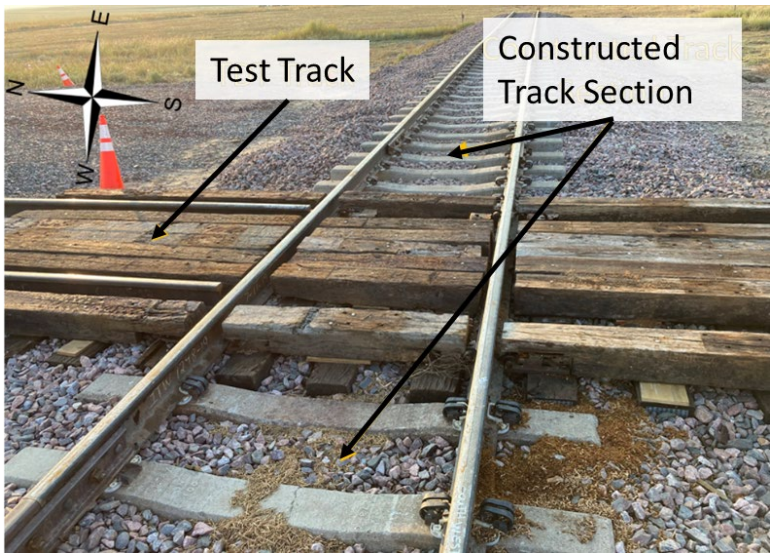


**Figure 12. Level Crossing Surrogate Constructed from Wooden Ties to Emulate a Grade Crossing**

### *2.3.5 Roll Inhibitor*

There remained a risk that the fuel tender could shift with or onto the freight trucks and roll over during impact. The objective of the test did not require an assessment of the structural integrity of the fuel tender in a dynamic rollover event since the objective of the test was mainly focused on the impact event and the first few seconds after impact. M-1004 does not limit rollover during the evaluation of the grade crossing impact scenario; however, during a full-scale test, rollover creates logistical challenges associated with cleaning up the site if the tender was on its side. A structure was constructed from railroad ties and soil to inhibit the fuel tender from fully rolling over after impact (see the two pyramidal mounds shown in white and grey in Figure 13). These structures were positioned in line with the body bolsters to inhibit excessive movement and body roll. The concept of these "roll inhibitors" and the fuel tender in its upright (red) and rolled (blue) conditions are shown in Figure 13. Figure 14 shows one of the roll inhibitors as constructed for the test.

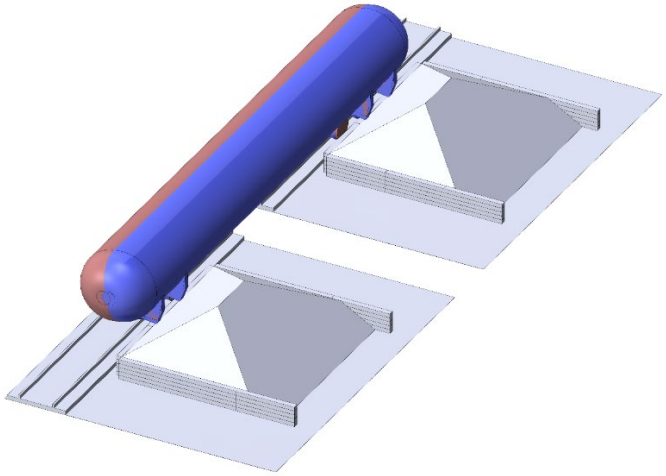

**Figure 13. Concept of Structure to Prevent Body Roll of the Fuel Tender after Impact**

**Figure 14. Roll Inhibitor Structure to Prevent Excessive Body Roll of the Fuel Tender after Impact**

### *2.3.6 Test Implementation*

The highway-grade crossing impact test was performed on September 22, 2021, at the TTC in Pueblo, Colorado. For the execution of the test, the locomotives were lifted onto the section of track and moved to either end. The fuel tender was lifted onto the track and positioned with the center of the protective housing in the center of the level crossing, as shown in Figure 15. The locomotives were coupled to the fuel tender and the couplers were forced into a draft condition. There were no brakes on the fuel tender, but the locomotives' hand brakes were set. Wedges were welded to the rails at the locomotive wheels closest to the tender to keep the locomotives from rolling closer to the fuel tender. The fuel tender was filled with LN2, and the dump truck was prepared for the test. The test arrangement is shown in Figure 16. Figure 17 displays the dump truck's position near the tender protective housing. An aerial view of the test setup with the locomotives, tender, and dump truck in their pre-test positions is laid out in Figure 18.

**Figure 15. Alignment of the LNG Fuel Tender Housing with the Center of the Track**

**Figure 16. Overview of Test Setup with Locomotives and Fuel Tender**

**Figure 17. Pre-test Test Setup with Dump Truck Close to the Housing of the Fuel Tender**

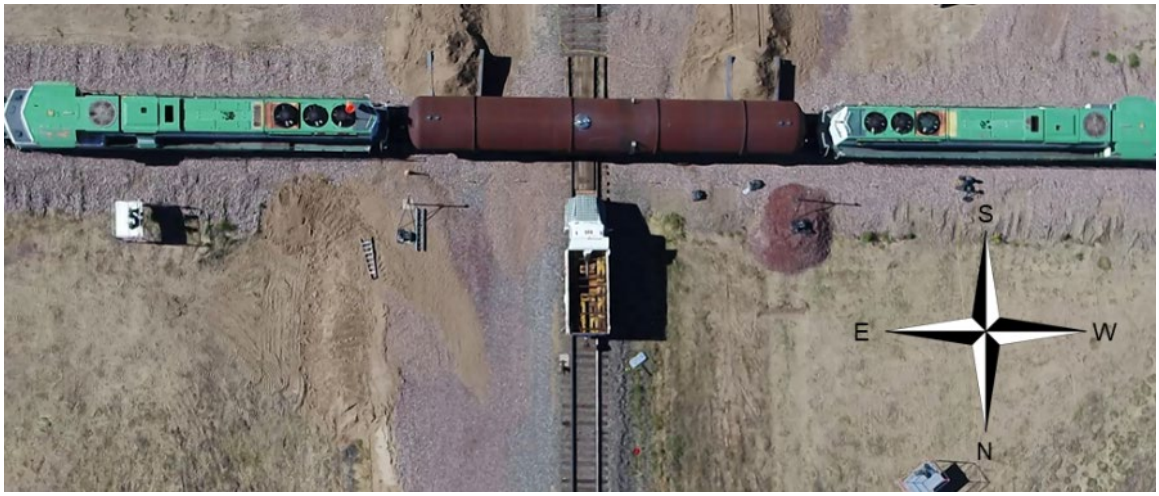


**Figure 18. Aerial View of the Test Setup with the Locomotives, Tender and Dump Truck in Position**

# 3. Test Instrumentation

To evaluate the crashworthiness of the protective housing surrounding the external piping and valves and the proper functioning of the cut-off valves, the team created an FE model of the grade crossing impact based on the setup discussed in Section 2. The team performed validation of this model to assess the suitability of the modeling requirements and modeling outcomes of the M-1004 specifications. The transducers that were used to collect data and the cameras used to record the impact are discussed in this section. The transducers measured the accelerations, displacements, speed, pressure, and position of the fuel supply valve. In total, 41 channels were recorded. The transducer types and counts along with the number of high-speed and high-definition cameras used in the testing are summarized in Table 3.

**Table 3. Summary of Transducers Used During the Impact Test**

| Type of Transducer | Channel Count |
|---|---|
| Accelerometers | 25 |
| String potentiometers | 10 |
| Speed sensors | 2 |
| Pressure transducers | 3 |
| Position indicator | 1 |
| **Total Data Channels** | 41 |
| High-speed cameras | 6 |
| High-definition cameras | 4 |

The coordinates X,Y, and Z are defined to be (i) in the direction of motion of the truck, (ii) normal to the motion of the truck, and (iii) vertical direction, respectively. Positive X, Y, and Z directions are forward, left (east), and up relative to the front end of the dump truck. Figure 19 shows the coordinate system of the test setup.

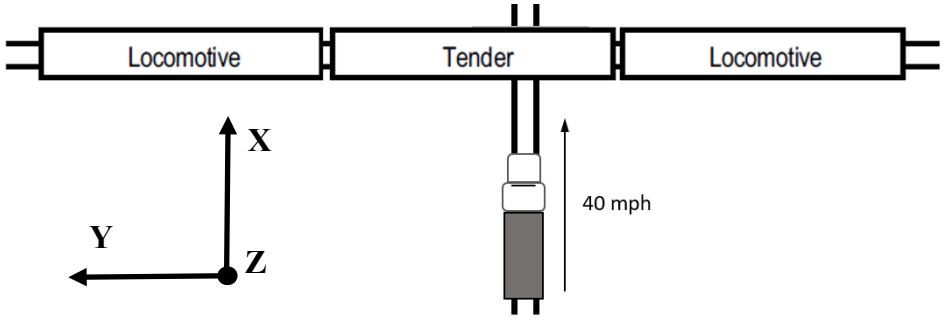


**Figure 19. Definition of the Coordinate System Used for the Test Instrumentation (Schematic Adapted from [1])**

## 3.1 Dump Truck Instrumentation

Accelerometers and string potentiometers were distributed throughout the dump truck to measure the accelerations and displacements at the ends, sides, and middle of the dump truck. These accelerometers had a typical scale factor calibration error of 2 percent. Table 4 summarizes the names, locations, and ranges of the various accelerometers mounted on the dump truck. Table 5

summarizes the names, locations, and ranges of the various string potentiometers mounted on the dump truck.

Redundant speed sensors measured the impact speed of the dump truck when it was within 20 inches of the impact point. The speed sensor used ground-based reflectors separated by a known distance and a vehicle-based light sensor that was triggered as the impacting vehicle passed over the reflectors. The last reflector was placed within 10 inches of the impact point. The interval that passed while the dump truck traveled between the reflectors was recorded so the speed could be calculated from distance and time. A backup speed measurement was taken with a handheld radar gun. The two channels of the speed sensors were named BSPDL and BSPDR.

Figure 20 shows the locations of the accelerometers, string potentiometers, speed sensors, data acquisition DataBRICK (DB) units, multiple trigger units (MTU), and the flash mounted on the dump truck.

**Table 4. Name, Location and Range of Accelerometers Mounted on the Dump Truck**

| Channel Name | Description of Location | Range (g) |
|---|---|---|
| VCTFX | Center of top of engine - longitudinal | 400 |
| VCBFX | Center of bottom of engine - longitudinal | 400 |
| VCTMX | Center of bottom of transmission - longitudinal | 400 |
| VCPX | Center of vehicle below piston - longitudinal | 400 |
| VLFX | Eastern C-channel above front tire - longitudinal | 400 |
| VLFZ | Eastern C-channel above front tire - vertical | 200 |
| VRFX | Western C-channel above front tire - longitudinal | 400 |
| VRFZ | Western C-channel above front tire - vertical | 200 |
| VCMX | Top of rear transverse C-channel - longitudinal | 400 |
| VLMX | Eastern side of rear transverse C-channel - longitudinal | 400 |
| VLMY | Eastern side of rear transverse C-channel - lateral | 200 |
| VLMZ | Eastern side of rear transverse C-channel - vertical | 200 |
| VRMX | Western side of rear transverse C-channel - longitudinal | 400 |
| VRMY | Western side of rear transverse C-channel - lateral | 200 |
| VRMZ | Western side of rear transverse C-channel - vertical | 200 |
| VCBX | Back plate for hitch attachment - longitudinal | 400 |
| VCBY | Back plate for hitch attachment - lateral | 200 |
| VCBZ | Back plate for hitch attachment - vertical | 200 |
| VCGX | Center of gravity of vehicle on dump bed - longitudinal | 400 |
| VCGY | Center of gravity of vehicle on dump bed - lateral | 200 |
| VCGZ | Center of gravity of vehicle on dump bed - vertical | 200 |
| VRACFX | Center of structure below railway axle at the front - longitudinal | 400 |
| VRACFZ | Center of structure below railway axle at the front - vertical | 200 |
| VRACBX | Center of structure below railway axle at the rear - longitudinal | 400 |
| VRACBZ | Center of structure below railway axle at the rear - vertical | 200 |

**Table 5. Name, Location and Range of String Potentiometers Mounted on the Dump Truck**

| Channel Name | Description of Location | Range (inch) |
|---|---|---|
| VUL1X | Eastern C-channel at front end - longitudinal | +5/−45 |
| VUR1X | Western C-channel at front end - longitudinal | +5/−45 |
| VUL2X | Eastern C-channel 2-ft from front end - longitudinal | +5/−45 |
| VUR2X | Western C-channel 2-ft from front end - longitudinal | +5/−45 |

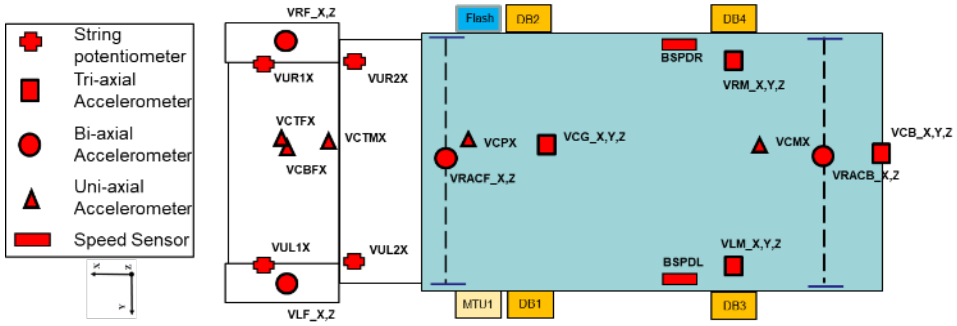


**Figure 20. Top View of Dump Truck Showing Location of the Various Transducers**

## 3.2 LNG Fuel Tender Instrumentation

The LNG fuel tender was instrumented with string potentiometers, pressure transducers, and a system to capture the operation of the fire block (FB) valve. The FB valve allows LNG fuel flow to the two locomotives when opened. The valve's state is controlled by a pneumatic actuator that allows the valve to open when air pressure is supplied to the actuator. In the event of an accident, the air pressure to the pneumatic actuator is released and the valve closes, preventing any release of fuel through the supply line. For the test, a pneumatic supply system was set up to open and close the FB valve remotely. This system comprised roughly 400 feet of hose running to the FB valve from a pressurized air tank far removed from the impact site. Once the impact occurred, the air was drained from the hose to close the valve. An optical sensor, with the channel name REFL, was mounted on the center sill to determine the state of the FB valve. The sensor was connected in such a fashion that it would give a value of zero volts when the valve was in the open position and approximately −3.5 volts when in the closed position. Table 6 and Table 7 summarize the names, locations, and ranges of the string potentiometers and pressure transducers fitted to the LNG fuel tender. Figure 21 shows the locations of the string potentiometers, pressure transducers, and DBs fitted to the LNG fuel tender.

**Table 6. Name, Location and Range of String Potentiometers Mounted on the LNG fuel tender**

| Channel Name | Description of Location | Range (inch) |
|---|---|---|
| TVLX | Valve protective housing – East | +1/−9 |
| TVRX | Valve protective housing – West | +1/−9 |
| TCLY | Eastern locomotive-to-tender coupler | +10/−10 |
| TCRY | Western locomotive-to-tender coupler | +10/−10 |
| TLHX | Eastern head of tender | +5/−45 |
| TRHX | Western head of tender | +5/−45 |

**Table 7. Name, Location and Range of Pressure Transducers Mounted on the LNG fuel tender**

| Channel Name | Description of Location | Range (psig) |
|---|---|---|
| TTPBV5 | Before FB valve | 0–250 |
| TTPAV5L | After FB valve on the western pipe | 0–250 |
| TTPMW | Manway pressure | 0–250 |

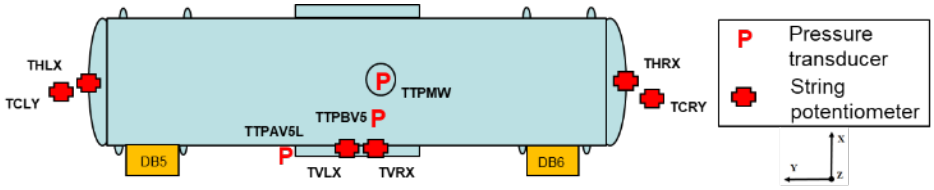


**Figure 21. Top View of LNG Fuel Tender Showing Location of the Various Transducers**

## 3.3 Real-Time High-Speed and High-Definition Photography

High-speed and real-time high-definition video cameras documented the impact. All the high-speed cameras were crashworthy and rated for peak accelerations of 100 g. The locations and views of the various cameras together with the grid applied to the hood of the dump truck are described in Appendix B.

## 3.4 Data Acquisition

Several 8-channel, battery-powered, on-board data acquisition systems recorded the test data from instrumentation mounted on the dump truck and the LNG fuel tender consist. These systems provided 1) excitation to the instrumentation, 2) analog anti-aliasing filtering of the signals, 3) analog-to-digital conversion, and 4) recording of each data stream.

The data acquisition systems were GMH Engineering DB units. Data acquisition complied with the appropriate sections of SAE J211 [9]. Data from each channel was anti-alias filtered at 1,735 Hz then sampled and recorded at 12,800 Hz. Each DB was ruggedized for shock loading up to at least 100 g. The on-board battery power was provided by GMH Engineering 1.7 Amp-hour 14.4 Volt NiCad Packs. The data recorded on the DBs was synchronized to have the time of zero seconds at initial impact. The time reference was derived from the closure of the tape switches on the front of the dump truck and the LNG fuel tender. Tape Switches, Inc., model 1201-131-A tape switches provided the initial contact trigger. The alignment of the tape switches is shown in Figure 22.

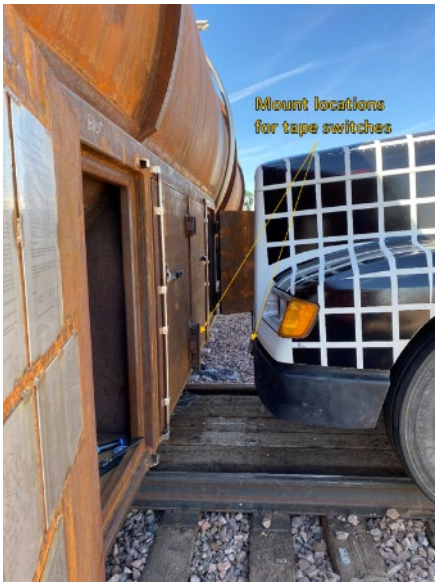


**Figure 22. The Dump Truck in Proximity to the LNG Fuel Tender Showing the Mount Locations of the Tape Switches**

Rather than relying on set gains and expecting no drift, the software in the DBs was used to determine zero levels and calibration factors. The DBs on the dump truck were set to record one second of data before the initial impact and seven seconds of data after the initial impact. The DBs mounted on the LNG fuel tender were set to record one second of data before the initial impact and at least thirty seconds of data after the initial impact.

## 3.5 Track Shift

The connection of the rails to the ties and the ties to the ground is one of the model parameters mentioned but not well defined in M-1004. In the test, flexible rail fasteners were used to connect the rails to the ties and Class 3 AREMA ballast was used to construct the track bed. Additionally, a small marker was placed on the northern edge of each tie to assist in measuring displacement between pre-test and post-test tie positions. The movement of the ties relative to fixed ground points was measured before and after the impact to assess the track shift that occurred during the impact. Figure 23 shows one such fixed measurement point represented by rebar driven into the ground. Additionally, point clouds of the test area were produced before and after the impact using a drone-based system. The displacement of each tie marker during the test was approximated by post-processing the pre- and post-test drone scan data as described in Appendix J.

**Figure 23. Fixed Measurement Point used to Assess Track Shift After the Impact**

## 3.6 Data Post-Processing

Each data channel was offset adjusted in post-processing. The offset adjustment procedure ensures that the plotted and analyzed data contain only impact-related accelerations and exclude electronic offsets or steady biases. The data collected from the 0.55 second just prior to impact was averaged together to determine the necessary offset. This offset was subtracted from the entire dataset for each channel except for the pressure transducer channels. This post-test offset

adjustment was independent of, and in addition to, the pre-test offset adjustment made by the data acquisition system.

According to the requirements of SAE J211 [9], only the acceleration data recorded during the impact was filtered using a CFC60 filter. Post-test filtering of the data was done with a two-pass phaseless four-pole digital filter algorithm consistent with the requirements of SAE J211 [9]. During this process, the data was first filtered in the forward direction with a two-pole filter. The first pass of the filtering process introduced a phase lag in the data. In the next pass, the data was filtered in the reverse direction with the same filter. This pass introduced a phase lead into the data, and this phase lead canceled the phase lag from the forward-direction filtering, resulting in data filtering done with a four-pole filter without the introduction of a phase change. The video data was kept in its native uncompressed formats and then converted to an .mp4 format.

# 4. Impact Test Results

The highway-grade crossing impact test between a single-frame highway truck and an LNG fuel tender was conducted on September 22, 2021, at the TTC in Pueblo, CO. The impact speed of the dump truck was measured at 42.6 mph before the impact. The following section describes the condition of the dump truck and LNG fuel tender after the impact and the most relevant measurements taken during the impact.

During the impact, the dump truck was shortened in length by about 12 feet. The tender protective housing, a protective compartment around the primary valves, was not compromised. The housing doors were able to operate post-impact and the valves were confirmed to be functioning properly.

Upon impact, the tender began to roll and shift. One of the two rails beneath the tender and locomotives rolled from the lateral load applied by the tender's wheels and the ties shifted laterally. These measurements were captured with instrumentation, videos, and photographs. The tender's couplers experienced roll and yaw and plastically deformed but did not break. The coupled locomotives shifted due to the track shift but all three vehicles in the consist remained upright.

Figure 24 shows still photos before and during the impact, captured by a drone positioned above the impact point. The cloud observable in the third frame is dust, not released LN2.


(1) (2) (3)

**Figure 24. Still Photos from the Drone Camera Showing: 1) the Dump Truck Traveling at 42.6 mph just Prior to Impact, 2) the Dump Truck Front End Crushed, 3) the Train Consist Displacement**

## 4.1 Post-impact Condition of Dump Truck

The kinetic energy of the dump truck was calculated to be 4.94 million foot-pounds (ft-lbf). The main components of the dump truck capable of energy absorption were the dump truck cab, underframe, and bed. The cab was constructed mainly from fiberglass with some structural steel and the underframe of the truck consisted of two C-channels interconnected by cross members. For the test, the dump bed was loaded with steel weights, increasing the structural rigidity of the truck bed. Figure 25 shows the condition of the dump truck before and immediately after the impact. Most of the dump truck cab was destroyed, and some components, such as the seats, were compressed against the rear of the cab. The C-channel forming the underframe peeled back above the front tire of the dump truck. The rear railway wheel of the dump truck derailed.

**Figure 25. Pre- and Post-Test Condition of the Dump Truck**

The dump bed remained largely intact, and it, along with the underframe, moved as a self-contained unit for most of the impact. The dump bed separated from and slid on the underframe during the impact. The welds that were shown in Figure 8 and the welds between the dump bed's hinges all failed during the impact. Some of the weld failures are shown in Figure 26. The weights and their restraining system functioned as expected with the weights remaining attached to the dump bed and the restraining beams deforming, which allowed the weights and the dump bed to slide as a unit. The weights and restraining system can be seen in their post-impact condition in Figure 27. When the bed was removed from the dump truck during test site cleanup, researchers noted that the engine had pushed the piston used to tip the dump bed into the recess

of the bed. The engine moved into the bottom part of the recess and under the weight closest to it.

(a) (b)

**Figure 26. Failed Welds Between Dump Bed and Underframe at (a) the Rear Hinges and (b) the Angle Iron Shown in Figure 8(a)**

**Figure 27. Condition of the Weights and Restraining System Post-Impact**

## 4.2 Post-Impact Condition of the Track

The track was not the main concern during impact. The track experienced two failures simultaneously: it shifted laterally on the ballast bed (Figure 28), and the rail on the opposite side of the struck housing rolled over (Figure 29).

**Figure 28. Track Shift on Ballast Bed**

(a) (b)

**Figure 29. Rolled Rail Under (a) the East-side Locomotive and (b) the South-side LNG Fuel Tender Housing (Non-impacted Side)**

The track shift was recorded manually at several of the ties and calculated for all visible ties using the point clouds obtained from drone scans. The lateral tie displacement along the section of track below the eastern locomotive is shown in Figure 30. While lateral tie displacement was obtained from both manual measurements and the pre- and post-test point clouds, longitudinal and elevational tie displacement data was obtained using the point cloud position changes only. It should be noted that positive values indicate a displacement toward the south (i.e., the direction in which the dump truck was running before the impact). Negative displacements indicated a displacement in the opposite direction (i.e., toward the dump truck). The protective housing was not located in the exact center of the tender, and, after impact, the tender was offset toward the

east. It should also be noted that there is strong correlation between the lateral tie displacements measured manually and the lateral tie displacements calculated from the point clouds. This indicates that for this scenario, tie displacements measured from scans are sufficiently precise to be used in place of those measured manually, as well as in locations where tie displacements were not measured manually. The highest lateral tie displacement was recorded below the truck of the eastern locomotive closest to the tender, followed by the freight trucks of the fuel tender. There was effectively no tie displacement at either end of the consist at the F-end trucks of the locomotives.

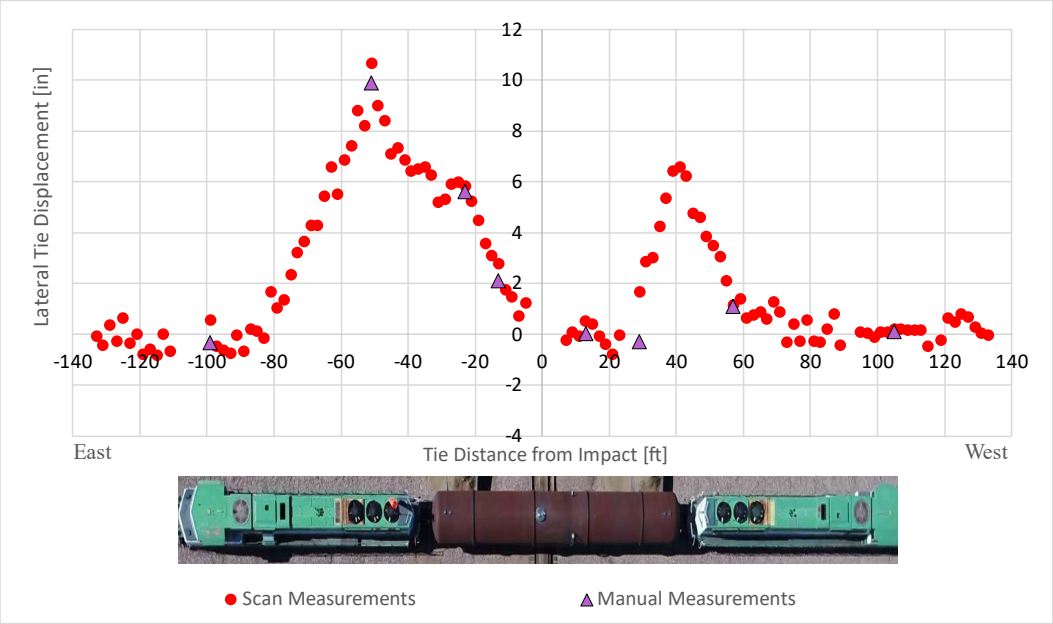


**Figure 30. Lateral Tie Displacement Along the Section of Track with the Overhead Picture of the Test Setup Aligned with the Plot to Provide Scale and Positioning**

## 4.3 Post-impact Condition of LNG Fuel Tender

The fuel tender was evaluated for damage post-test and the valve system that would cut off any supply of fuel to the locomotives was assessed. Additionally, the exterior tank, the interior tank, and the protective housing were assessed. A reading of the vacuum between the two tanks was taken before and after the impact. Based on the measurement taken directly after the test, the fuel tender maintained its vacuum, indicating neither the exterior nor the interior tank was compromised during the impact. The exterior of the housing showed signs of minor damage in the form of a dent on the housing door, indentations on the center post of the housing structure, and deformation of the door locking mechanisms and handles (highlighted in yellow in Figure 31). Also, the team noted the imprint on the housing doors from the front grill and hood structure of the dump truck. The valves inside the housing were inspected and no visual damage or LN2 leakage was detected. The operation of the FB valve, the valve that allows fuel flow to the locomotives, was recorded during the impact. The signal of the optical sensor during the impact is shown in Figure 32. The hose that supplied air to the FB pneumatic actuator was severed during the test. Approximately 1.6 seconds later, the sensor voltage changed from zero to -3.3 V. The minimal damage to the fuel tender protective housing and the change in the state of the FB

valve achieved the main objective of the test, i.e., demonstrating the crashworthiness of the protective housing and the proper functioning of the cut-off valves.

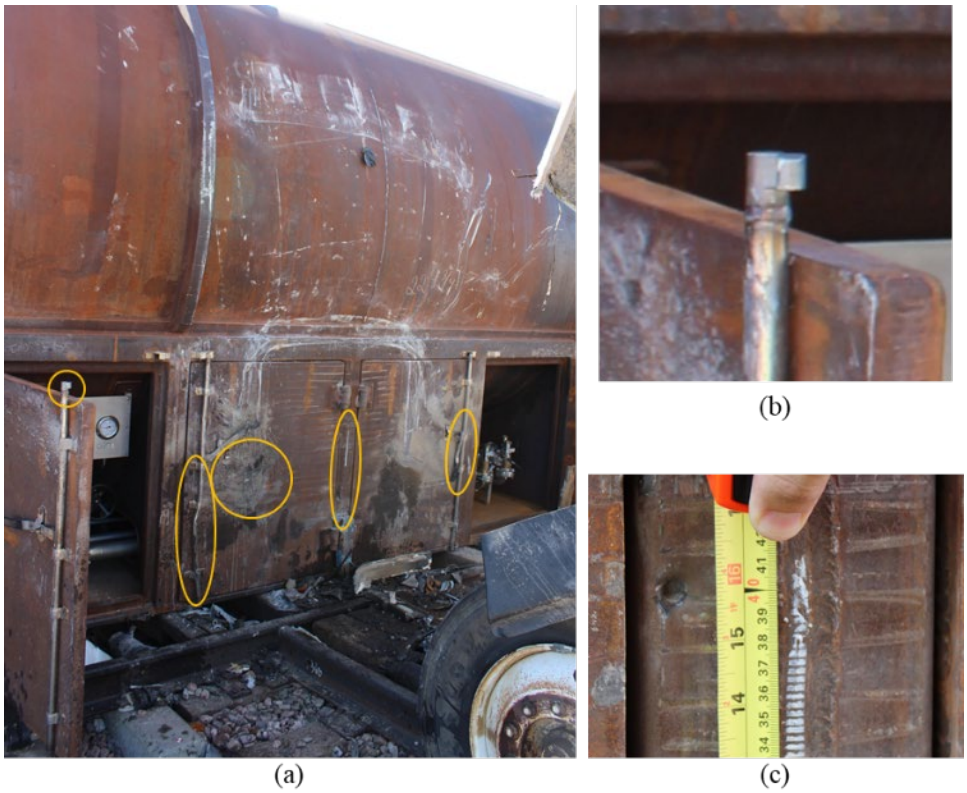


**Figure 31. Damage Done to Fuel Tender's Protective Housing. (a) Overview of Damage, (b) Door Locking Mechanism Damage, and (c) an Indentation in the Center Post**

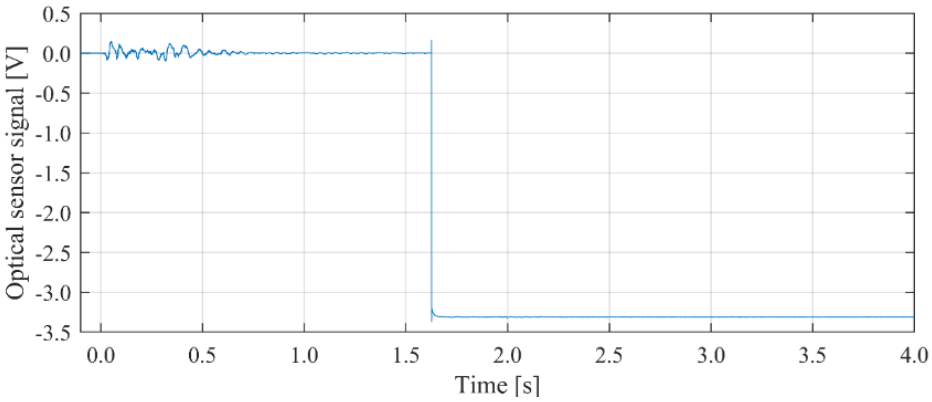


**Figure 32. Optical Sensor Signal Recorded During Impact Test**

## 4.4 Summary of Measured Results

The impact sequence occurred in three phases based on a review of the high-speed footage. The first phase lasted around 0.165 seconds. During this phase, the cab of the dump truck was crushed and the underframe deformed. After the first 0.165 seconds, the deformation of the cab and underframe ended, and the second phase of the impact began. During this phase, the dump bed separated from the underframe and slid along the underframe. The dump bed moved in the

x-direction until the bed collided with the rear of the cab roughly 0.25 seconds after the start of the impact. The third phase of the impact began after 0.25 seconds and was characterized by the gross movement of the tender, the locomotives, and the track mainly in the x-direction. The third phase ended around 0.8 seconds when the gross motions ended and only the structural vibration and the settlement of dust and debris remained.

Figure 33 shows the acceleration response measured on the dump bed roughly at the center of gravity of the dump truck measured in the x-direction. As stated in Section 3.6, the acceleration data was filtered at 60 Hz using a two-pass phaseless four-pole digital filter algorithm consistent with the requirements of SAE J211 [9]. The three phases of the impact are highlighted in Figure 33 and can be seen as the amplitude of the acceleration response of the dump bed changed.

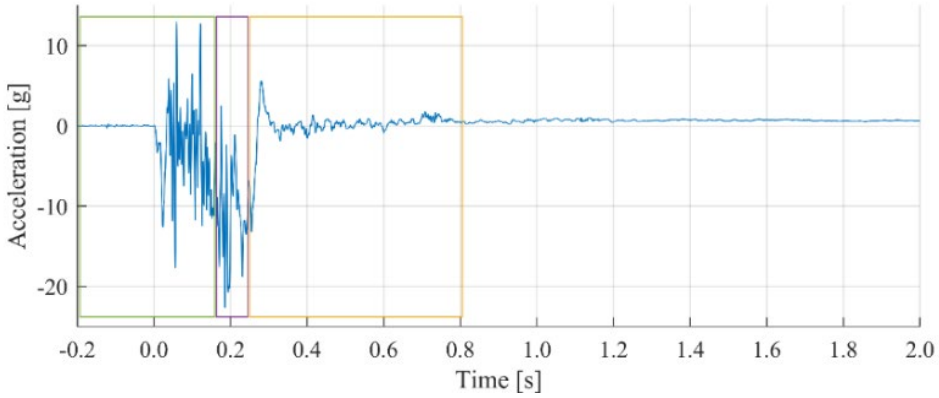


**Figure 33. Acceleration Response of the Dump Bed in the X-direction (Channel VCGX) Showing the Three Phases of the Impact**

The displacements measured at the end of the fuel tender heads are shown in Figure 34. The displacement of the east side head reached 45 inches, the maximum travel potential of the string potentiometer. When the displacement reached the maximum distance, the string snapped, rendering the displacement measurement meaningless. The west side head reached a maximum of roughly 35 inches. The head displacement results correlate with the measured tie displacements shown in Figure 30 that show the east side displaced more than the west side because of the fuel tender being struck offset from its center.

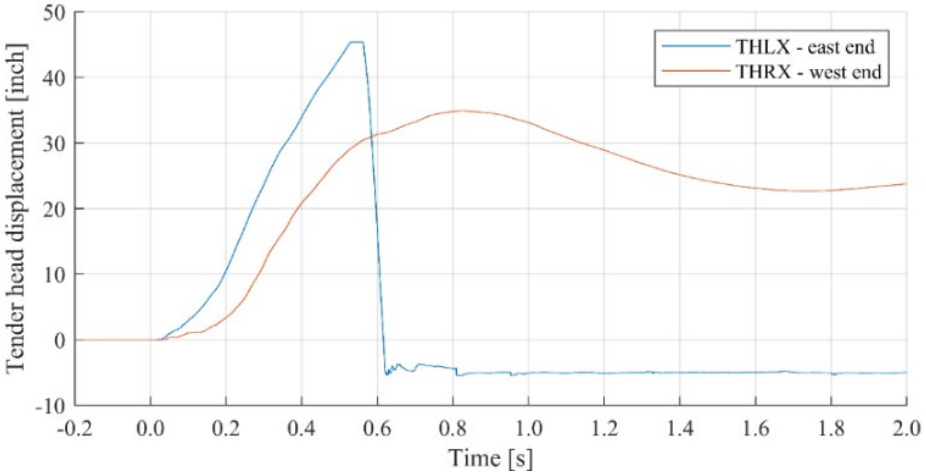


**Figure 34. Displacement of the Fuel Tender Heads**

The displacements measured at the couplers are shown in Figure 35. Each coupler reached its maximum displacement around 0.3 seconds, shortly after the start of the third phase of the impact. The east side coupler displaced more than the west side coupler. This difference could be attributed to the off-center impact on the fuel tender.

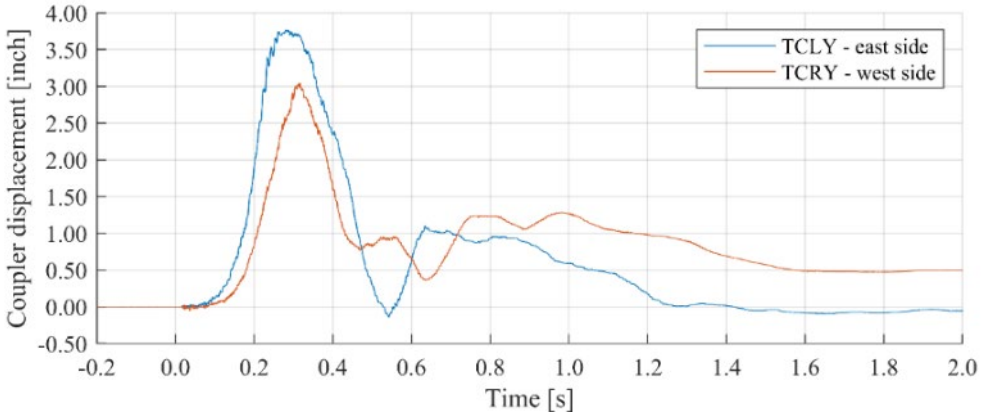


**Figure 35. Displacements Between the Couplers**

The displacements measured inside the protective housing are shown in Figure 36. These included some transients in the measurements directly after the impact. After these changes, the displacements settled to around 0.29 inches and 0.12 inches of inward displacement on both the east and west side of the protective housing. There was a loss in signal of the displacement transducer on the east side around 0.55 seconds. The loss in signal was caused by damage to the wires connecting the transducer to the data acquisition system. The data after this loss in signal may be ignored.

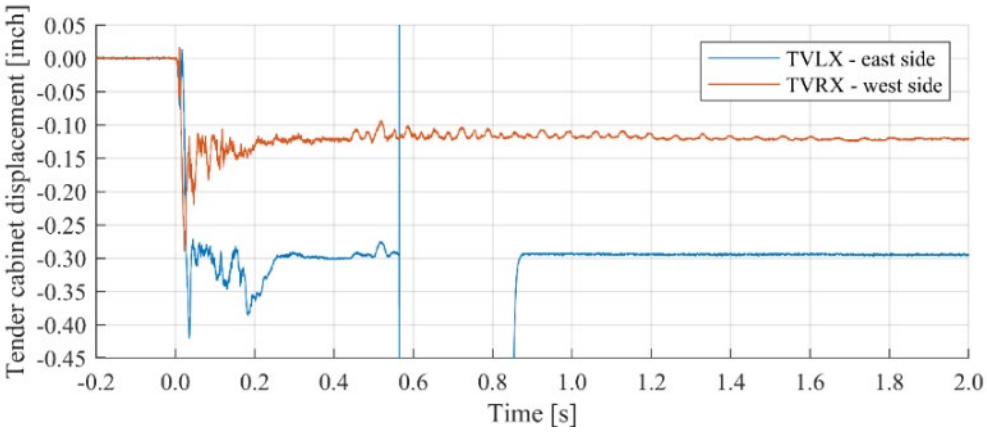


**Figure 36. Displacements Measured Inside the LNG Fuel Tender Housing**

Figure 37 shows that there was a pressure drop of roughly 4.5 psig directly after the impact due to the cryogenic liquid self-cooling after being agitated. The pressure before the FB valve stabilized at 22.8 psig for the duration of the measurement. It should be noted that the pressure measurements were not zeroed before the impact test, but they were zeroed before the LNG fuel tender was filled with LN2 to measure the pressure that existed in the tank after the fill. There may have been drift in the pressure measurements due to the five days that passed since the pressures were last zeroed. Also, there was a loss in signal of the manway pressure transducer (channel TTPMW) around 0.3 seconds and the data after this point may be ignored. The loss in

signal was caused by damage to the wires connecting the transducer to the data acquisition system.

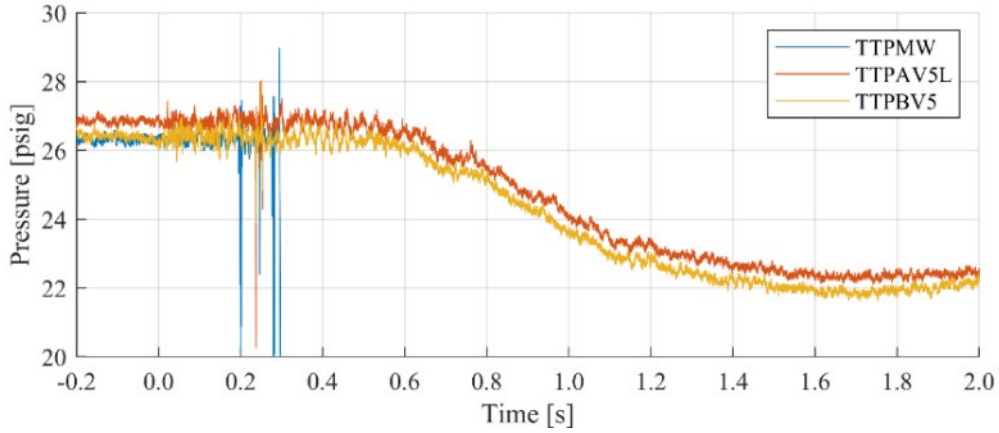


**Figure 37. Pressures Measured at the Manway, Before and After the FB Valve**

# 5. Model Development

Researchers developed two different types of models to assist in planning the test setup and estimating the fuel tender response to the impact. A FE model included detailed geometry and material behaviors of the locomotives, tender, highway vehicle, and track structure. This model was used to examine a limited number of specific impact conditions prior to the test and to conduct a post-test simulation using the actual test conditions. A lumped-mass model featured simplified representations of the same parts included in the FE model, which allowed it to run much more quickly.

## 5.1 FE Model

The assembled FE model is shown in Figure 38, with callouts indicating the various substantial components that were tracked. The fuel tender in the FE model had its long and short ends flipped relative to the position of the tender in the physical test (this discrepancy will be discussed further in the discussion alongside the comparison of test measurements and model data). This section summarize the FE models of the fuel tender, dump truck, locomotives, and track. In addition to the geometry seen in the figure below, numerous constraints, contacts, and connectors were defined throughout the model to define the interactions between components. Additional details on the FE model can be found in the Appendices to this report. Throughout this section, the global directions of the assembled FE model will be used unless otherwise noted. As seen in Figure 38, the X-direction is the direction of impact (i.e., transverse to the tender and locomotives), the Y-direction is the vertical direction, and the Z-direction is parallel to the locomotive-tender-locomotive consist's track direction.

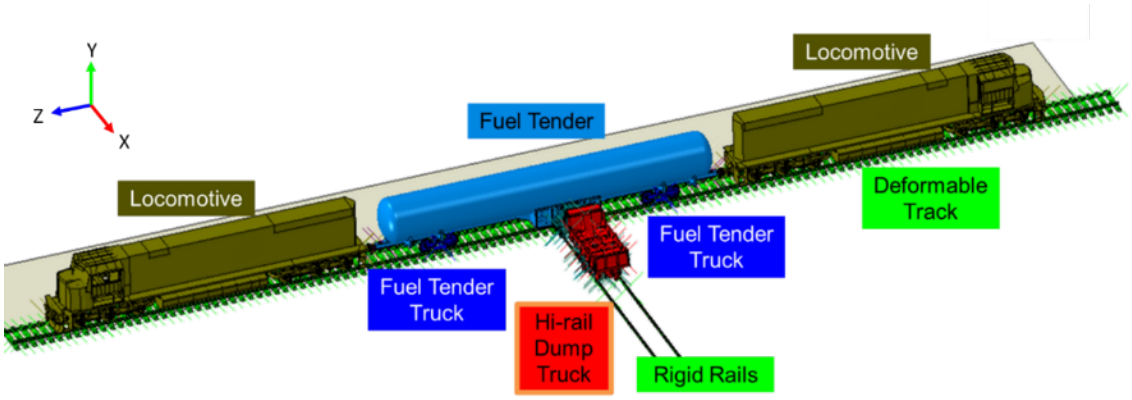


**Figure 38. Annotated FE model**

### *5.1.1 Fuel Tender*

The FE model of the fuel tender was developed using a computer-aided design (CAD) geometry file provided by the tender's manufacturer. The CAD file included the tender's geometry but did not include the tender's three-piece freight trucks. Discussion of the fuel tender's model is broken into separate sections for the carbody, the lading, and the three-piece freight trucks.

#### *5.1.1.1 Carbody*

The CAD file provided by the tender's manufacturer contained substantial detail (e.g., nuts, bolts, valves, etc.) that was unnecessary for modeling the tender impact. The geometry was

simplified and unnecessary details were removed from the FE model. The model did not include any piping, openings in the tanks, or housing doors on the non-impact side of the tank. The carbody portion of the tender model is shown in Figure 39. The FE model included geometry of the inner and outer tanks, center sill, housing, couplers, and the connections between the tanks. The tender carbody was meshed using shell elements with appropriate thickness values and elastic-plastic material properties. The couplers, draft gear followers, and center plates were modeled as rigid bodies. Appendix D discusses the development of the tender carbody FE model in detail. The protective housing on the tender is not located in the center but offset from the centerline of the tank by approximately 3.5 feet.

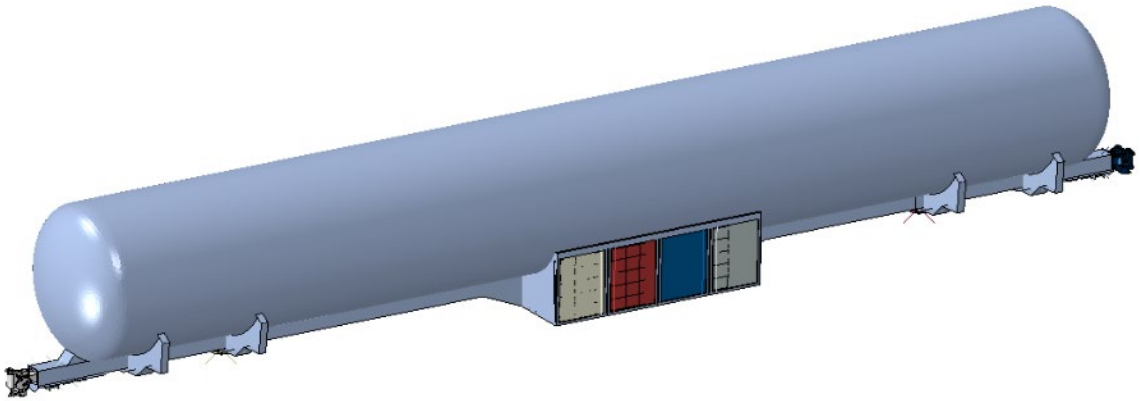

**Figure 39. Fuel Tender Carbody Portion of FE Model**

#### *5.1.1.2 Lading*

In addition to the geometry of the tender carbody, the tender portion of the FE model included simulated lading. As was previously discussed in Section 2.2.1, the mass of LN2 planned for the test was chosen to match the mass of LNG that the tender would carry under normal operating conditions. This mass of LN2 had a filling level of approximately 45 percent by volume. Thus, substantial liquid sloshing within the tank would be possible owing to the large vapor volume. At the same time, the impact from the highway vehicle was not expected to result in a substantial indentation to the inner tank. Therefore, the volume of the inner tank was expected to remain constant.

Previous tank car impact research featured various methods of modeling the two-phase (i.e., liquid and vapor) fluid response within a tank under impact conditions. Approaches examined under this program have included Arbitrary Lagrangian-Eulerian (ALE) modeling [10], Lagrangian elements for the liquid with an ideal gas pressure-volume relationship for the vapor [11] [12][13], Lagrangian elements for both fluids [14], Lagrangian liquid with smoothed particle hydrodynamics (SPH) vapor [15], and hydraulic and pneumatic cavities [16], [17], [18]. Based on its relatively simple implementation and the expectation that the inner tank would undergo little deformation, the pneumatic and hydraulic cavity modeling techniques were used in the fuel tender model. Details of this modeling technique are described in [16].

A flexible membrane was defined within the inner tank. The membrane part included a horizontal surface, as shown in the cross-section view in Figure 40. This surface represented the boundary between the liquid and vapor phases. A reference point defined above this plane was

used to define the volume of the pneumatic cavity and a reference point below this plane defined the hydraulic cavity. The mass of the liquid was incorporated into the light-colored portion of the membrane using a "nonstructural mass" keyword. The mass of the vapor was incorporated into the dark-colored portion of the membrane using a similar technique.

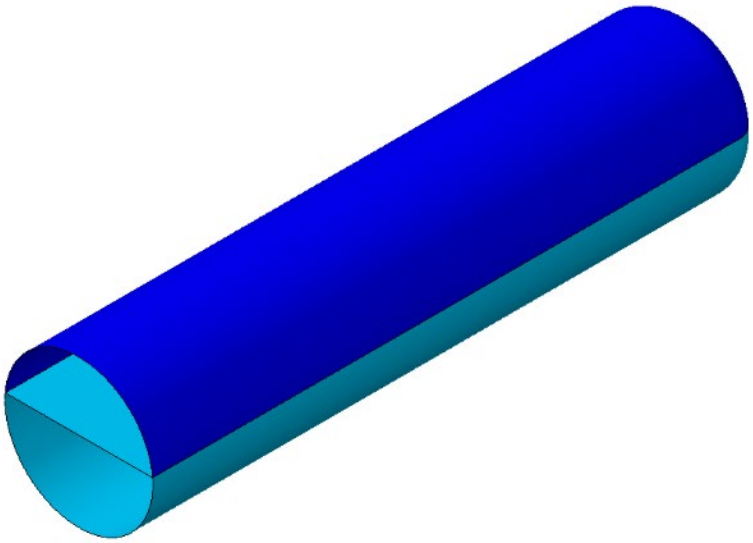

**Figure 40. Membrane Used to Define Pneumatic and Hydraulic Cavities within Inner Tank**

Table 8 contains a summary of the parameters used to define the liquid and vapor phases of the lading and then used in the baseline FE model. Some parameter values were subsequently varied as part of a parametric study conducted with the pre-test model. Any variations from the values in this table are discussed in the section of this report describing the corresponding parametric study.

**Table 8. Summary of Input Parameters for LN2**

| Parameter | Value | Notes |
|---|---|---|
| Saturated Liquid Temperature | 105.5 K | |
| Saturated Vapor Temperature | 105.5 K | |
| Liquid Pressure | 162.3 psia | Varied in parametric study |
| Vapor Pressure | 162.3 psia | Varied in parametric study |
| Liquid Mass | 233.33 lbf-s$^2$/in | |
| Vapor Mass | 13.5 lbf-s$^2$/in | |
| Liquid Density | 6.12 x 10$^{-5}$ lbf-s$^2$/in$^4$ | [6] |
| Universal Gas Constant | 73.583 in-lbf/(mol-K) | [19] |
| Vapor Molecular Weight | 1.6 x 10$^{-4}$ lbf-s$^2$/in/mol | Calculated value using data from [19] |
| Vapor Molar Heat Capacity | 431.83 in-lbf/mol-K | Calculated value using data from [6] |
| Liquid Bulk Modulus | 27,311.2 lbf-s/in$^2$ | Calculated value using data from [6] |

#### *5.1.1.3 Three-piece Freight Trucks*

The fuel tender would be standing on typical freight trucks at the time of the impact, rather than any simplification or approximation of trucks. This provided a realistic impact condition representing the actual condition of the tender in service. However, this also added complexity to the model, as the three-piece freight truck would be resisting the lateral forces developing during the impact in addition to supporting the vertical weight of the tender. Modeling the three-piece

freight truck required a compromise between simplifying the complex behaviors associated with a suspension and including enough detail that the tender-truck-rail interactions were a reasonable approximation of the test conditions.

The geometry of the three-piece freight truck model is shown in Figure 41. Each freight truck assembly included two wheelsets, two sideframes, one bolster, and two constant contact side bearings (CCSB). The wheelsets were modeled using solid hexahedral brick elements with an elastic steel material property. All other parts were modeled as rigid bodies with assigned inertial properties. Connector element properties were defined to allow the side bearings and the secondary suspension to deflect. Contact was enabled between the sideframes and axles, and between the bolster and sideframes. Appendix E discusses development of the three-piece freight truck model.

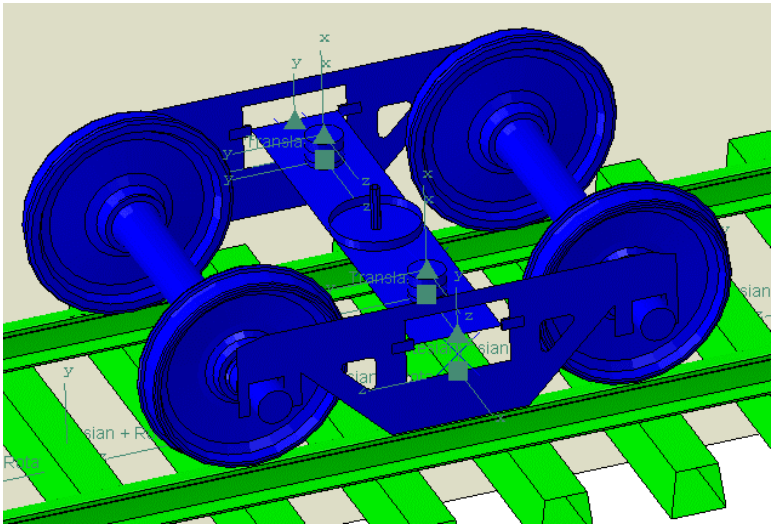

**Figure 41. Three-piece Freight Truck FE Model**

### *5.1.2 Dump Truck*

M-1004 specifies an 80,000 lb single-frame highway vehicle as the impacting vehicle. A 1994 FLD 120 dump truck was selected as the single-frame vehicle and was modified to travel on rails (see Section 2.3.1). The team modified a publicly available FE model of a semitrailer truck tractor[7] [20] to create the FE model of the modified dump truck (see Figure 42). This semitrailer tractor model was originally developed for use in the LS-DYNA software. This model was converted for use in Abaqus/Explicit to simulate the LNG tender impact. A description of the process of modifying the existing FE model of the semi tractor is discussed in Appendix K.

[7] The tractor model was originally developed by the National Crash Analysis Center (NCAC) at George Washington University (GWU), and subsequently modified by National Transportation Research Center, Inc., Battelle, Oak Ridge National Laboratory, and the University of Tennessee at Knoxville. Additional background and history of the semi tractor FE model that served as the base model for the dump truck model's development is described in Appendix K.

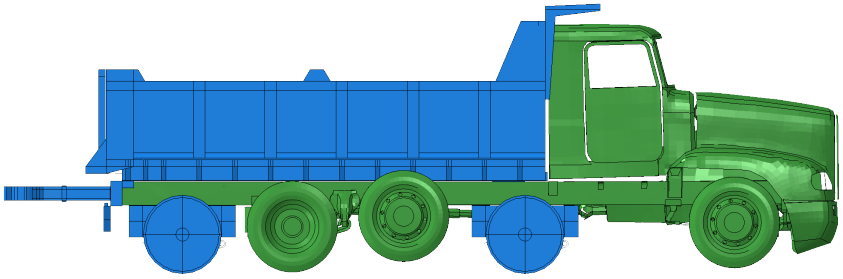

**Figure 42. Finite Element Model of Modified Dump Truck**

After conducting a literature review, researchers were not able to find a publicly available FE model of a dump truck. However, Texas A&M Transportation Institute (TTI) had conducted pre-test FE modeling [21] and a series of tests [22] of an impact between heavy duty trucks and highway bridge piers. TTI researchers modeled impacts of bridge piers from a semitrailer truck and a dump truck, and their tests used a semitrailer truck. TTI provided the research team with two dump truck models they had developed (see Figure 43).

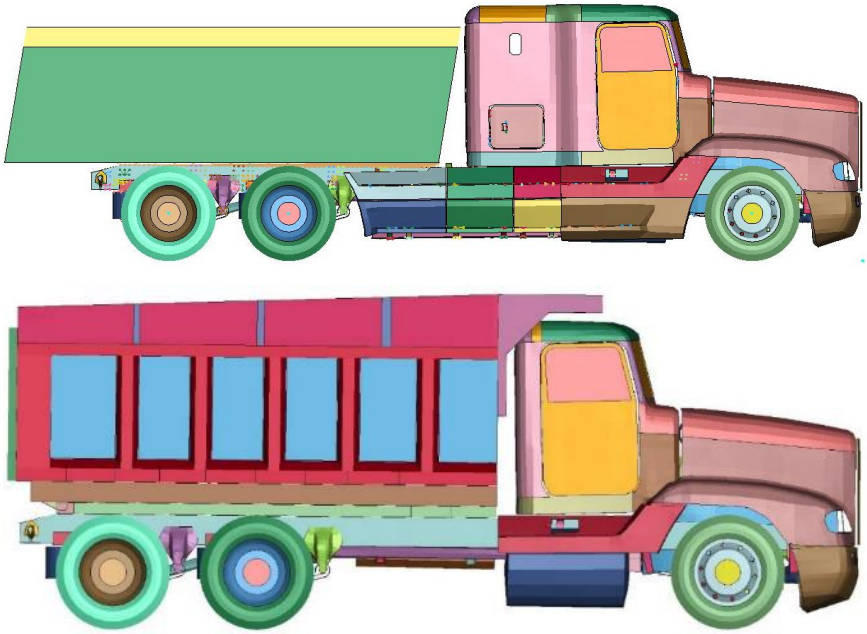

**Figure 43. Preliminary (Top) and Finalized (Bottom) Finite Element Models of Dump Trucks Shared by TTI**

The dump truck with the sleeper cab shown in Figure 43 (top) had a 241-inch wheelbase and featured a simple rigid dump body. The dump truck with a day cab shown in Figure 43 (bottom) had a 212-inch wheelbase and featured a deformable dump body. Each vehicle had a weight of approximately 65,000 lbs.

The team determined that the wheelbase on the TTI sleeper cab dump truck model matched the actual dump truck planned for use in the tender impact test (241 inches). However, the model was in a preliminary state and the dump body was attached to the frame with rigid beam elements that unrealistically stiffened the frame under the dump body. The dump truck with a day cab featured a more realistic attachment between the dump body and frame, but the

wheelbase was too small compared to the actual dump truck selected for this test. Therefore, the modeling team took a similar approach to the researchers at TTI and created an FE model of a dump truck by modifying a publicly available FE model of a semitrailer truck [20]. The models provided by TTI were used in initial simulations into a rigid wall, which produced a force-crush characteristic that served as an input to the MBD model (discussed in Section 5.2.2).

Figure 44 shows the FE model of the dump truck situated on rigid rails in Abaqus after the team modified the semitrailer truck model. The features colored in grey were adapted from publicly available models of semi-tractors (refer to Appendix K) [20]. The rail wheel assemblies (colored in dark green) were created using CAD files provided by TTCI (see Appendix C), and the dump body (colored in red) was created based on physical measurements. A drop axle (colored in light green) was added to the base truck by copying its front axle and adding constraints.

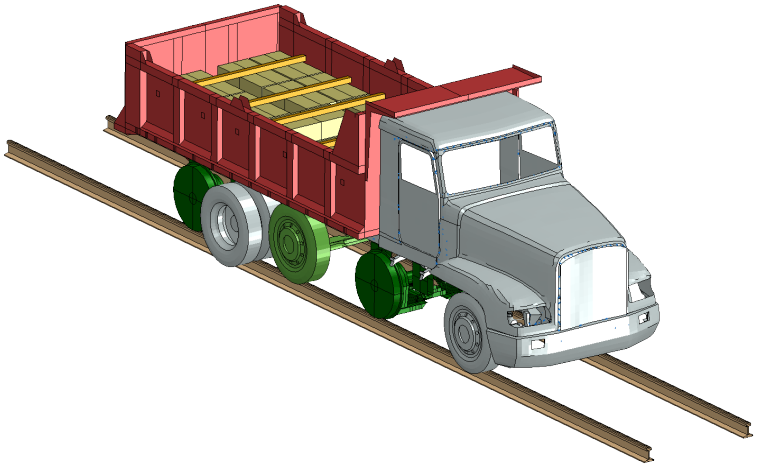

**Figure 44. Dump Truck Positioned on Rigid Rails Isometric View**

Figure 45 shows a top view (top) and section view (bottom) of the dump truck FE model. The 16 rectangular ballast blocks (colored in tan) each weighed 3,200 lbf and were included based on the ballast arrangement in the actual dump truck. After adding the ballast, the total weight of the dump truck model was approximately 80,163 lb, which can be compared to the actual dump truck weight of 81,350 lbf (refer to Section 2.3.1). Ballast restraints (colored in orange) were created based on measurements from TTCI, and chains additionally used in the actual test to secure the ballast were not included in the model. Simple representations of the rear dump body hinges as discrete connectors and the front 5-stage hydraulic piston (colored blue) were also included because, while the dump body was welded to the frame by TTCI, it was expected that the dump body could detach during the impact due to rapid deceleration of the dump truck's frame. The rear coupler (colored in brown) was also included for visualization.

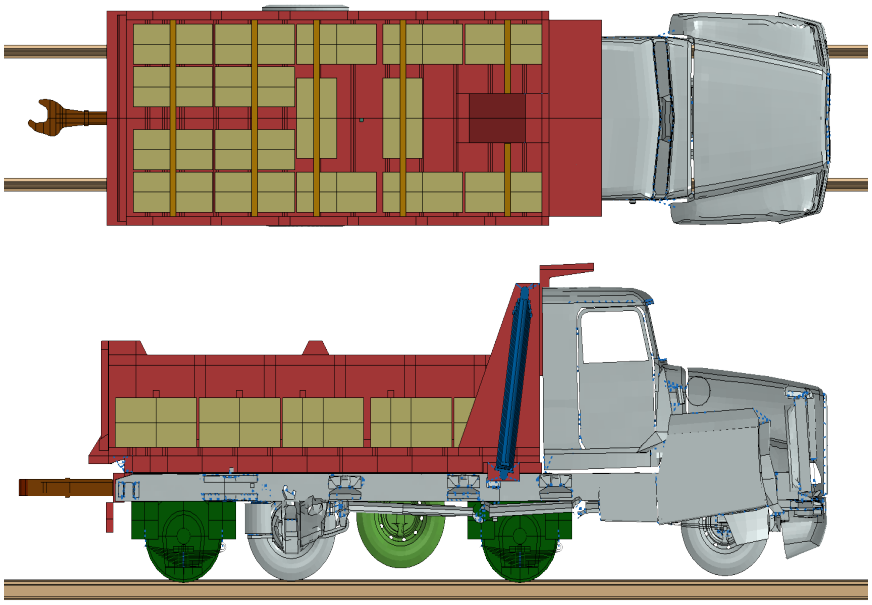

**Figure 45. Dump Truck Positioned on Rigid Rails Top View (Top) and Section View (Bottom)**

Additional details about the dump truck model development can be found in Appendix K.

### *5.1.3 Locomotives*

An FE model of a locomotive (shown in Figure 46) was prepared by Applied Research Associates (ARA). The locomotive model was previously used in LNG fuel tender grade crossing FE analyses performed by Kirkpatrick et al. [3]. ARA modified a locomotive model that was created by QinetiQ North America, Inc. (QNA) to create the locomotive FE model used in their LNG fuel tender grade crossing impact simulations. The original QNA model was developed for FRA. The model provided by ARA had approximately 417,000 deformable elements and weighed approximately 420,000 lb.

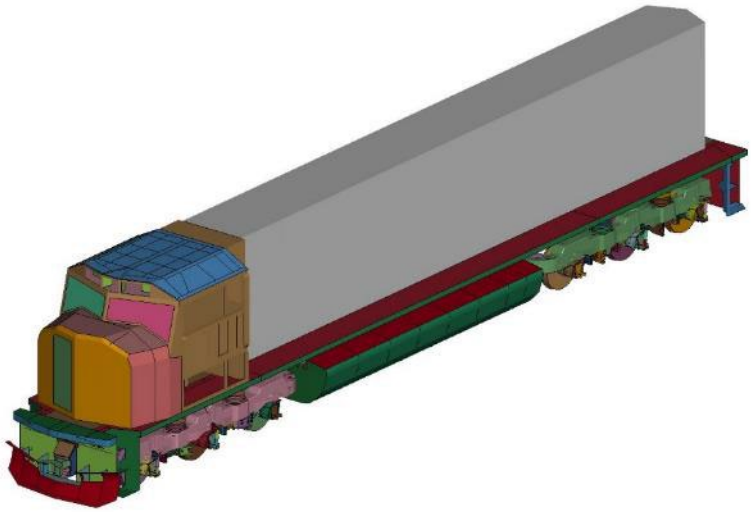

**Figure 46. Locomotive FE Model in LS-DYNA**

Using the same procedure from the LS-DYNA to Abaqus/Explicit conversion of the highway truck model, the team used Abaqus CAE to automatically convert the locomotive's input deck and manually reassigned model features that were not automatically translated. Figure 47 shows the locomotive FE model after it was converted to Abaqus and included in the LNG fuel tender grade crossing impact simulation.

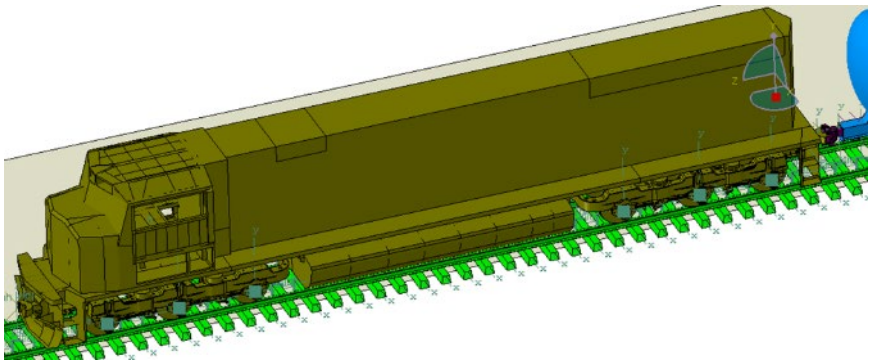

**Figure 47. Locomotive FE Model in Abaqus on Rails and Coupled to LNG Fuel Tender**

### *5.1.4 Track*

Two distinct sets of railroad track were used in the test setup and required modeling. The high-rail dump truck would coast down an existing length of track on its railroad wheels, and the tender and locomotives would stand on another set of tracks. Different modeling approaches were used for each set of tracks. The tracks are shown in Figure 48. Additional details on the track modeling techniques used in the FE model are contained in Appendix F.

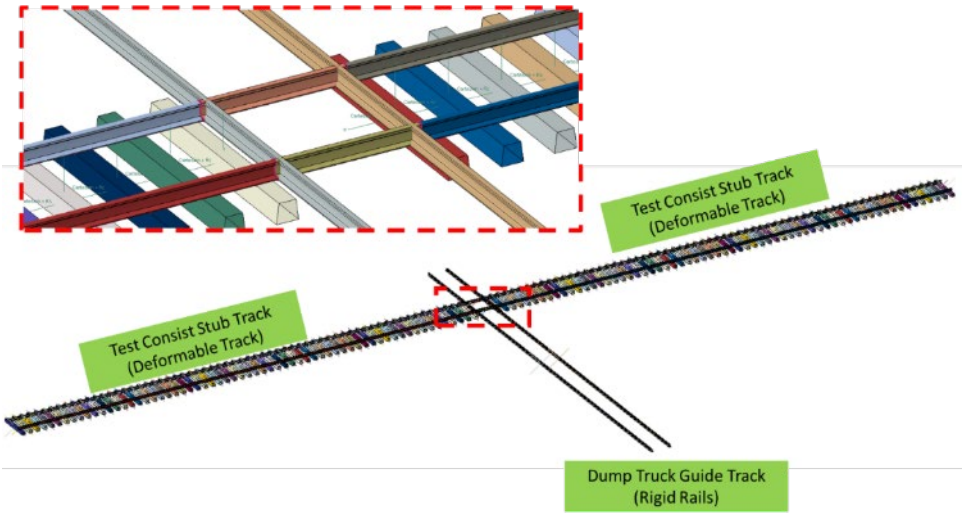


**Figure 48. Annotated Image Showing Test Consist Stub Track and Dump Truck Guide Track in FE Model**

The continuous track that the dump truck coasted along served as a guideway for this vehicle. The dump truck imparted loads to this track far below what a typical freight railcar or locomotive would impart. Additionally, once the impact occurred, the dump truck was expected to derail off the rails, so the effect of the rails on the model results was expected to be negligible. Therefore,

the dump truck rails were modeled as fixed, rigid rails that served only as a guideway for the high-rail dump truck in the model.

The "stubs" of track that supported the two locomotives and the tender were specifically built for this test. At the beginning of the simulation process, these stubs were modeled as two rigid rails that were fixed in space. That is, the rails could neither deflect nor deform, regardless of the magnitude of the forces and/or moments applied to them. This was a modeling choice intended to simplify the modeling process since it only required a rail profile (i.e., cross-section geometry) to be defined. The total forces and moments in each direction and for each rail were calculated in this early model. These forces and moments were large enough that it was apparent that the rails and track structure would be likely to deform during the impact. Thus, a more sophisticated approach was required to model the stubs of track.

#### *5.1.4.1 Dump Truck Guide Track*

The dump truck guide track consisted of two RE 136 [23] rails that were modeled as rigid bodies. Each rail was fully constrained against both translations and rotations. Each rail measured 1,300 inches long to provide sufficient distance for the dump truck to travel during the initial settling period. The two rails extended beyond the intersection with the test consist stub track because in the test setup the dump truck would be traveling along a continuous, existing section of track. If the dump truck guide track were terminated at the intersection with the test consist stub track in the model, any potential interaction between the tender and the dump truck guide track on the non-impact side (e.g., tender-rail contact following a rollover) would not be captured by the model.

The rigid rail parts are shown in Figure 49. The inset image on the top shows a zoomed-in view of the mesh in the center of one rail, adjacent to where the boundary conditions are applied. The bottom view shows an end-on view of the two rail profiles. The rails were constrained in all six degrees-of-freedom (DOF).

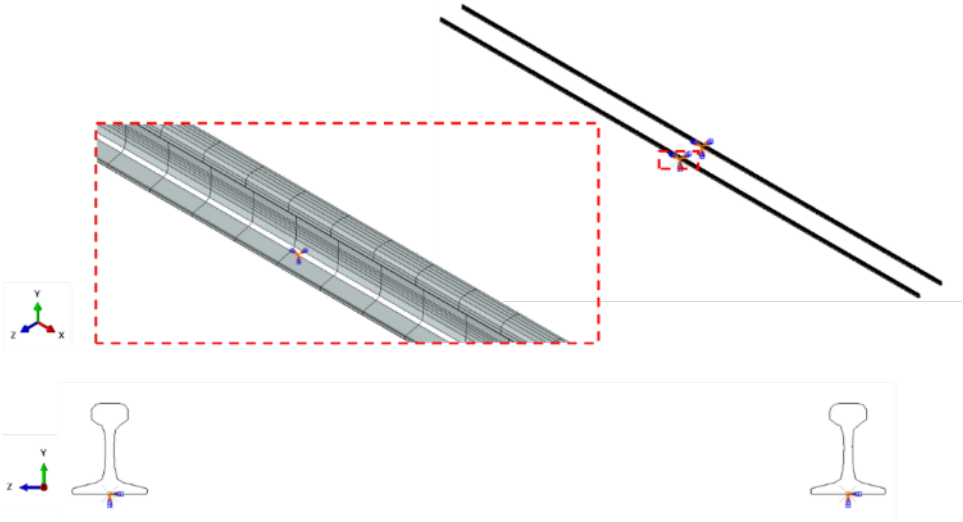

**Figure 49. Images of Rigid Rail Parts and Mesh**

#### *5.1.4.2 Test Consist Stub Track*

Developing a detailed model of a deformable track complete with ballast, concrete ties, fasteners, and rails was outside of the scope of the modeling plan to support this test. At the same time, simply assuming the rails upon which the tender and locomotive stood would remain fixed and rigid was not reasonable, as the test consist stub track would be providing lateral resistance to the impact load. The deformable track arrangement in the model was a compromise between the competing needs of capturing potential rail and/or tie motion and allowing the model to increase in complexity only as necessary. Additionally, the model was limited by the availability of input data to describe the various track behaviors. As the model was being developed to support an impact test to a fuel tender, the project scope did not include plans to conduct laboratory tests or measurements on track components to generate model input data.

The deformable track model was made up of a combination of rigid and deformable parts and consisted of four deformable rails (long), 126 rigid concrete ties, and 126 rigid ground planes. Initially, the deformable rails (long) were discontinuous, terminating adjacent to the rigid rails of the dump truck guide track. During construction of the test setup, the team verified that the test consist stub track could be made continuous. The model was thus updated to include an additional deformable rail (short) between the terminations of the deformable rails (long). The overall arrangement of the test consist stub track model (with short deformable rails included) is shown in Figure 50. The tie gap in the center of the rails is where the dump truck guide track (not shown) intersects the test consist stub track.

**Figure 50. Test Consist Stub Track Arrangement**

Each deformable rail was modeled using an RE136 rail profile [23]. The deformable rail was assigned an elastic-plastic material response based on tensile measurements made on head-hardened rails [24]. The concrete ties were modeled as rigid bodies having overall dimensions and inertial properties based on published values for concrete ties [25].

The various parts were attached through a combination of constraints and connectors. Additionally, boundary conditions were used to fix the ground planes in space and remove several DOF from the concrete ties. Each deformable rail (long) was connected to a series of rigid concrete ties using a TIE-type constraint in Abaqus. This constraint defined a perfect connection between nodes on the deformable rail (long) and nodes on the rigid concrete tie. This simplified connection essentially represented the clips, shoulders, and other mounting hardware between the rail and concrete tie as a rigid, unbreakable connection. In cases where a deformable rail (short) was installed between the deformable rails (long), a similar TIE-type constraint was used to attach each end of the short rail to the mating end of a long rail.

Each concrete tie had a companion rigid ground plane. Each rigid ground plane was fully constrained in all 6 DOF. Boundary conditions on each concrete tie prevented translation in the

global Z-direction (i.e., parallel to the deformable rails) and rotation about a vertical axis. Connector elements with prescribed translational and rotational behaviors for the remaining DOF were defined between each concrete tie and its companion ground plane. The prescribed behaviors of the connectors were used as a simplified means of representing the vertical, lateral, and rotational compliance of the track structure below the level of the ties. Development of the connector behaviors is described in Appendix F.

## 5.2 Lumped Mass MBD Model

The lumped mass MBD model was developed to quickly test iterations and possibilities that would be difficult to do in a timely manner with an FEA model. This dynamics model was used to examine the major behaviors of the tender car, dump truck, and locomotives. There were safety concerns raised during the development of this test – particularly regarding the tender car and locomotives rolling over – that a lumped mass model could explore and assess the possibility of occurring. Some properties of the various bodies were known, while others were approximated to a range, and certain properties could be specifically varied for the test. Figure 51 shows the various bodies included in the lumped mass model.

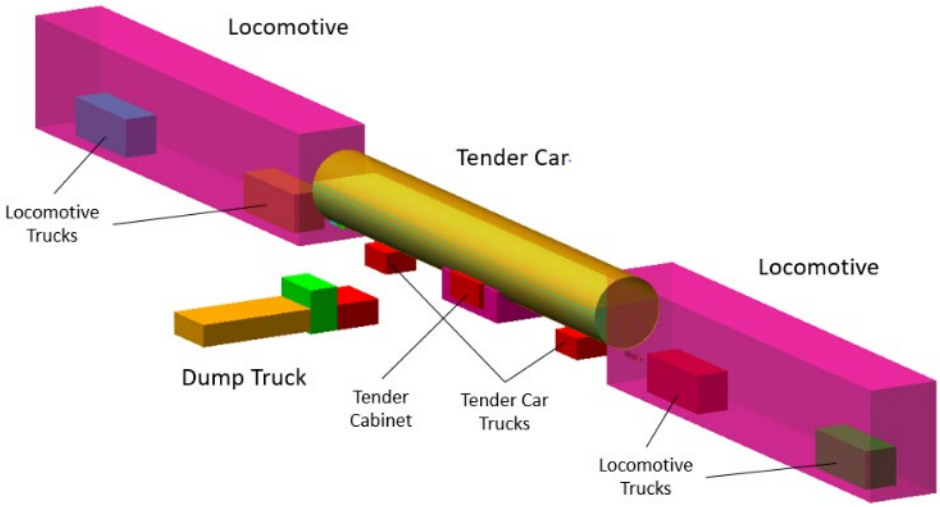


**Figure 51. Lumped Mass Model**

The model was created in Adams View 2017 [26]. Adams is a commercially available multibody dynamics simulation solver capable of running nonlinear systems with numerous connections. The software has some limited flexible body simulation capabilities but is much more adept at handling rigid bodies with defined geometries or inertial values. The software has several common connection, force, and spring types built in, and it can also handle function-defined stiffnesses, forces, and other parameters.

### *5.2.1 Equipment*

The dump truck was modeled using measurements taken of the actual dump truck used in the test and simplifying it into three different "blocks": the engine block, the cab, and the dump bed. These three blocks were all rigidly attached to one another, in effect making the three blocks one solid body. The density was calculated from the mass of the truck, the geometry, and an assumed

even distribution. The dump truck was also constrained to a one-dimensional linear slide toward the tender car. If a full three-dimensional model of the dump truck was created, it would be necessary to know its inertial values or at least a better estimate of its mass distribution. However, in this simplified one-dimensional model, only the mass and initial velocity are needed. The estimated geometry gives a better visual sense of how the model behaves, which is why it is used instead of a point mass. A nonlinear spring was attached to the front end of the truck model to represent the crush that the dump truck would experience. Preliminary FEA modeling of the impact scenario showed that the engine block and cab would likely crush significantly, which would affect the forces applied to the tender car's protective housing. Further explanation of this nonlinear spring is given in Section 5.2.2. Figure 52 shows a side view of the Adams dump truck model.

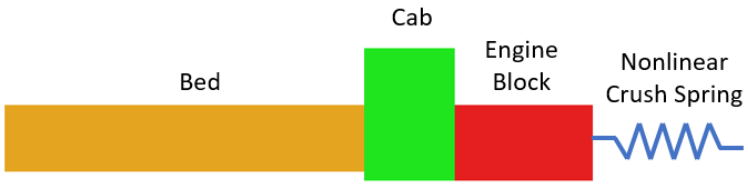


**Figure 52. Dump Truck Model**

The tender car model was similarly simplified to include just the tank, lading, housing, and trucks. Major dimensions were taken from an engineering drawing of the tank, and others were measured in the CAD model. The tender car without trucks (i.e., the tank and housing bodies in this model) weighed approximately 175,000 lbf (or 175 kilopounds (kips)) and the trucks about 15 kips, but the inertial values were largely unknown for this model. All bodies were instead assigned a uniform density depending on what was known about each body. If the volume of the body could be easily approximated, like the tank, then it was assigned the density of its respective material (typically steel) to approximate its weight and inertia values. Conversely, if the weight of the body was known, it was assigned a theoretical density that met the target weight based on body geometry. The trucks and housing were modeled as cuboids and the tank was modeled as a thin shell cylinder. Since the tank geometry approximation was closer to its actual geometry than the housing, it was assigned the density of steel and the housing was given a uniform density; the combined weight of the tank and housing was 175 kips. The lading was modeled as a solid cylinder inside the tank and given the density of LN2, and its outage was modeled using an intersecting cuboid and a Boolean operator that could cut into the lading to give the desired outage. The lading was fixed with a rotational joint parallel to the car's longitudinal axis to represent fluid slosh.

The SD60 locomotives were modeled using dimensions and weights found online [27]. The locomotives' HT-C trucks were modeled as separate blocks using weights from a technical paper [28]. The cuboids were assigned uniform densities in a similar manner to the tender car. While the center of mass in the locomotive model is likely inaccurate, the locomotives were primarily present to hold the tender car in place. Figure 53 shows the model of the tender car and locomotives.

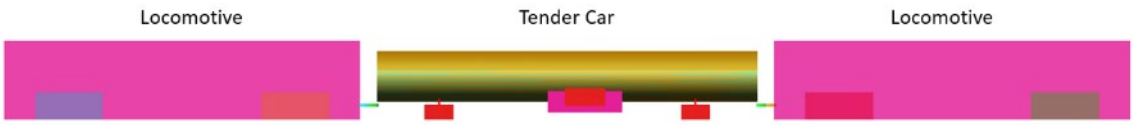


**Figure 53. Train Consist Model**

The track stubs that the tender car and locomotives rested on were modeled separately. With such high lateral forces, the track stubs were likely to experience panel shift, so the separate model would estimate the amount of lateral travel allowed in the main model. The rails were modeled as I-beams and given similar cross sections and area moments of inertia as the rail profiles used in the test. Adams has a flex link body that splits a body into discrete rigid links that are connected by beam-like forces dependent on the links' Young's modulus and inertia values. Given many links for a high resolution, the body can act similarly to a flexible body. The rails were converted into long flex links that were attached to concrete tie cuboids every two feet. The ties could travel laterally with a friction constant equal to empirical tie push tests for concrete [29]. A wheelset was centered along the rails and was allowed to settle using basic contact forces. Then, a force roughly equivalent to the peak impact force of the dump truck was applied to the wheelset laterally to push the rails. The amount of panel shift seen in this model was then transferred to the main model as the amount of lateral travel allowed by the trucks before they rotated about a theoretical rail. Figure 54 shows the separate Adams model developed for the track.

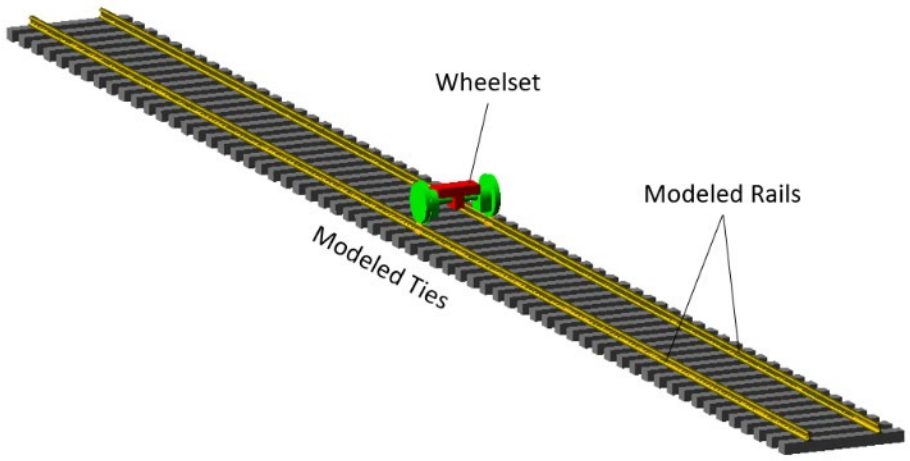


**Figure 54. Wheelset Model**

### *5.2.2 Parameters*

There were many different parameters required to input the forces acting between the various bodies. Most were estimates chosen from a range of possibilities from various sources.

Figure 55 shows the force-time history and force-crush behavior from the preliminary TTI dump truck FE model with a sleeper cab (shown in the top of Figure 43). The team used this preliminary model early in the grade-crossing impact modeling process to estimate a force-crush spline. This was the first dump truck model available and the lumped-mass model results would be less valuable for test planning if delayed until the team completed development of the detailed

FE model of the modified dump truck. The 65,000 lb dump truck was impacted into an analytic rigid wall in LS-DYNA at 40 mph. Normal reaction force was requested from the rigid wall, and displacement in the x-direction (U1) was requested from history nodes on the bumper, rear frame, and rear axle to estimate crush. The simplified force-crush spline (red line) was manually overlayed over the model results. A hard stop at approximately 127 inches and 2.5 million lbf was added to represent the dump body impacting the LNG fuel tender.

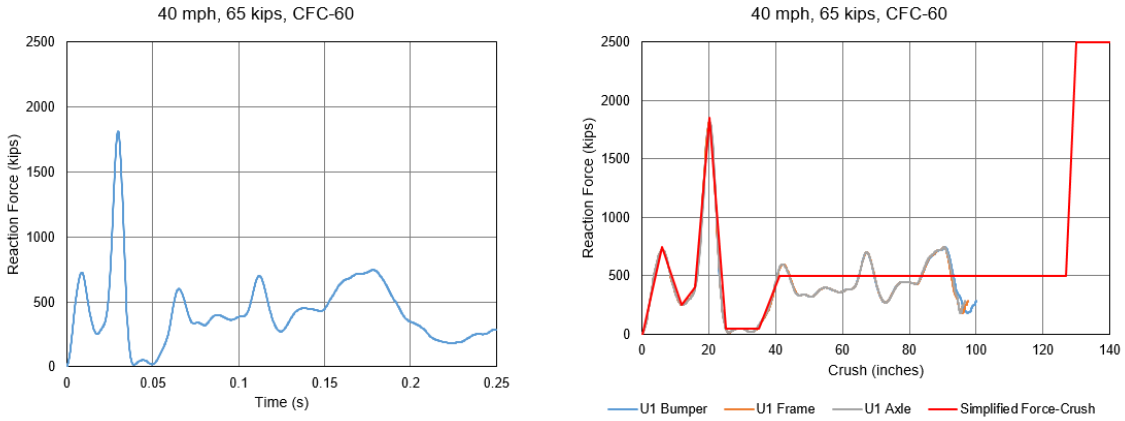


**Figure 55. Force Crush Spline for TTI Dump Truck**

The output forces from the FEA model were simplified as shown, and the force-crush behavior was applied in the MBD model as an elastic spring between the truck front-end and the protective housing that would activate once the bodies made contact. An elastic spring was used as a conservative estimate of tender rollover. It would likely exacerbate the tendency of the tender to roll over as the dump truck was able to exert force on the tender for the longer duration of a simulation than if the dump truck was modeled as perfectly plastic.

The coupler forces were also important parameters since the couplers were possible points of failure. CFRs and industry standards require couplers to be able to withstand minimum shear and torsional values [30] [31][8]. These were used to create force splines that were mostly linear, but then dropped to zero representing a failure in that direction. The linear stiffnesses for these splines were estimates, but there were some empirical studies performed on the torsional stiffness of couplers [32]. Failure in torsion was a primary concern for this model since it could contribute to the tender car rolling over.

The track panel shift was represented as another spline in the primary model. This force acted between the trucks of the tender and the ground of the model. It used both the friction constant from the tie push test and the panel shift approximation from the track model. The spline as shown in Figure 56 was level for a value of (total weight on the rails) × μ and then spiked at the maximum panel shift value. This force would act as a traditional friction force before stopping at the desired lateral deflection value once the stiffness of the force spiked.

[8] A value of coupler torsion strength is found in the APTA Recommended Practice for a common H-type tightlock coupler used as a pushback coupler. This value was presumed to be a lower bound estimate for a freight style coupler.

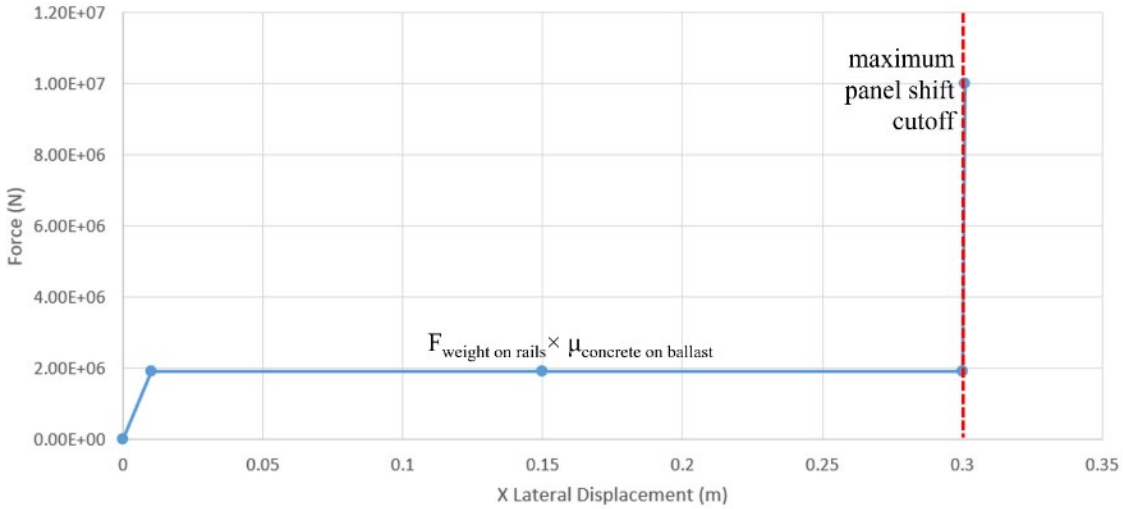


**Figure 56. Modeled Track Panel Shift Spline**

Many of the parameters for this model were chosen from a range of possible values to make the model susceptible to rollover. If the tender car did not roll over in its least robust modeled state, then increasing those parameters would only further prevent rollover. More discussion on critical parameters for this model and how their alterations changed any outcomes is in Appendix I.

# 6. Test and Model Behavior Comparison

As previously discussed, the assembled FE model included numerous behaviors that were challenging to characterize accurately. While the scenario prescribed in M-1004 is intended to represent a "real world" situation with few idealizations and simplifications, the reality of running a test meant that these complex behaviors could have caused an unexpected outcome if the simulations used a faulty assumption. For example, the test setup called for the tender undergoing evaluation to be coupled to two locomotives. While the models of the locomotives were provided by AAR, the conditions of the actual locomotives used in the test could vary substantially from that of a standardized virtual locomotive. Furthermore, a simulation can be run using the assumption that the couplers can resist any force or moment without breaking, but the couplers would eventually fail if sufficient force or moment were applied. Determining the combinations of forces and/or moments that could break a coupler under various loading conditions was outside of the scope of work when preparing for this test.

Nonetheless, it was important to consider the potential effects such a failure could have on the outcome of the test. The team considered two potential outcomes. First, the team examined how a certain less-than-ideal behavior (e.g., a component failure, strength less than that assumed in the baseline model, etc.) could cause the tender to experience a failure of the criteria set out in the M-1004 standard. This was important to consider during test setup to understand whether the outcome of the impact scenario was highly sensitive to certain conditions in the setup. If certain behaviors that were difficult to control, such as the stiffness of the ballast, had a substantial influence over whether the tender passed or failed the criteria of the scenario, then this behavior would need to be examined and potentially defined more specifically in the standard.

Even if the model demonstrated that the impact was unlikely to cause the tender to fail to meet the M-1004 criteria, the second consideration focused on the safety and practicality concerns associated with running a full-scale test. M-1004 does not prohibit rollover of the tender in a simulation, but it also would complicate the post-test cleanup if rollover happened during the test. Understanding whether the outcome of the simulation was sensitive to certain conditions or assumptions in the model was deemed important to the test preparations and planning.

Since it was beyond the scope of the test preparations to conduct a full characterization program for each difficult-to-control behavior, a modeling plan was developed that attempted to model the upper and lower limits of each behavior of interest. If the results of a simulation at the upper and lower limits of a behavior produced substantially similar results, then the actual value of that behavior would not be critical. If the results of the upper and lower limit analyses were substantially different, however, then that behavior would require further investigation and possibly need to be controlled during the test.

A total of 10 pre-test simulations (Cases A through J) were run using the assembled FE model. In each simulation, one or more behaviors were varied from the baseline model to assess the effects on the outcome. These behaviors are highlighted in each case. The conditions used in each case simulated with the pre-test FE model are summarized in Table 9. Case E and Case J have been italicized in the table since those two cases are discussed in more detail below.

**Table 9. Summary of Pre-test FE Model Conditions**

| Case | Tender-to-locomotive Couplers | Bolster Pin and Center Bowl | Rail Base to Concrete Tie | Track Vertical Stiffness | Track Lateral Stiffness | Stub Track Connection | Impact Speed | Initial Pressure | Notes |
|---|---|---|---|---|---|---|---|---|---|
| A | Yes | Yes | Tied | Default | Default | Discontinuous | 40 mph | 150 psig | Baseline model |
| B | No | Yes | Tied | Default | Default | Discontinuous | 40 mph | 150 psig | Simulate instant coupler failure |
| C | No | No | Tied | Default | Default | Discontinuous | 40 mph | 150 psig | Simulate instant coupler and center pin/bowl failure |
| D[9] | No | Yes | Not Tied | Default | Default | Discontinuous | 40 mph | 150 psig | Simulate instant coupler failure and unrestrained rail |
| *E* | *Yes* | *Yes* | *Not tied* | *Default* | *Default* | *Discontinuous* | *40 mph* | *150 psig* | *Simulate unrestrained rail* |
| F | Yes | No | Tied | Default | Default | Discontinuous | 40 mph | 150 psig | Simulate instant center pin/bowl failure |
| G | Yes | Yes | Tied | Default | Default | Discontinuous | 45 mph | 150 psig | Simulate 5 mph overspeed impact |
| H | Yes | Yes | Tied | Default | Default | Continuous rail | 40 mph | 150 psig | Simulate continuous rail under tender |
| I | Yes | Yes | Tied | Default | Default | 48-ft grade crossing | 40 mph | 150 psig | Simulate upper limit of grade crossing stiffness |
| *J* | *Yes* | *Yes* | *Tied* | *Default* | *Default* | *Continuous rail* | *40 mph* | *25 psig* | *Simulate proposed outage pressure* |

This section contains discussion of two cases, the simulation most closely matching the test conditions (Case J) and the model that simulated an unrestrained rail (Case E). Case J reflected the evolving test conditions, specifically the proposed change to outage pressure under consideration by AAR and the as-built track segment using continuous rail. Case E is presented for comparison since it most closely approximated how the rail in the physical test separated from its restraining clips and rolled over. The results from all the pre-test FE simulations are included in Appendix H.

## 6.1 FE Model

In Figure 57, overall views of the post-impact test for model Case E and model Case J are shown on the top, middle, and bottom, respectively. In all three images the tender and locomotives are observed to be upright and proximate to their initial positions. The cab of the dump truck has been reduced in length significantly in all three cases.

[9]Due to an input error, the results of Case D are not credible. The model is included in this table in the interest of thoroughness. Additional information on this case is found in Appendix H [3].

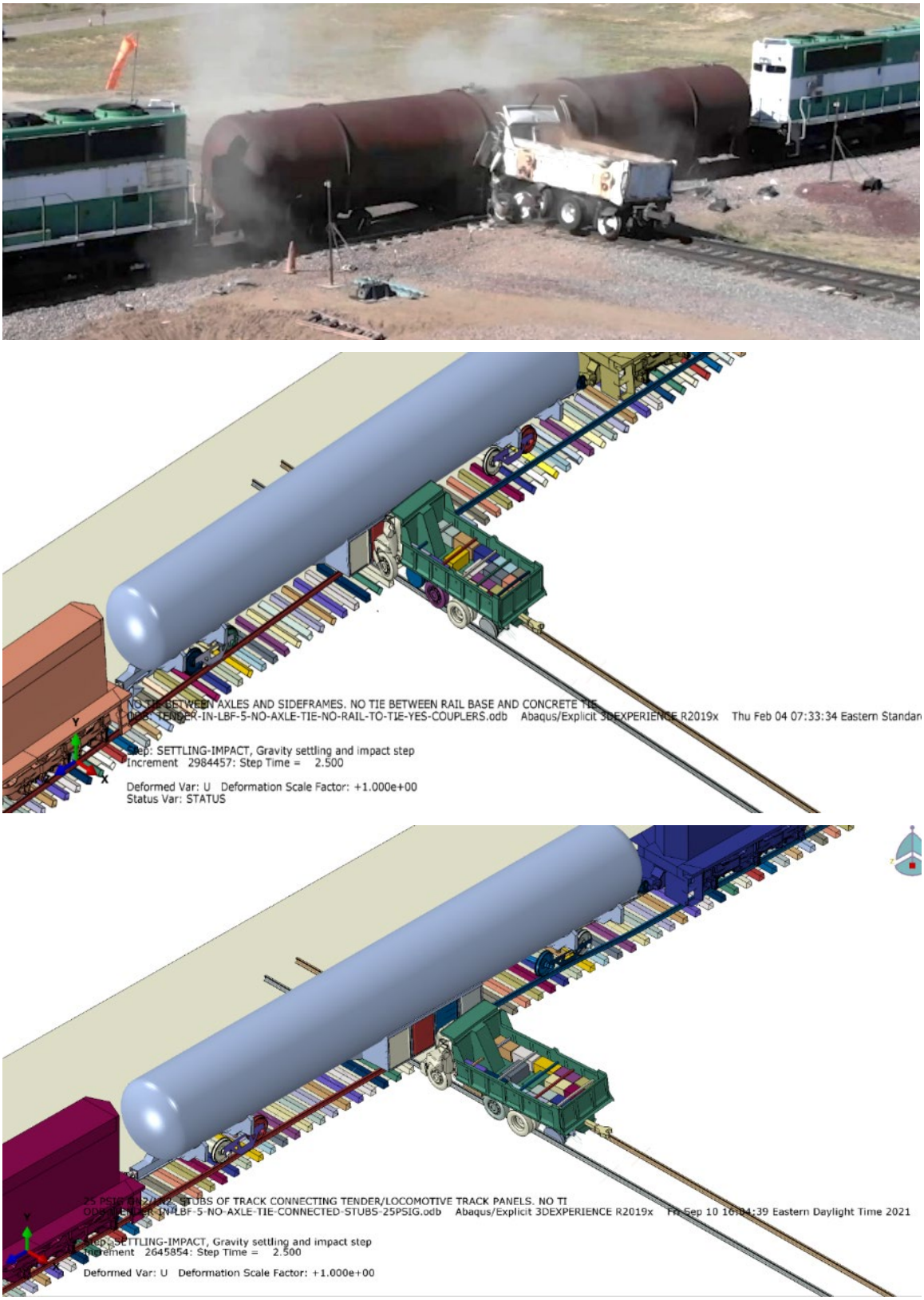


**Figure 57. Post-impact State of Test (top), Model Case E (Center), and Model Case J (Bottom)**

Figure 58 shows side views of the post-impact dump truck for model Case E and model Case J on the top, middle, and bottom, respectively. In the middle image of Figure 58, taken from model Case E, the eastern locomotive has been removed to clarify the view of the dump truck. In this test, the dump truck's lead railroad axle remained on the rails and its rear railroad axle derailed. The dump bed separated from the frame of the truck when the welds attaching the hinge sheared. Neither pre-test FE model included the ability of the dump bed to separate from the frame. Each pre-test FE model had its rear railroad axle derail, with the front axle of the Case J model also derailing.

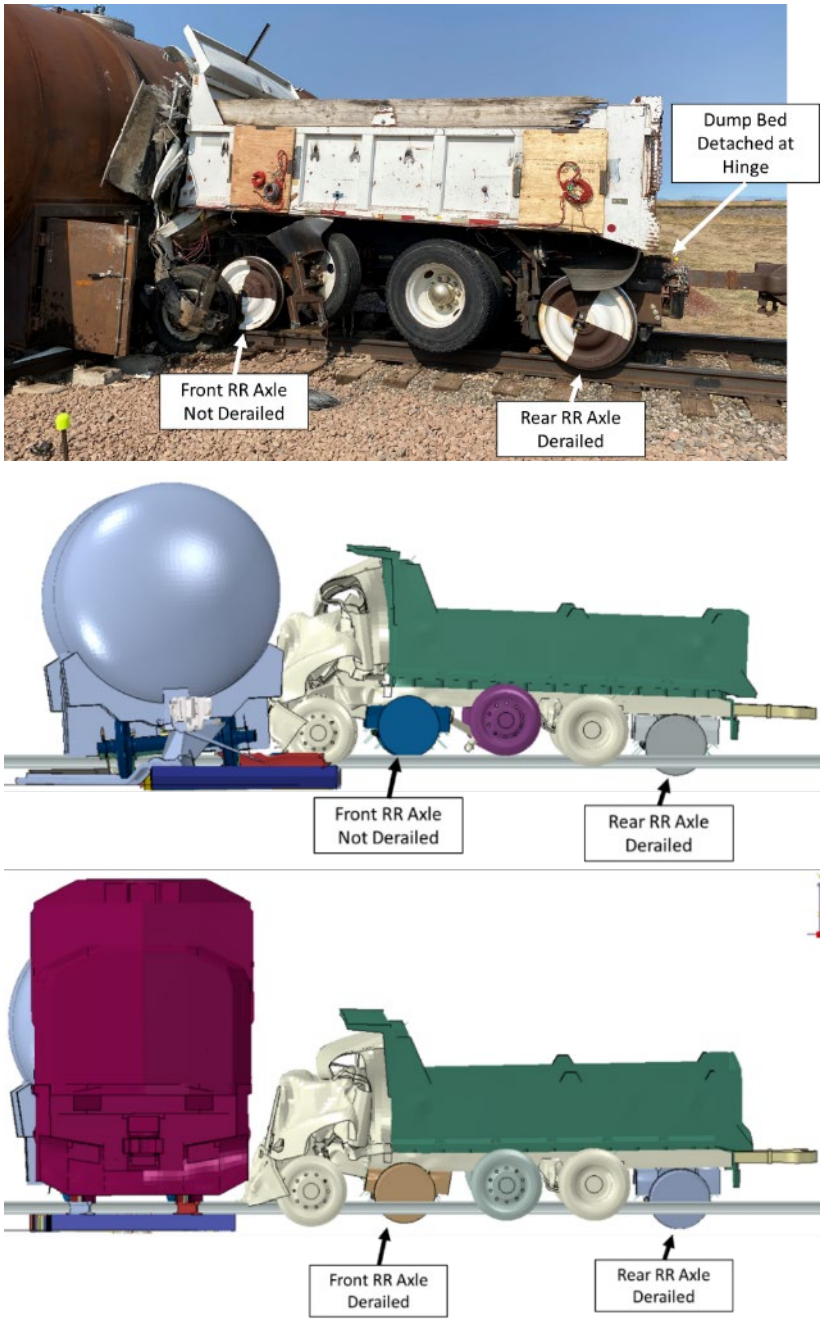


**Figure 58. Post-impact Dump Truck in Test (top), Model Case E (center), and Model Case J (bottom)**

The dump truck's point of impact was aligned with the center of the housing and the housing was offset from the center of the tender by approximately 3.5 feet. However, in the test the housing was offset to the opposite side than in the model. Test and model data are compared to one another in two ways below. First, the model and test data are presented "as-is," meaning that the data from the east end of the test is compared to data from the east end of the model. This means that the data from the "long" end of the tender (i.e., the end with a longer length of shell between the end of the tank and the housing) in the test is compared to data from the "short" end of the tender in the model. Second, the data are presented with an east-west flip of the model data, so that the results from the short end of the tender in the model are compared with the data from the short end of the tender from the test.

The lateral displacement between the pre-test and post-test positions of each tie was obtained for all the model cases to facilitate comparison between the predicted and recorded track shift. The lateral tie displacement obtained from the test is shown alongside the original tie lateral displacement data from Cases E and J on the left side of Figure 59 and Figure 60, respectively. Lateral displacement data from the models was also reflected on the point of impact, and is compared to the reflected data on the right side of Figure 59 and Figure 60 for Cases E and J, respectively.

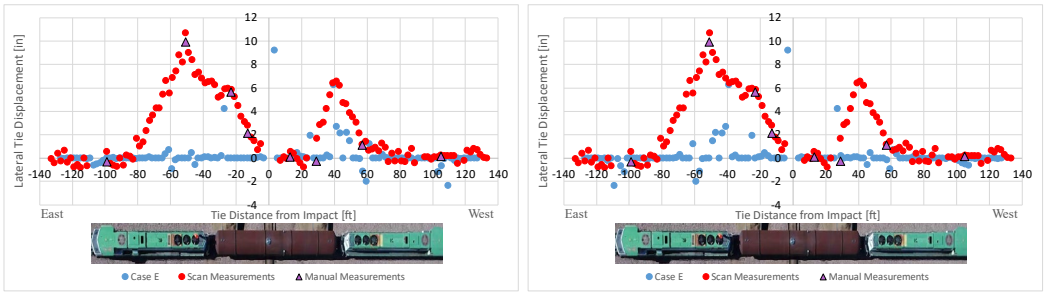


**Figure 59. Comparison of Lateral Tie Displacements Between the Test and Case E (left) and Test and Case E Flipped East-West (Right)**

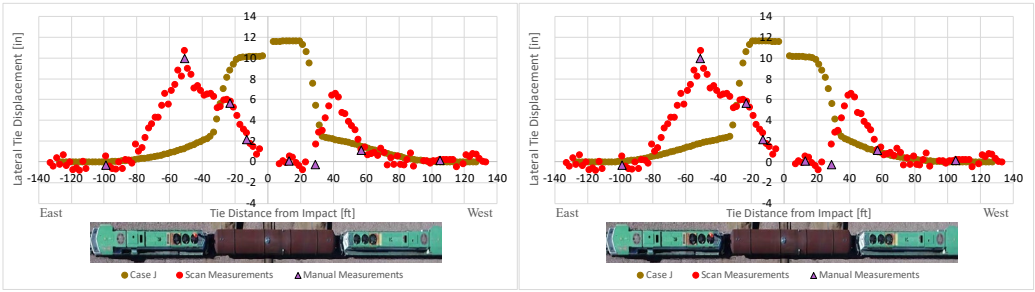


**Figure 60. Comparison of Lateral Tie Displacements Between the Test and Case J (left) and Test and Case J Flipped East-West (Right)**

In each of the model cases, data for velocity over time was recorded at several locations corresponding to the locations of accelerometers in the test. Of the lateral (x), longitudinal (y), and elevational (z) components of these velocities in the tender track coordinate system, longitudinal velocity of the truck was deemed to be the most important to compare between the model and test data. The longitudinal velocities shown below contain an "x" in their channel names since the longitudinal axis of the dump truck corresponds to the lateral axis of the fuel tender track, and vice-versa. Additionally, since the model and test are flipped in the longitudinal

direction (y axis), velocities on the left side of the dump truck in the test correspond to their right-side analogue in the test, and vice-versa.

Accelerometer data from the test was integrated to obtain velocity data at the locations of the accelerometers. However, due to damage from the impact, several of the data channels in the test data were unusable beyond certain times and could not be fully compared to the model data. Plots in this section compare only the data channels which did not become unusable due to damage. Comparison of all data channels is included in Appendix H.

Additionally, the velocity data for channel VRMX was compared with its direct model analogue (left side of dump truck vs. left side of model), as well as its reflected model analogue (left side of dump truck vs. right side of model). Plots of the test velocity data over time of channels VCMX, VCGX, and VRMX were compared with Case E in Figure 61, and Case J in Figure 62.

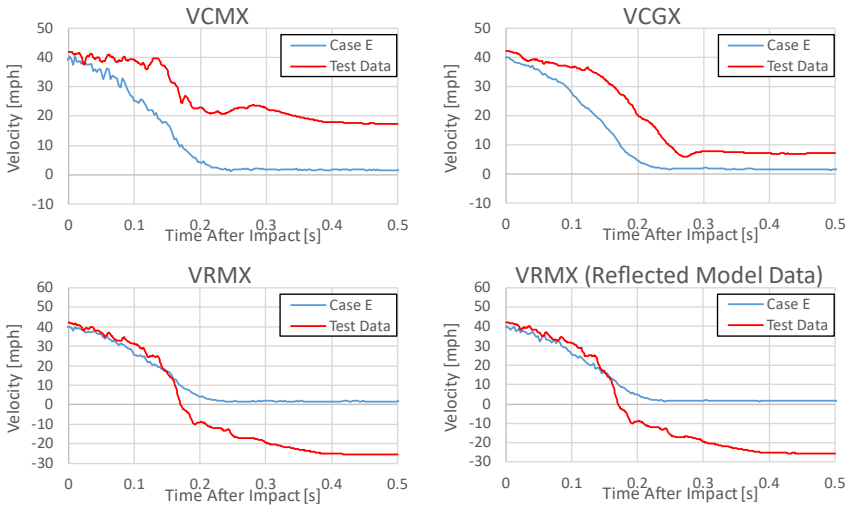


**Figure 61. Measured and Case E Velocities from Channels VCMX, VCGX, and VRMX. VRMX Test Data is also Compared with Reflected Model Data.**

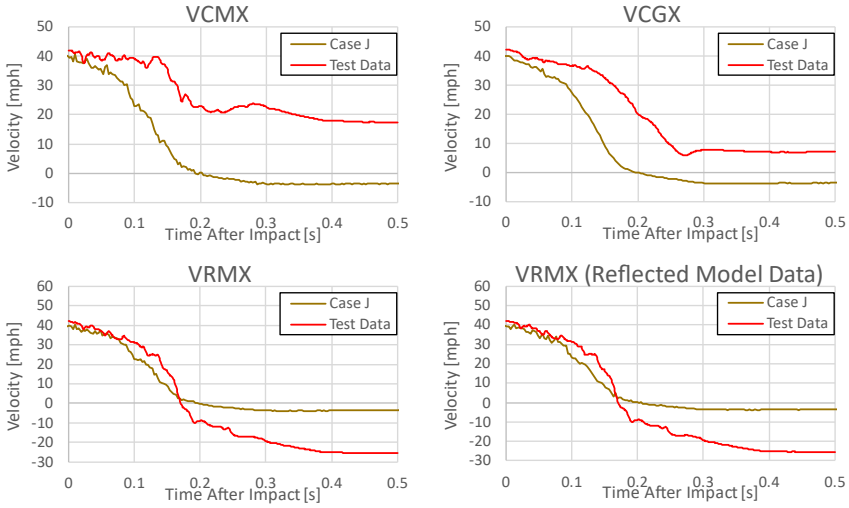


**Figure 62. Measured and Case J Velocities from Channels VCMX, VCGX, and VRMX. VRMX Test Data is also Compared with Reflected Model Data.**

In each of the model cases, acceleration for each channel was derived from the corresponding velocity data channel using a 5-point Stencil calculation. Like the velocity plots above, acceleration plots in this section compare only the data channels which did not become unusable due to damage, with a comparison of all acceleration data channels in Appendix H.

Additionally, the acceleration data for channel VRMX was compared with its direct model analogue (left side of dump truck vs. left side of model), as well as its reflected model analogue (left side of dump truck vs. right side of model). Plots of the test acceleration data over time of channels VCMX, VCGX, and VRMX were compared with Case E in Figure 63 and Case J in Figure 64.

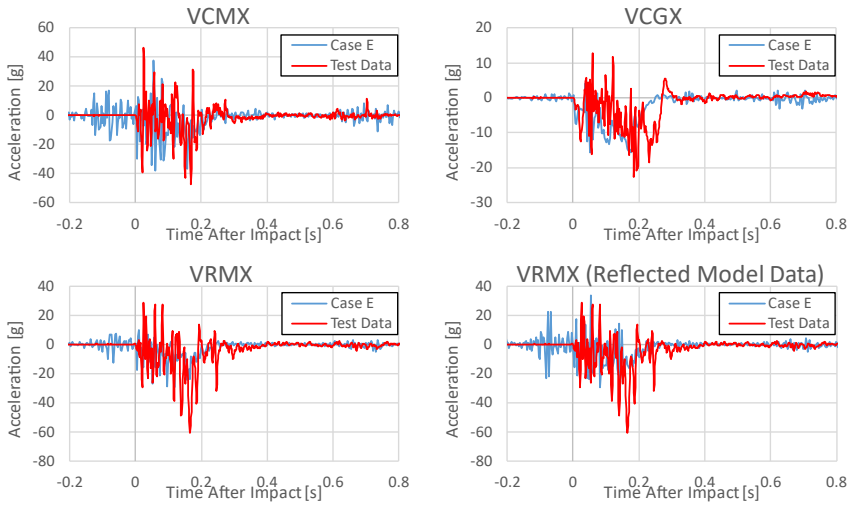


**Figure 63. Measured and Case E Accelerations from Channels VCMX, VCGX, and VRMX. VRMX Test Data is also Compared with Reflected Model Data.**

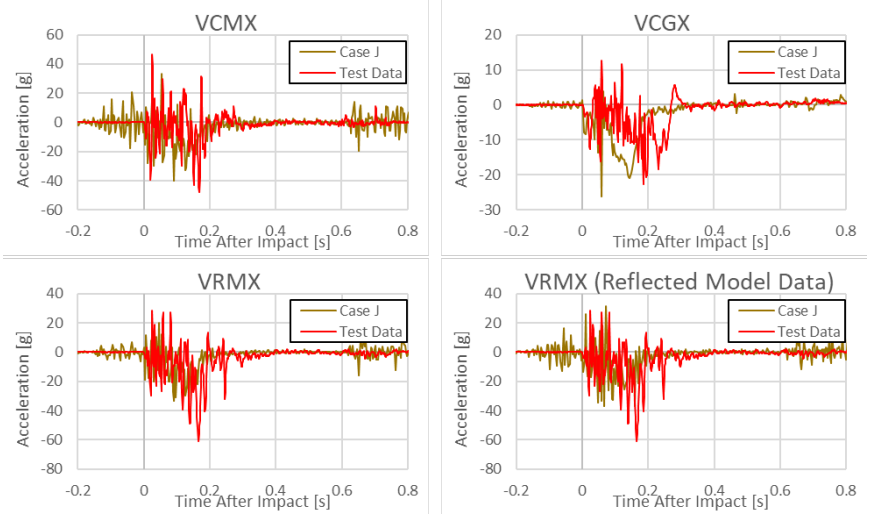


**Figure 64. Measured and Case J Accelerations from Channels VCMX, VCGX, and VRMX. VRMX Test Data is also Compared with Reflected Model Data.**

String potentiometers were installed within the housing surrounding the external piping and valves on the impacted side of the tender. One string potentiometer was installed in the housing compartment on the east side of the point of impact above the piping passthrough (referred to as

the “high” potentiometer, above the passthrough) ; another was installed in the compartment on the west side of the point of impact below the piping passthrough (referred to as the “low” potentiometer, below the passthrough). Displacement data were requested from approximately the same areas in the FE model. The string potentiometers in the east and west housing compartments are shown alongside the corresponding locations in the FE model in Figure 65 and Figure 66.

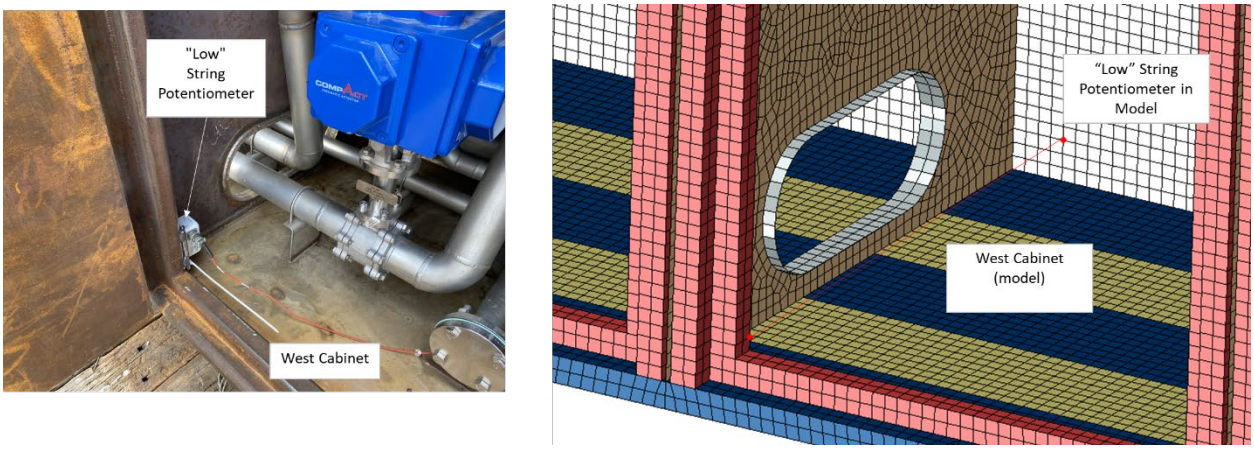


**Figure 65. West Housing String Potentiometer Location in Test (left) and FE Model (Right)**

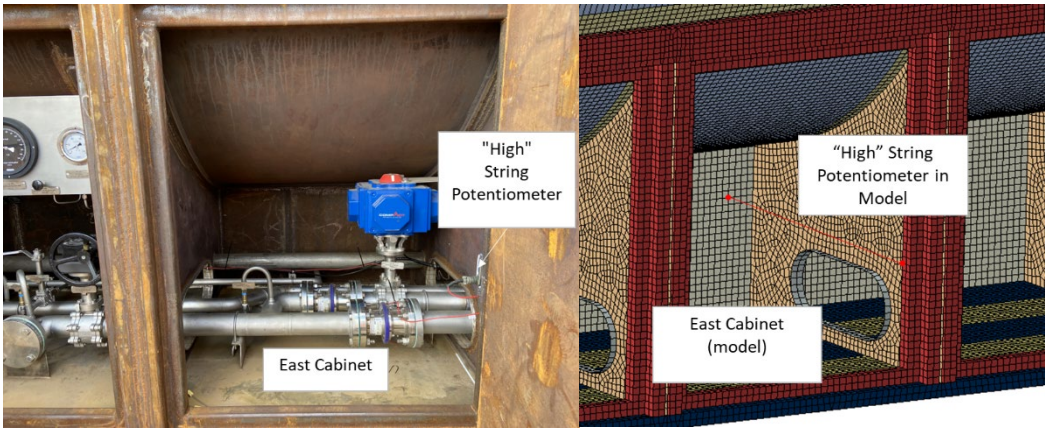


**Figure 66. East Housing String Potentiometer Location in Test (left) and FE Model (right)**

The complete set of internal string potentiometer results compared between each model case and the test data are provided in Appendix H. Results from Cases E and J are presented and discussed below. The results contain two different test and model comparisons for each case. Recall that the pre-test FE model had the tender’s east and west ends flipped relative to the position of the tender in the test. The model results are compared with the test results first without accounting for this swap. That is, the relative displacement of the east housing in the model used nodes on the “high” side of the passthrough and the relative displacement of the west housing used nodes on the “low” side of the passthrough, consistent with the placement of string potentiometers in the tender. Model results are also presented for nodes representing the relative displacement of the high side of the western housing and the low side of the eastern housing, effectively flipping the model results to account for the discrepancy between tender arrangement in the test and the pre-test models. Figure 67 and Figure 69 present the results from Case E and Case J,

respectively, plotted against test data taken from the corresponding sides. Figure 68 and Figure 70 present the results from Case E and Case J, respectively, with the model locations swapped from east-west to match the relative positions of the string potentiometers in the test.

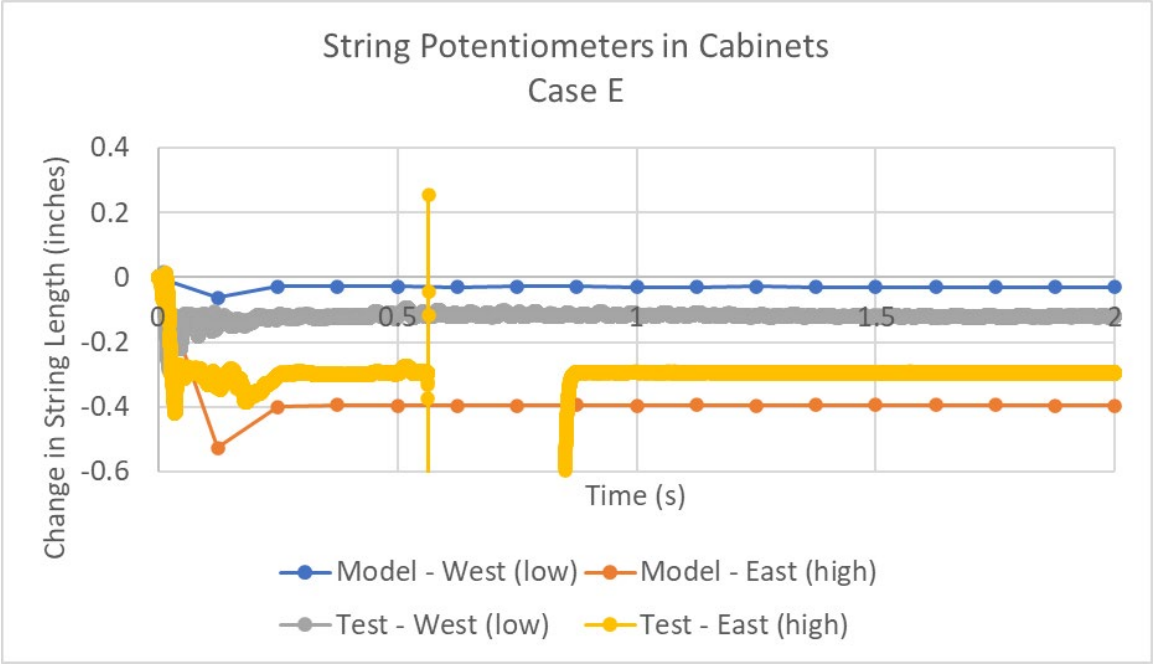


**Figure 67. String Potentiometers in Piping Housing, Case E**

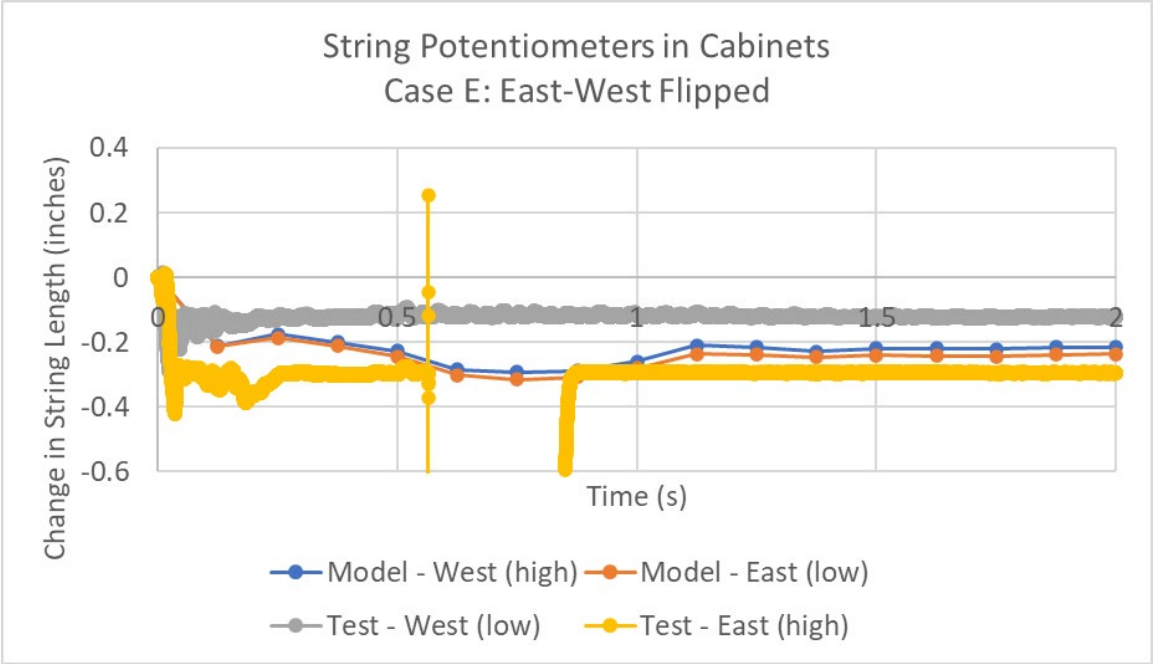


**Figure 68. String Potentiometers in Piping Housing, Case E, East-West Flipped**

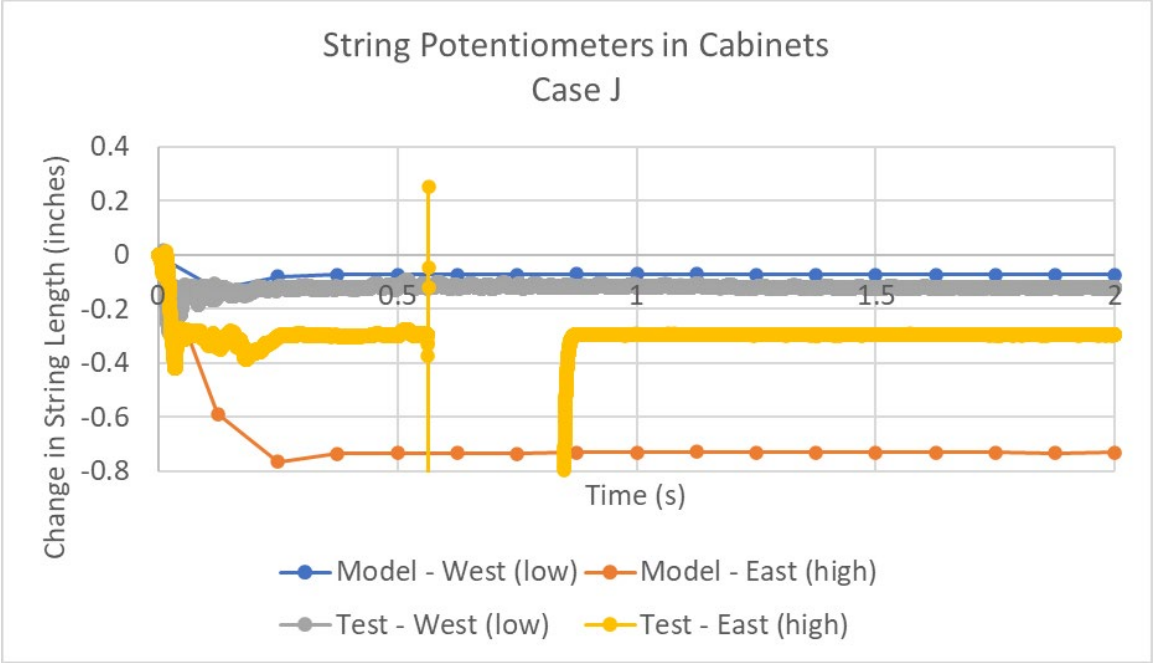


**Figure 69. String Potentiometers in Piping Housing, Case J**

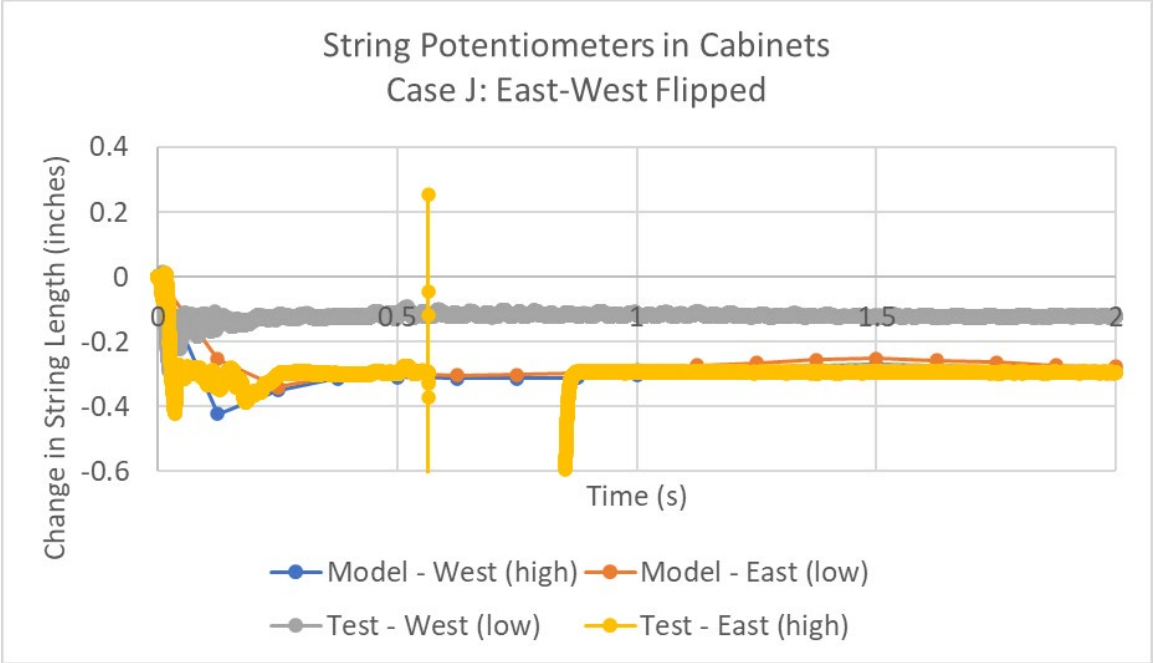


**Figure 70. String Potentiometers in Piping Housing, Case J, East-West Flipped**

In general, the test measurements of housing deformation are consistent with the pre-test model results. While no model result matches the test data exactly, the deformations in both models and

in the test were minimal for both instrumented housing. The model results bound the results of the test measurements, which was the goal of the pre-test modeling.

The tender head displacement test data is compared directly with Case E in Figure 71 and Case J in Figure 73, and compared with the reflected Case E in Figure 72 and the reflected Case J in Figure 74.

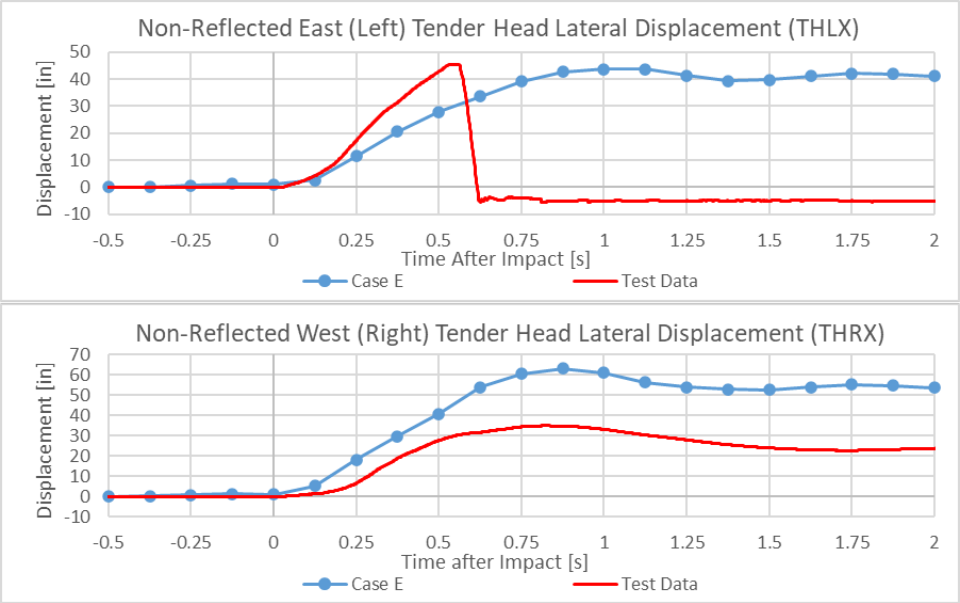


**Figure 71. Lateral Displacement of the East and West Tender Heads for Case E Directly Compared with Test Data**

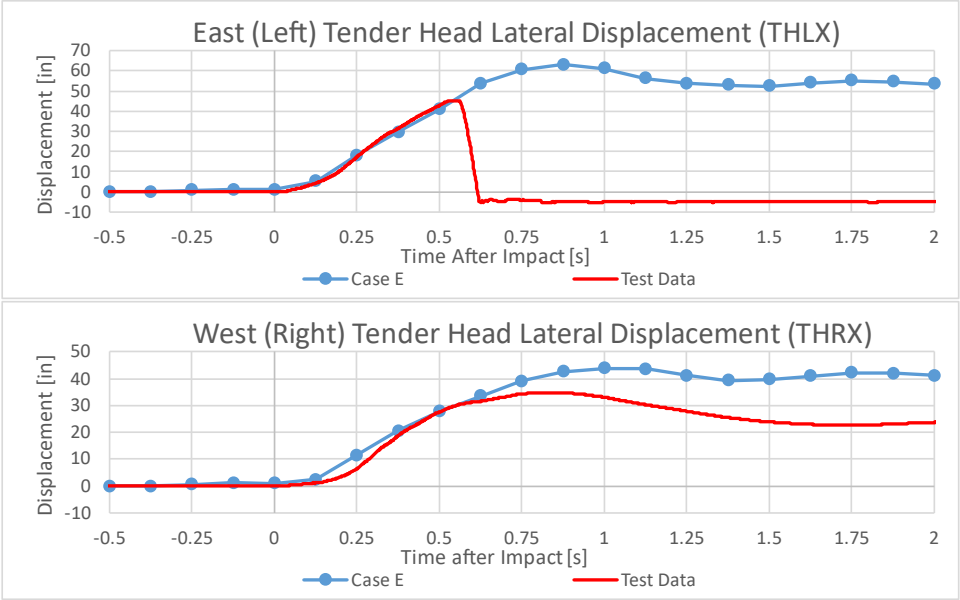


**Figure 72. Reflected Lateral Displacement of the East and West Tender Heads for Case E Compared with Test Data**

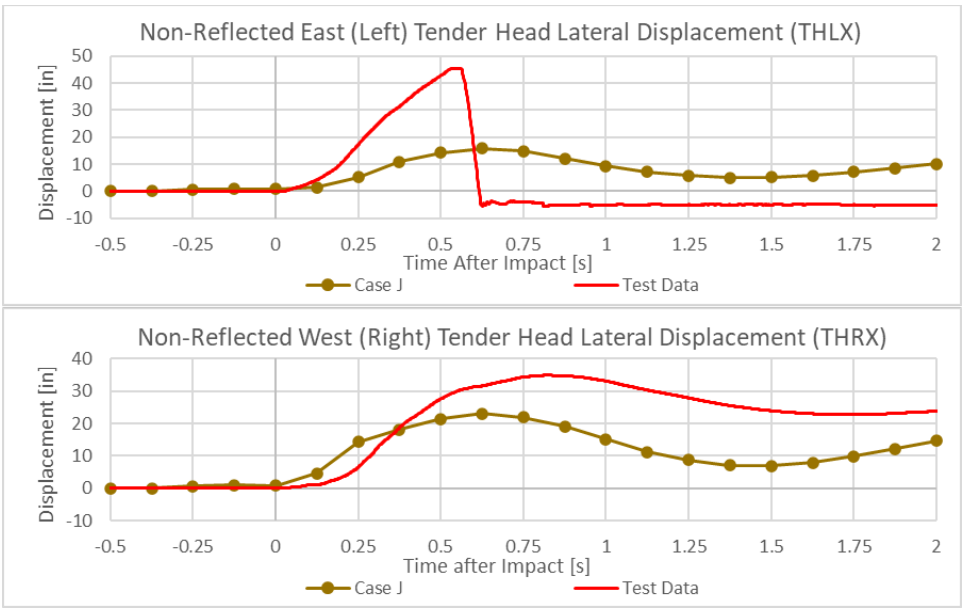


**Figure 73. Lateral Displacement of the East and West Tender Heads for Case J Directly Compared with Test Data**

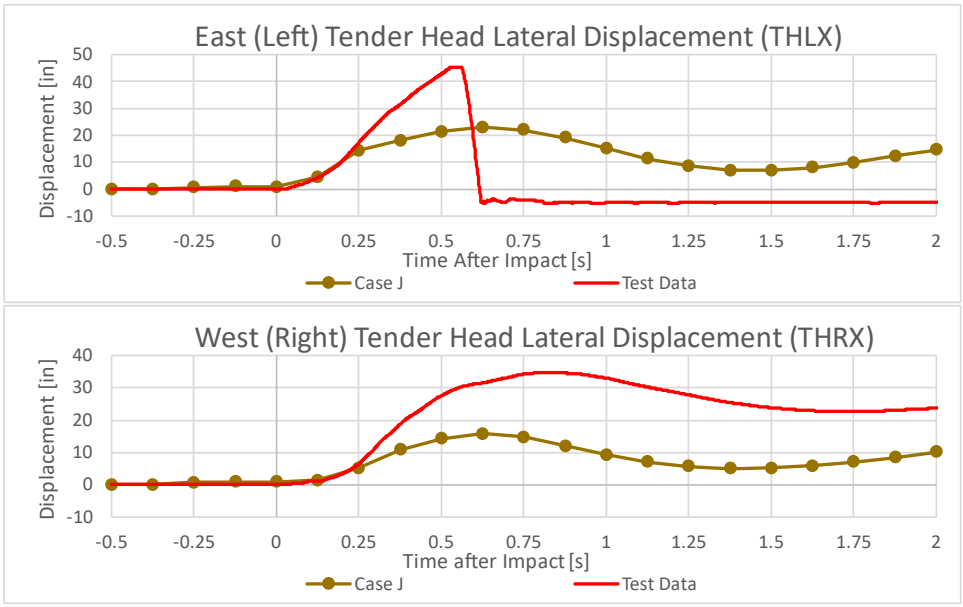


**Figure 74. Reflected Lateral Displacement of the East and West Tender Heads for Case J Compared with Test Data**

The head displacement data measured during the test was consistent with the results of these two pre-test models. In both models and in the test the two ends of the tender had slightly different displacement-time histories. This was expected, as the point of impact on the housing was not centered on the centerline of the tender. The test-model agreement tended to be better earlier in the impact event, with larger discrepancies seen later in the impact event. Note that the test used rollover inhibitors which limited the tender's travel, but the models did not include these features.

Figure 75 shows the string potentiometer across the locomotive-to-tender coupled interface from the test on the top and from the corresponding location in the FE model on the bottom. In both images the path of the string has been highlighted for clarity. The string was principally oriented parallel to the coupler shanks (i.e., transverse to the direction of impact). String potentiometers only are able to measure an extension or a retraction of the string as a function of time. The data collected by these instruments cannot be used to identify which direction(s) the ends of the string moved to produce an extension or retraction. For example, a string extension could be caused by the locomotive and tender moving apart from each other longitudinally, or by the tender rolling parallel to the direction of impact while the locomotive remained stationary. The results of these string potentiometer measurements should be interpreted and compared with model results with caution due to this inherent limitation in the data.

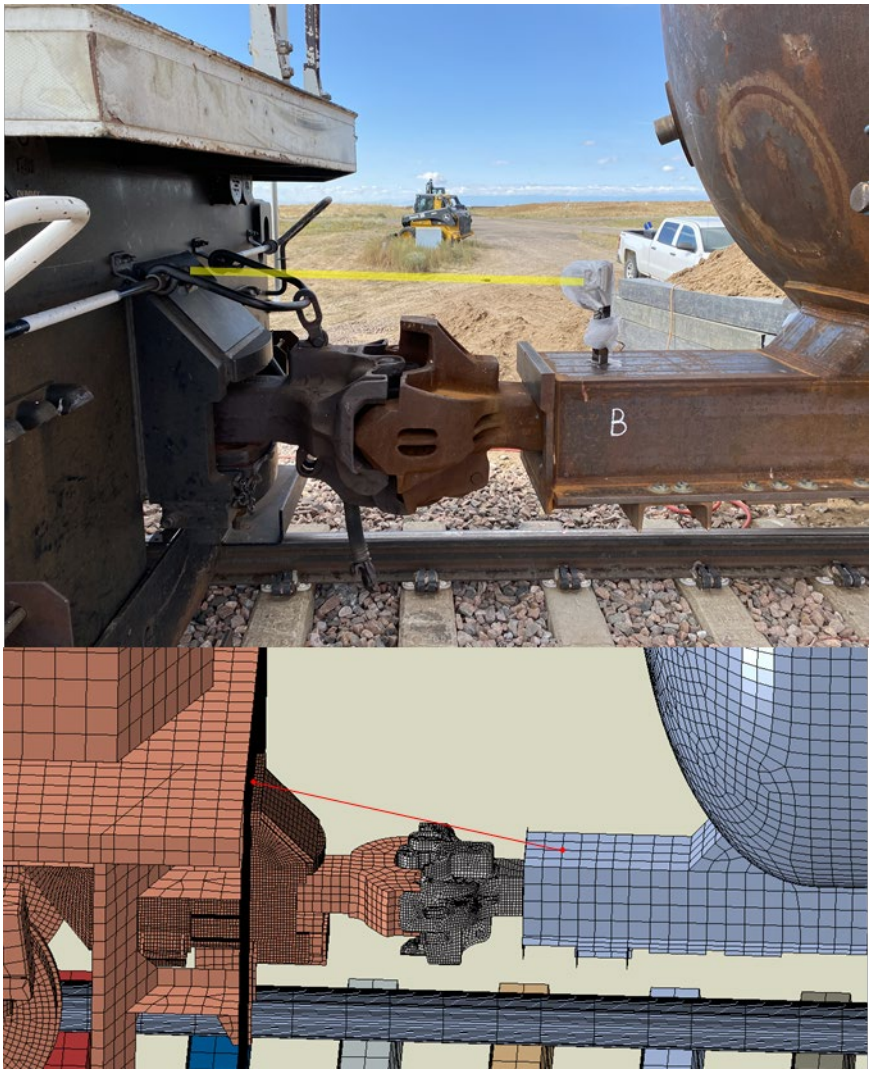


**Figure 75. Locomotive-to-tender String Potentiometer in Test (top) and FE Model (bottom)**

Figure 76 contains plots of the string potentiometer measurements across the east (top) and west (bottom) coupled interfaces in the test and FE model for Case E. In this figure, the left and right side results from the model are plotted against the same side results of the test. Figure 77 contains the same data, but with the left side measurements from the test compared to the right

side measurements from the model and vice versa. This flipped comparison was included to account for the tender being flipped east-west in the test compared to the pre-test FE model.

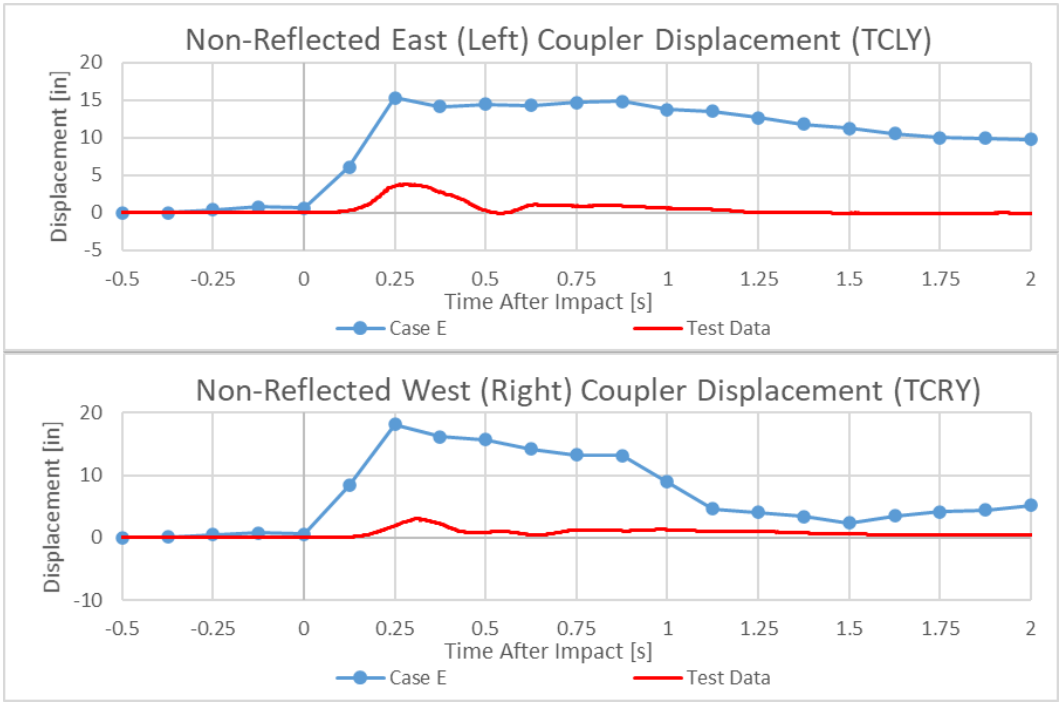


**Figure 76. Locomotive-to-Tender Coupler Displacements for Case E Directly Compared with Test Data**

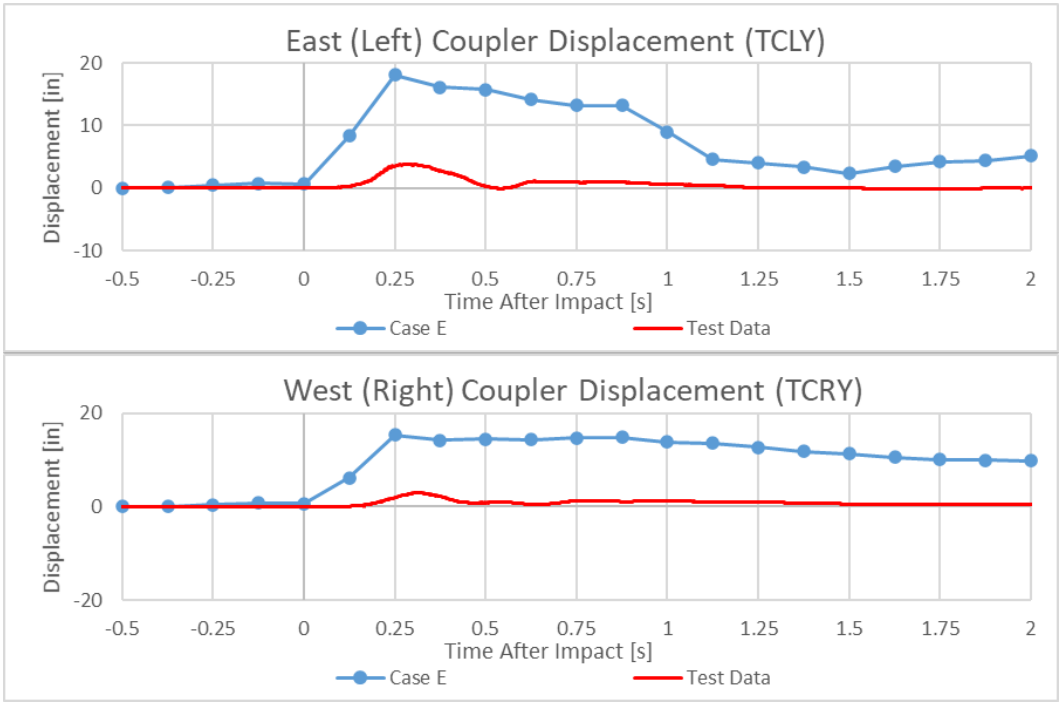


**Figure 77. Reflected Locomotive-to-Tender Coupler Displacements for Case E Compared with Test Data**

Figure 78 contains plots of the string potentiometer measurements across the left (top) and right (bottom) coupled interfaces in the test and FE model for Case J. In this figure, the left and right side results from the model are plotted against the same side results of the test. Figure 79 contains the same data, but with the left side measurements from the test compared to the right side measurements from the model and vice versa.

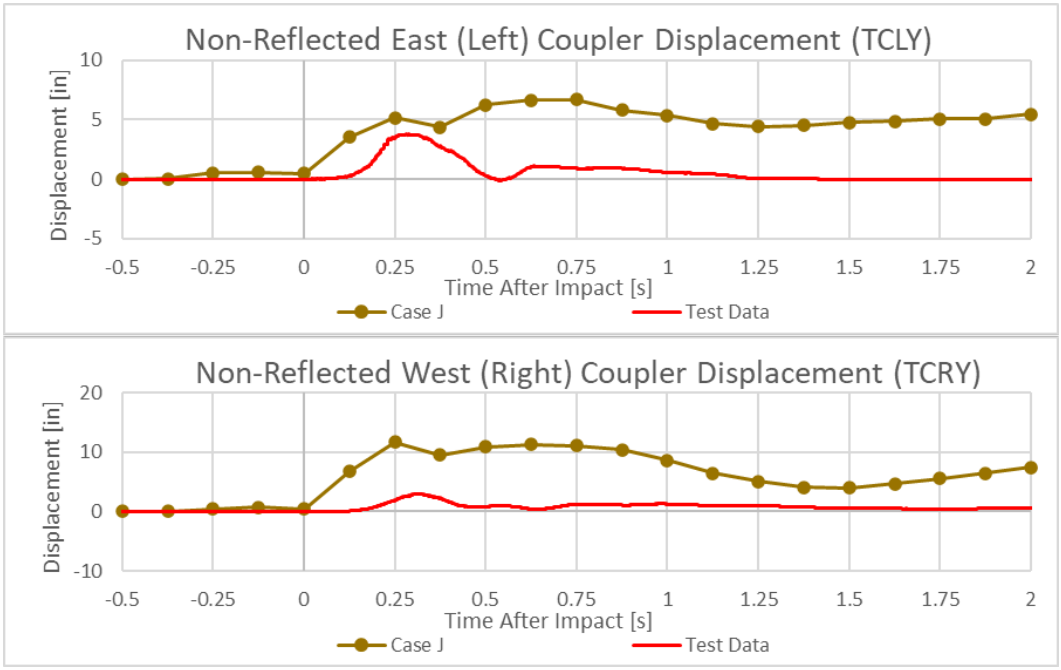


**Figure 78. Locomotive-to-Tender Coupler Displacements for Case J Directly Compared with Test Data**

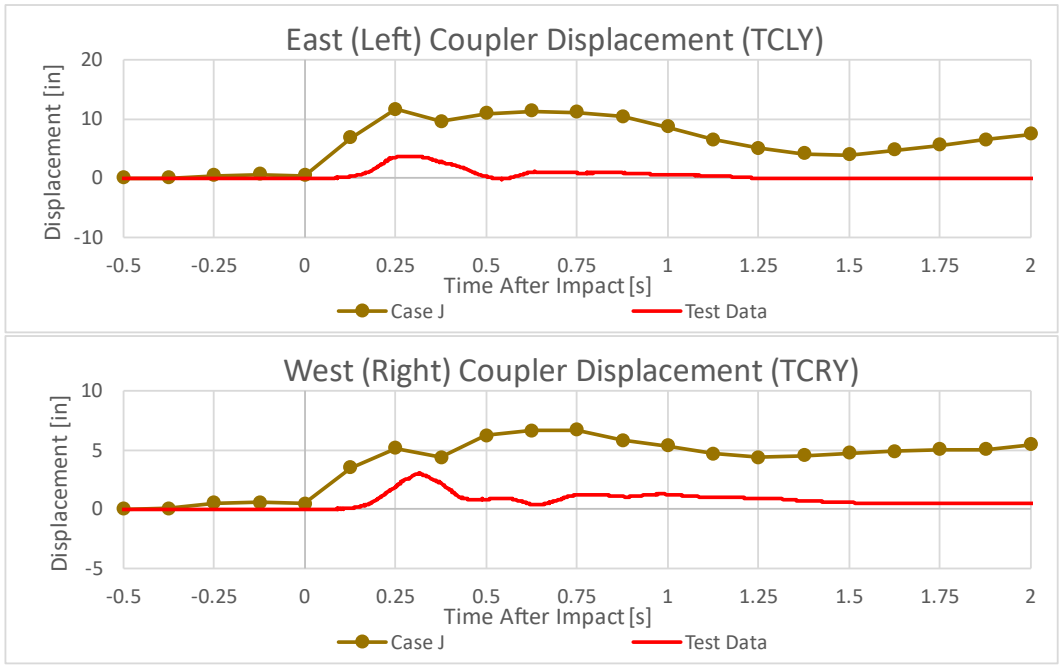


**Figure 79. Reflected Locomotive-to-Tender Coupler Displacements for Case J Compared with Test Data**

Both Case E and Case J models produced string potentiometer displacements that were larger than the test measurements at both coupled interfaces. The Case J results qualitatively agreed with the test measurements, featuring an initial peak value followed by a decrease in value. Rollover inhibitors included in the test setup that were not included in the model could have served to restrict the amount of relative coupled interface motion that could occur in the test.

## 6.2 Lumped Mass MBD Model

Like the FE model, the lumped mass MBD model was developed to find the bounds of possibilities that were likely to occur during the test. However, this model was less concerned with whether the tender would meet the requirements in M-1004 and was instead focused on macro behaviors during the test that could affect the outcome. A primary concern was tender rollover, which could create secondary impact forces on the housing that could complicate interpretation of the test results as well as test cleanup. MBD test cases helped to determine whether to build a roll inhibitor for the test.

Six parameters were varied from baseline: the force cutoff of the rotation coupler spline, the shape of the rotation coupler spline, the impact speed of the dump truck, the allowable distance of track panel shift, the truck rollback "braking" force, and the primary dump truck/tender force-crush location above ground. While dozens of parameters could have been selected, these six were chosen because they were shown to be likely points of failure during the model build process (e.g., the couplers failing in torsion) or they were unknowns that would not be determined until test day (e.g., speed and panel shift). The conditions used for each case are summarized below in Table 10.

**Table 10. Summary of Pre-test Lumped Mass Model Conditions**

| Case | Coupler Cutoff | Coupler Spline | Speed (mph) | Panel Shift (m) | Truck Rollback | Force Location Height | Notes |
|---|---|---|---|---|---|---|---|
| I | 202,500 n-M (149,356 ft-lbs) | Linear stiffness | 40 | 0.3 (11.811 in) | Yes | 1.3462 m (53 in) | Rollover |
| II | none | Linear stiffness | 40 | 0.3 (11.811 in) | Yes | 1.3462 m (53 in) | Rollover |
| III | 1,550,000 n-M (1,143,221 ft-lbs) | Abaqus output | 40 | 0.3 (11.811 in) | Yes | 1.3462 m (53 in) | No rollover |
| IV | 202,500 n-M (149,356 ft-lbs) | Linear stiffness | 45, 35 | 0.3 (11.811 in) | Yes | 1.3462 m (53 in) | Rollover |
| V | 202,500 n-M (149,356 ft-lbs) | Linear stiffness | 40 | 0.6 (23.622 in) | Yes | 1.3462 m (53 in) | Rollover |
| VI | 202,500 n-M (149,356 ft-lbs) | Linear stiffness | 40 | 0.3 (11.811 in) | No (friction on) | 1.3462 m (53 in) | Rollover |
| VII | 202,500 n-M (149,356 ft-lbs) | Linear stiffness | 40 | 0.3 (11.811 in) | Yes | 0.8462 m (33.315 in) | No rollover |

A tender roll angle measurement was plotted to examine how much the tender car rolled in each case. This measurement is the angle between a vector fixed to the tender carbody's vertical and the global vertical. Before the tender car is struck, this measurement is zero. This measurement

also settles back to zero in the cases where the car does not completely roll over, while it continues to increase when there is tender rollover. Figure 80 shows the time history of this measure for all cases.

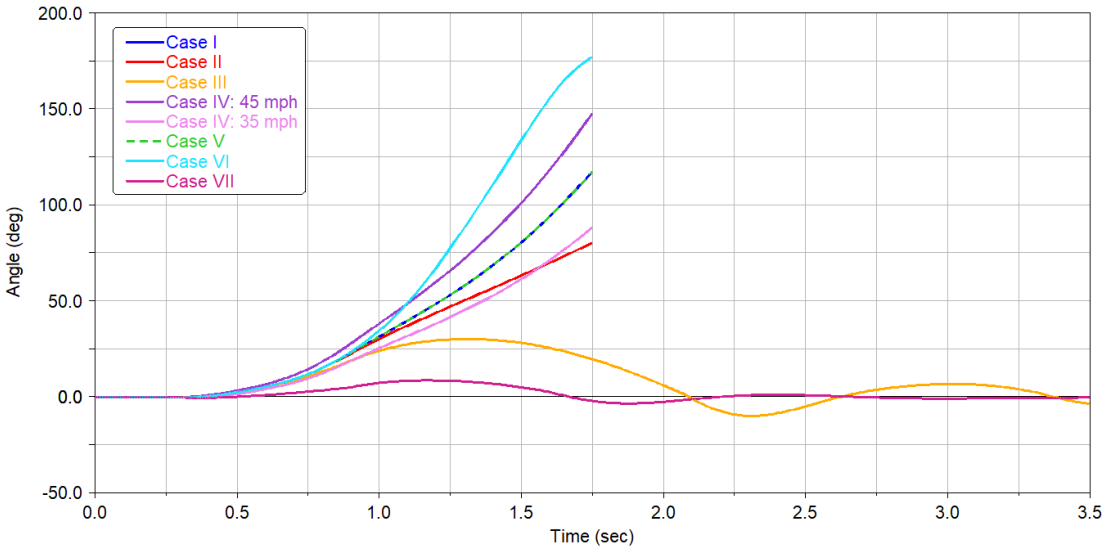


**Figure 80. Tender Roll Time History for All Cases**

Further details about the modeling effort and results for each case are found in Appendix I.

# 7. Conclusions

Researchers developed a test derived from the M-1004 standard that emulated the highway-grade crossing impact between a dump truck and an LNG fuel tender and executed the test on September 22, 2021, at the TTC in Pueblo, Colorado. A dump truck was converted to a hi-rail vehicle, loaded to 81,350 lbf, and run into the valve protective housing on the side of an LNG fuel tender. The dump truck impacted the fuel tender, at the location of the protective housing for the critical valving, at 42.6 mph. The tender was loaded with approximately 13,123 gallons of LN2.

The objective of the test was to demonstrate the crashworthiness of the protective housing surrounding the external piping and valves and the proper functioning of the cut-off valves. The post-impact analysis of the fuel tender showed little damage to the protective housing and no harm to the valves within it, proving the crashworthiness of the protective housing. The functionality of the cut-off valve was proven shortly after the impact.

The test conditions either met or exceeded the requirements specified in M-1004; the weight (81,350 lbf) and velocity (43 mph) of the dump truck were slightly above the 80,000 lbf and 40 mph requirements given in M-1004. The test produced the results required by M-1004 (i.e., no leakage from outer tank, inner tank not breached, and only release occurring through the PRV). The tender used in this test was designed to meet the quasi-static requirements for the protective housing specified in M-1004. The test showed that a tender designed to meet the static requirements in M-1004, may also meet the dynamic impact requirements.

## 8. References


[1] Association of American Railroads (2020, draft). Manual of Standards and Recommended Practices - Interoperable Fuel Tenders for Locomotives (M-1004). Association of American Railroads, Washington, DC.

[2] Iden, M. (2012). Liquefied Natural Gas (LNG) as a Freight Railroad Fuel: Perspective From a Western U.S. Railroad. *ASME 2012 Rail Transportation Division Fall Technical Conference*, Omaha, NE.

[3] Kirkpatrick, S. W., Wagner C., & Northrup, C. (2019). Crashworthiness and Puncture Protection Analyses of LNG Tenders. Association of American Railroads, Washington, DC.

[4] The Engineering Toolbox (n.d.) Air - Density and Specific Volume vs. Altitude. Accessed 17 March 2020.

[5] United States Geological Survey (USGS) (2002). Geographic Names Information System (GNIS) Detail - City of Pueblo. Accessed 18 January 2022.

[6] Lemmon, E. W., Bell, I. H., Huber, M. L., & McLinden, M. O. (2023). Thermophysical Properties of Fluid Systems. *NIST Chemistry WebBook, NIST Standard Reference Database Number 69*, P. J. Linstrom and W. G. Mallard, Eds., National Institute of Standards and Technology.

[7] Belport, S., Carolan, M., Trevithick, S., Eshraghi, S., & Krishnamurthy, A. (2022). Side Impact Test and Analyses of a DOT-113 Surrogate Tank Car Filled with Cyrogenic Lading (Report No. DOT/FRA/ORD-22/33). Federal Railroad Administration.

[8] Federal Railroad Administration (2020). CFR 2020: Part 213 - Track Safety Standards. Accessed 15 December 2021.

[9] SAE International (2022). Instrumentation for Impact Test - Part 1: Electronic Instrumentation, Standard J211/1_202208. SAE, Warrendale, PA.

[10] Kirkpatrick, S. W., Rakoczy, P., MacNeill, R. A., & Anderson, A. (2015). Side Impact Test and Analyses of a DOT 111 Tank Car (Report No. DOT/FRA/ORD-15/30). Federal Railroad Administration, Washington, DC.

[11] Kirkpatrick, S. W. (2010). Detailed Puncture Analyses of Various Tank Car Designs - Final Report - Revision 1. Applied Research Associates, Mountain View, CA.

[12] Rakoczy, P., Carolan, M., Eshraghi, S., & Gorhum, T. (2019). Side Impact Test and Analyses of a DOT-117 Tank Car (Report No. DOT/FRA/ORD-19/13). Federal Railroad Administration, Washington, DC.

[13] Trevithick, S., Carolan, M., & Eshraghi, S. (2020). Side Impact Test and Analyses of a DOT-111 Tank Car (Report No. DOT/FRA/ORD-15/30). Federal Railroad Administration, Washington, DC.

[14] Carolan, M. E., Jeong, D. Y., Perlman, B., Murty, Y. V., Namboodri, S., Kurtz, B., Elzek, R. K., Anankitpaiboon, S., Tunna, L., & Fries, R. (2013). Application of Welded Steel Sandwich Panels for Tank Car Shell Impact Protection (Report No. DOT/FRA/ORD-13/19). Federal Railroad Administration, Washington, DC.

[15] Rakoczy, P., & Carolan, M. (2016). Side Impact Test and Analysis of a DOT-112 Tank Car (Report No. DOT/FRA/ORD-16/38). Federal Railroad Administration, Washington, DC.

[16] Carolan, M., & Rakoczy, P. (2019). Side Impact Test and Analyses of a DOT-105 Tank Car (Report No. DOT/FRA/ORD-19/12). Federal Railroad Administration, Washington, DC.

[17] Wilson, N., Eshraghi, S., Trevithick, S., Carolan, M., & Rakoczy, P. (2020). Side Impact Test and Analyses of a DOT-105 Tank Car – 6 X 6 Inch Indenter (Report No. DOT/FRA/ORD-20/38). Federal Railroad Administration, Washington, DC.

[18] Trevithick, S., Carolan, M., Eshraghi, S., & Wilson, N. (2021). Side Impact Test and Analyses of a Legacy DOT-113 Tank Car (Report No. DOT/FRA/ORD-21/28). Federal Railroad Administration, Washington, DC.

[19] The Engineering Toolbox (2004). Universal and Individual Gas Constants. Accessed 12 March 2020.

[20] National Transportation Research Center, Inc. FEM Models for Semitrailer Trucks.

[21] Buth, C. E., Williams, W. F., Brackin, M. S., Lord, D., Geedipally, S. R., & Abu-Odeh, A. Y. (2010). Analysis of Large Truck Collisions with Bridge Piers: Phase 1. Report of Guidelines for Designing Bridge Piers and Abutments for Vehicle Collisions (Report No. FHWA/TX-10/9-4973-1). Texas A&M Transportation Institute.

[22] Buth, C. E., Brackin, M. S., Williams, W. F., & Fry, G. T. (2011). Collision Loads on Bridge Piers: Phase 2. Report of Guidelines for Designing Bridge Piers and Abutments for Vehicle Collisions (Report No. FHWA/TX-11/9-4973-2). Texas A&M Transportation Institute.

[23] American Railway Engineering and Maintenance-of-Way Association (1999). AREMA Manual for Railway Engineering. AREMA, Lanham, Maryland.

[24] Jeong, D. Y., Woelke, P. B., Nied, H. F., DuPont, J. N., Kizildemir, S., Fletcher, F. B., & Hutchinson, J. W. (2019). Defect Growth Characterization in Modern Rail Steels. *ASME/IEEE 2019 Joint Rail Conference*, Snowbird, UT.

[25] LBFoster (n.d.). CXT (R) Concrete Ties - 200S-13 Tie. Accessed 1 February 2022.

[26] MSC Software Corporation (Hexagon) (2017). About Adams 2017. Hexagon, Irvine, CA.

[27] Conrail Historical Society (n.d.). SD60 Technical Information.

[28] Marta, H. A., Mels, K. D., & Itami, G. S. (1972). Design Features and Performance Characteristics of the High Traction, Three-Axle Truck. *ASME/IEEE 1972 Joint Rail Conference*, Jacksonville, FL.

[29] Kish, A. (2011). On the Fundamentals of Track Lateral Resistance. *AREMA 2011 Annual Conference*, Minneapolis, MN.

[30] 49 CFR § 238.205 - Anti-climbing mechanism.

[31] American Public Transportation Association (2012). Pushback Couplers in Passenger Rail Equipment (Report No. APTA PR-CS-RP-019-11). APTA Standards Development Committee, Washington, DC.

[32] Trent , R., Prabhakaran, A., & Sharma, V. (2010). Torsional Stiffness of Railroad Coupler Connections (Report No. DOT/FRA/ORD-10/13). Federal Railroad Administration, Washington, DC.

## Abbreviations and Acronyms

| ACRONYM | DEFINITION |
|---|---|
| ASTM | American Society for Testing and Materials (former) |
| AAR | Association of American Railroads |
| ALE | Arbitrary Lagrangian-Eulerian |
| ARA | Applied Research Associates |
| AREMA | American Railway Engineering and Maintenance-of-Way Association |
| B-W | Bao-Wierzbicki |
| CAD | Computer-Aided Design |
| CCSB | Constant Contact Side Bearing |
| CFC | Channel Frequency Class |
| DB | DataBRICK |
| DOF | Degrees of Freedom |
| DOT | Department of Transportation |
| FAST | Facility for Accelerated Service Testing |
| FB | Fire block |
| FRA | Federal Railroad Administration |
| FEA | Finite Element Analysis |
| FE | Finite Element |
| GN2 | Gaseous Nitrogen |
| HMR | Hazardous Materials Regulations |
| HD | High Definition |
| HHFT | High-hazard Flammable Trains |
| ISO | International Organization for Standardization |
| kip | Kilopound |
| LIDAR | Light Detection and Ranging |
| LNG | Liquefied Natural Gas |
| LN2 | Liquid Nitrogen |
| MBD | Multibody Dynamics |
| MLI | Multi-layer Insulation |
| MTU | Multiple Trigger Unit |

| ACRONYM | DEFINITION |
|---|---|
| MW | Molecular Weight |
| NCAC | National Crash Analysis Center |
| NGFT | Natural Gas Fuel Tender |
| NPRM | Notice of Proposed Rulemaking |
| PEEQ | Plastic Equivalent Strain |
| PHMSA | Pipeline and Hazardous Materials Safety Administration |
| PRV | Pressure Relief Valve |
| ROW | Right-of-way |
| SAE | Society of Automotive Engineers (former) |
| SCFM | Standard Cubic Feet per Minute |
| SPH | smoothed particle hydrodynamics |
| STDP | Start-to-discharge Pressure |
| TRIAX | Stress Triaxiality |
| TAG | Technical Advisory Group |
| TC | Transport Canada |
| TTC | Transportation Technology Center |
| TTCI | Transportation Technology Center, Inc. |
| TTI | Texas A&M Transportation Institute |